E-ELT PROGRAMME
CODEX Phase A

SCIENCE CASE

E-TRE-IOA-573-0001 Issue 1

18-Jan-2010

Author	M. Haehnelt	18-Jan-2010	
WP Manager	M. Haehnelt	18-Jan-2010	
Principal Investigator	L. Pasquini		
	Name	Date	Signature

Co-authors

Name	Affiliation
M. Haehnelt	Institute of Astronomy, University of Cambridge
S. Cristiani, V. D'Odorico, P. Molaro, M. Viel, E. Vanzella	INAF – Osservatorio di Trieste
M. Dessauges, S. Udry, D. Naef	Observatoire de Geneva
R. Rebolo López, R. García López, M.R. Zapatero Osorio, A. Herrero, G. Israelian	Instituto de Astrofísica de Canarias
P. Bonifacio,	Observatoire de Paris – Meudon
J. Liske, L. Pasquini	ESO

Change record

Issue	Date	Section / Paragraph affected	Reason / Initiation Documents / Remarks
1	18-Jan-2010	All	Established

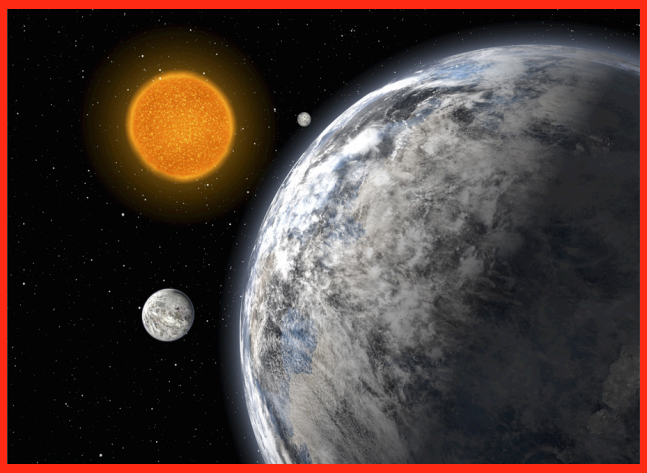

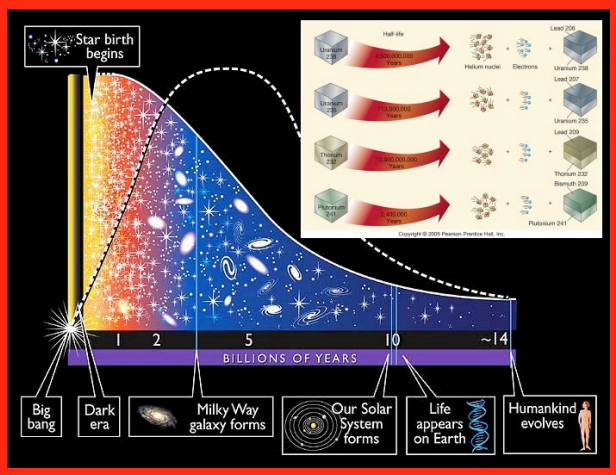

The science case for

CODEX

an ultra-stable high-resolution spectrograph for the E-ELT

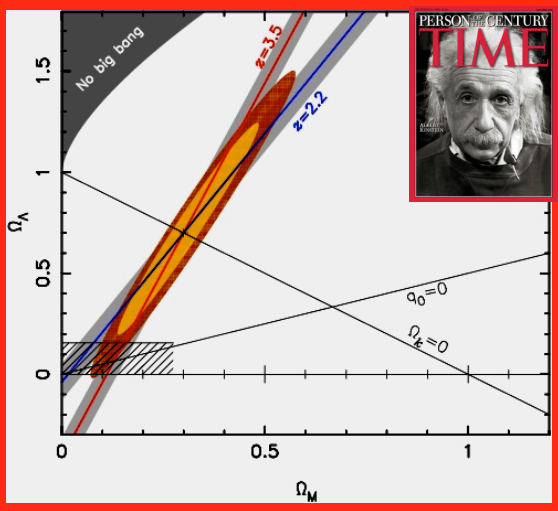

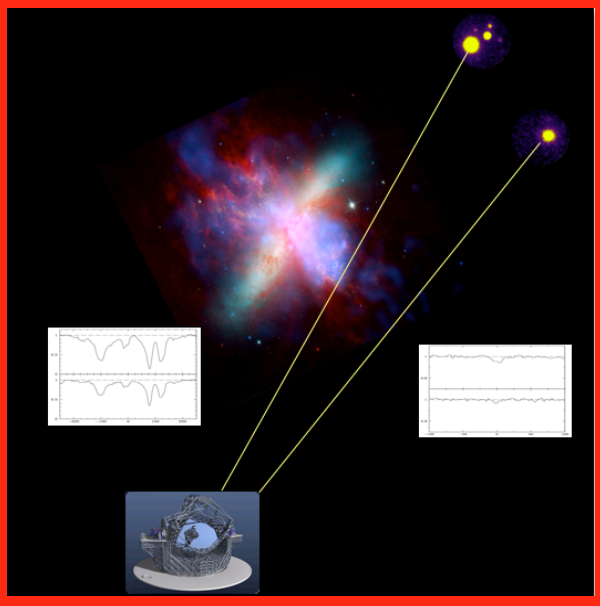

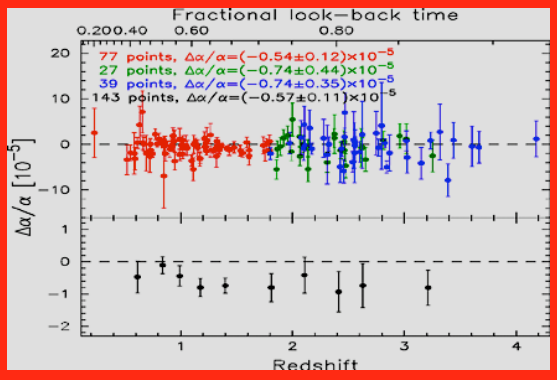

E-ELT PROGRAMME

CODEX Phase A Study

The Science Case (Version 7.0)

E-TRE-IOA-573-0001 Issue 1

January-2010

prepared by the members of the Science WP:
Piercarlo Bonifacio, Stefano Cristiani, Miroslava Dessauges, Valentina D'Odorico, Martin Haehnelt (Project Scientist and WP manager), Artemio Herrero, Garik Israelian, Jochen Liske, Paolo Molaro, Dominique Naef, Luca Pasquini, Rafael Rebolo Lopez, Stephane Udry, Eros Vanzella, Matteo Viel, Maria Rosa Zapatero Osorio

The Science Case for CODEX

CONTENTS

Summary

CODEX, the proposed ultra-stable optical high-resolution spectrograph for the E-ELT, will use novel Laser Comb calibration techniques and an innovative design to open a new era for precision spectroscopy. With its unique combination of light-collecting power and precision, CODEX will facilitate progress across the range of the burning science questions of our time. CODEX will make it possible to realize a long-held dream of cosmologists: to directly measure the acceleration of the Universe, believed to be driven by the mysterious dark energy by monitoring the cosmological redshift drift of spectroscopic features at cosmological distances. The same combination of precision and aperture will allow the assembly of the first sizeable sample of earth-like planets in the habitable zones of their stars with the radial velocity technique which has proved to be so successful with HARPS. The increase in photon flux afforded by the large aperture of the E-ELT will take this technique to the level of cm/s radial velocity stability – a factor of about 20 improvement compared to HARPS. These are just two of the most spectacular scientific results anticipated for CODEX which will be complemented by a wide range of spectacular science in stellar, galactic and extra-galactic Astronomy as well as Fundamental Physics. CODEX is a spectrograph designed to make the most out of the unique light gathering power of the E-ELT. With its wide ranging science case and large discovery potential it appears as an excellent candidate for an first/early light instrument.

1 Introduction

1.1 CODEX - an ultra-stable high-resolution optical spectrograph for the E-ELT

The E-ELT project is designed to sustain the internationally leading role of Europe in ground-based Astronomy in the imminent transition from 10m to 30-50m apertures. While instruments geared towards the infrared (IR) will exploit the advantages of partially reaching the diffraction limit, photon-hungry high-precision spectroscopy will particularly benefit from the enormous light collecting power of the E-ELT. The substantially increased photon flux together with the huge advances in precision and stability in spectrograph building to be realized in CODEX will enable some new, truly spectacular science.

CODEX will facilitate progress across the range of the burning science questions of our time. With its unique combination of light-collecting power and precision, CODEX will enable a serious attempt to realize a long-held dream of cosmologists: to directly measure the acceleration of the Universe, believed to be driven by the mysterious dark energy by monitoring the cosmological redshift drift of spectroscopic features at cosmological distances. The same combination of precision and aperture will allow the assembly of the first sizeable sample of earth-like planets in the habitable zones of their stars with the radial velocity technique which has proved to be so successful with HARPS. The increase in photon flux afforded by the large aperture of the E-ELT will enable CODEX to take this technique to the next level with its cm/s radial velocity stability which is improved by a factor of about 20 compared to HARPS.

These are just two of the most spectacular scientific results anticipated for CODEX. We will not have the space and resources here to present the wide range of exiting problems CODEX will be able to tackle in detail. We will thus concentrate on five "Show Cases" which demonstrate CODEX abilities. These Show Cases cover a wide range of subject areas and technical demands on the spectrograph in order to aid in the necessary trade-offs in the spectrograph design. We have chosen the following five Show Cases.

- **A direct measurement of the accelerating expansion of the Universe: Detecting and measuring the cosmological redshift drift of the Lyman-alpha forest.** The cosmological redshifts of spectroscopic features originating at large distances are the signature of an expanding Universe. As the expansion rate changes with time, the change is expected to be mirrored by a corresponding change in redshift. This is a very small effect, but should become measurable with CODEX if the collective signal in a large number of absorption features is monitored. The most favourable target is the multitude of absorption features making up the Lyα forest in QSO absorption spectra.

- **Detection of Earth twins in the Habitable Zone of solar-type stars.** The search for extra-solar earth-like planets which at least in principle could sustain life similar to that on our planet catches the imagination of scientists as well as that of the general public. The required accuracy for radial velocity searches to detect rocky planets in the habitable zone of 10 cm/s is in reach with the proposed HARPS-like spectrograph ESPRESSO for the VLT. With the 2 cm/s accuracy of CODEX it will be possible to assemble and study sizeable samples of earth-like planets in the habitable zone of their parent stars.

- **Galactic Archaeology: Unraveling the assembly history of the Milky Way with nucleochronometry.** How galaxies assembled and came to look the way they do is another of the *big questions* in Astronomy. Much has been learned in this respect from our own Galaxy which we can study in so much more detail than other galaxies. CODEX will take the sensitivity with which weak features of rare isotopes in stellar spectra can be studied to new limits. This should turn nucleochronometry - the equivalent of dating materials on the Earth using radioactive nuclides – into an accurate quantitative astronomical tool. The resulting precise age determinations of stars should lead to substantial progress in unraveling the assembly history of the Milky Way.

- **Probing the interplay of galaxies and the Intergalactic Medium from which they form.** The formation of the first autonomous sources of radiation, stars and black holes will have led to the heating, reionization and pollution of the intergalactic medium (IGM) with metals. The sensitivity of CODEX to the expected weak absorption features of residual metals in the low-density IGM thus opens a window into this important period in the history of the Universe. CODEX will enable the study of the interplay of galaxies and the intergalactic medium from which they form in unprecedented detail.

- **Testing Fundamental Physics: Taking the test of the stability of fundamental constant to new limits.** The values of many fundamental constants in physics have little if any theoretical explanations. Fundamental constants have thus long been speculated to vary in space or time or both. A discovery of such variations would be a revolutionary step and would lead to the development of new Physics. The current evidence for small variations of the fine structure constant on cosmological timescales from studies of QSO absorption spectra is intriguing but rather controversial. CODEX will take tests of the stability of fundamental constants to largely improved new limits.

Note that three of the Show Cases are part of the Design Reference Mission (DRM) of the E-ELT (see `www.eso.org/sci/facilities/eelt/science/drm/`). The discussion of the Show Cases will be complemented by a list of further science questions we expect CODEX to address. Despite its ambitious precision and stability goals, CODEX will be a versatile general purpose high-resolution optical spectrograph. Past attempts to predict ahead of time what will be the most exciting science produced by instruments opening up new regions of discovery space have generally failed. We obviously hope that this will hold for CODEX as well.

1.2 The laser frequency comb – introducing an absolute and reproducible calibration standard into astrophysical spectroscopy

One of the most crucial subsystems of CODEX will be its wavelength calibration source. The spectrum of an ideal calibration source has a high density of unblended, regularly spaced lines of uniform intensity covering the entire spectral range of interest. The wavelengths of these lines should be known from first principles and they should remain stable and reproducible to high accuracy for many years.

Traditional methods of wavelength calibration (e.g. the use of ThAr comparison spectra) are not able to meet the high demands of CODEX on accuracy and stability. Instead, the best approximation of an ideal wavelength calibration source currently known, and hence the most promising device for CODEX, is a so-called laser frequency comb (LFC, see Fig. 1[1]).

The core of an LFC is a mode-locked laser emitting a repetitive train of femtosecond pulses. In frequency space this results in thousands of equally spaced modes covering a bandwidth of several THz. The mode spacing is given by the pulse repetition frequency which resides in the radio frequency domain. The repetition frequency can readily be synchronised with a precise radio frequency reference such as an atomic clock. These clocks provide by far the most precise measurements of time and frequency currently available, which are in turn the most reliably determined quantities in physics.

The novelty of the LFC and its tremendous benefit for many areas of physics has been widely recognized with the award of the 2005 Nobel Prize in Physics to T. Hänsch and J. Hall for fundamental and pioneering work in the development of the optical frequency comb technique.

An LFC offers a number of advantages over traditional wavelength calibration sources. (i) the absolute position of each line is known a priori (i.e. without reference to any laboratory measurements) with relative precision better than 10^{-12}, which is limited only by the radio frequency clock; (ii) the density of lines may be as high as permitted by the spectrograph's resolution while at the same time guaranteeing the absence of blended lines; and (iii) the line density is perfectly uniform.

Development and testing of a prototype Laser Comb system for HARPS is under way in collaboration with the MPI for Quantum Optics. As discussed in the RD study report these efforts proceed extremely well. We are thus confident that wavelength calibrations with a LFC is set to become the new standard in high-precision spectroscopy. With a LFC with pulse repetition rate in the range 5–30 GHz (so that the lines are resolved from each other by CODEX), and of a uniform intensity of all comb modes over the full CODEX wavelength range, a photon-noise limited wavelength calibration accuracy of $\sim$1 cm/s for every *single* exposure can easily be achieved by CODEX (Murphy et al., 2007, MNRAS, 380, 839). The built-in stability and reproducibility of the LFC spectra ensure that any evolution in the distortions of the wavelength scale induced by the spectrograph or detector may be accurately tracked over essentially arbitrary timescales.

1.3 A special ("experimental") observing mode for CODEX?

Monitoring the small cosmological redshift drift of about 1-2 cm/s per year in the spectra of what are rather faint sources at cosmological distances will pose unprecedented challenges. The required observing time adds up to substantial amounts (the Design Reference Mission proposal requests about 4000h over 15 years). The data have to be

[1]The Figure is taken from Thomas R. Schibli, "Frequency combs: Combs for dark energy", Nature Photonics, Volume 2, Issue 12, pp. 712-713 (2008). DOI: 10.1038/nphoton.2008.240

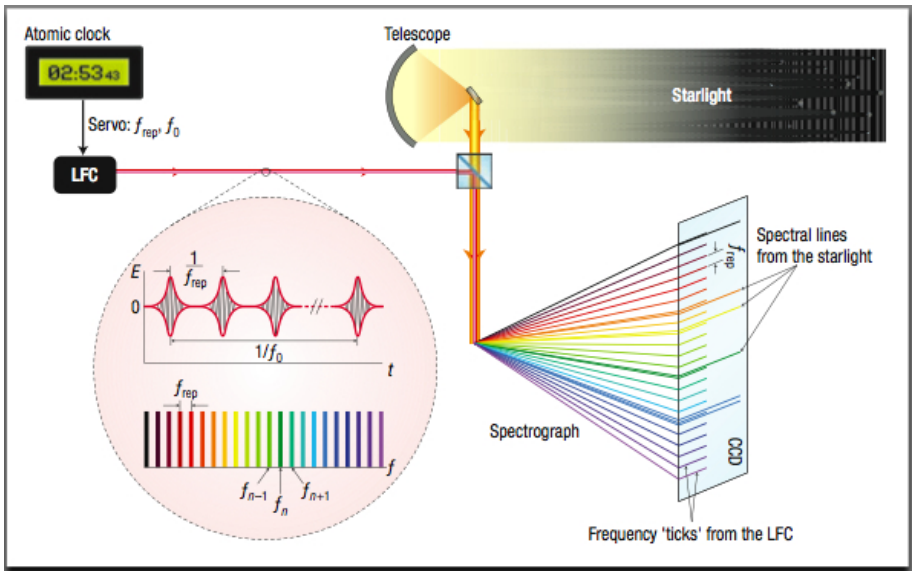

Figure 1: Wavelength calibration with a laser frequency comb. The LFC emits a periodic pulse train with a period of $1/f_{\rm rep}$. The associated optical spectrum shows a comb-like structure with a line-spacing of $f_{\rm rep}$ and an offset frequency f_0. The two radio-frequencies $f_{\rm rep}$ and f_0 are phase locked to a reference signal such as an atomic clock. This ensures precise knowledge of the frequencies f_n of every spectral line in the LFC. The Figure is taken from Schibli[1] (2008).

collected and processed in a homogeneous and consistent way. As results will become increasingly more interesting as time goes on there will hopefully be a strong case to continue the measurement over decades if successful. The successful introduction of service mode observations at the VLT goes a long way in accommodating what is similar to a Physics experiment in the scale of operation. The redshift drift "experiment" would probably nevertheless be carried out most efficiently in a special "experimental" observing mode. Many of the QSO absorption spectra taken for this purpose will be extremely valuable for other scientific purposes. At the same time many QSO absorption spectra taken for other purposes could contribute to the redshift experiment, and much more efficiently so if the benefit for the redshift drift experiment is taking into account in the planning phase. A special version of the VLT service mode operation modified with the aim of maximizing the benefit of CODEX QSO absorption spectra for both the redshift drift experiment *and* the many other science goals discussed here should be able to achieve this.

1.4 The CODEX exposure time calculator

The signal-to-noise (S/N) or exposure time estimates presented in this document were generally calculated with, or are consistent with, the generic spectroscopic E-ELT Exposure Time Calculator (ETC) provided by the E-ELT Science Office at ESO (see `http://www.eso.org/observing/etc/`). Details are given in the documentation accompanying the ETC. Here we briefly explain our input parameter choices for CODEX S/N calculations using the E-ELT ETC. For the redshift drift experiment the system transmission and its wavelength dependence and in particular the cut-off at blue wavelengths are rather critical. For the redshift drift experiment all calculations are thus based on the exact system transmission of the baseline design as described in the Executive Summary.

The target is always assumed to be a point source, and the site is always chosen to be the Paranal-like site. The ETC assumes an appropriate extinction curve and models the sky brightness as a pseudo-continuum appropriate for a moon phase of 3 days from new moon plus a standard set of night sky emission lines. The light is collected by a 42m telescope (with an appropriate central obstruction). Unless otherwise stated we assume a combined telescope/instrument throughput (including entrance aperture losses and detector quantum efficiency) of 0.2. Note that the ETC assumes a combined telescope/instrument throughput of 0.25, excluding the aperture losses and detector. Since it also assumes a detector quantum efficiency of 0.9, we must set the aperture loss to 0.9 to obtain the desired overall efficiency value of 0.2. This is achieved by selecting "AO mode = seeing limited" and " Radius of S/N reference area = 800 mas". Note that an efficiency of 0.2 is very close to the overall system transmission of the baseline design (~ 0.22) as presented in the executive summary. To get the detector noise right, we have set the parameter "number of spectra on detector" to 280. This number accounts for the number of pixel over which the

light at a given wavelength will be spread. Finally, we point out that the S/N estimates returned by the ETC are per resolution element, not per pixel.

1.5 The position of CODEX in relation to other optical high-resolution spectrographs

CODEX will be the natural progression towards ultra-stable high precision spectroscopy which so successfully started with HARPS for 4m class telescopes and will hopefully soon reach the 10m class with ESPRESSO. Due to the impressive progress in calibration techniques based on the Laser Frequency Comb, ESPRESSO should reach a Doppler precision of 10 cm/s with resolving power R>150 000 at one UT for relatively bright objects, and 1 m/s with R$\sim$40 000 in the 4-UT mode for fainter objects. CODEX is designed to be in a class of its own in this respect and should reach 2 cm/s with a goal of 1 cm/s. CODEX will thereby be nevertheless optimized for throughput and thus be more efficient than *e.g.* UVES despite its ambitious precision and stability goals. There will obviously be some overlap in the science goals between CODEX and ESPRESSO. ESPRESSO will constitute a big improvement compared to HARPS and UVES/X-Shooter but the Doppler accuracy and sensitivity will be typically 10 times worse than what we aim to achieve with CODEX at the E-ELT.

Here it is also appropriate to discuss PEPSI, a high-resolution spectrograph under construction for the LBT[2]. PEPSI will be located in a pressure and temperature controlled environment. The emphasis of the design is, however, on polarimetry rather than high Doppler precision. Some of the design choices adopted (image slicers, selectable central wavelength) do not appear to be optimized for precision spectroscopy. The maximum resolving power of PEPSI is higher than what we anticipate for CODEX. PEPSI should thus be able to contribute to the discussion of the variability of fundamental constants and to stellar spectroscopy science cases.

Until about a year ago CODEX was the only ultra-stable, high-resolution spectrograph proposed for an ELT. This has recently changed. A high-resolution optical spectrograph called Q-SPEC is amongst the instruments now under discussion for the GMT project [3]. Q-Spec appears to adopt many aspects of the optical design and concepts of CODEX (anamorphic pupil, pupil slicer) and aims at a precision of better than 1 m/s. The possibility of multi-object spectroscopy is also considered. With its effective aperture of 21.5 m the GMT is significantly smaller than planned for the E-ELT. Q-SPEC is thus similar to ESPRESSO in 4-UT mode rather than CODEX. A competitive feasibility study of a High Resolution Optical Spectrograph (HROS) for the TMT was performed in 2006 by two groups, one at UCSC and one at the University of Colorado. No journal publication is available from these studies, but the preliminary design concepts had no emphasis on stability and precision. The studies suggested to achieve wavelength precision with absorption cells in the optical path (e.g. iodine or similar). The proposed resolving power was in the range 30 000-50 000, a factor 3-5 lower than what we propose for CODEX. The design did not foresee any fibres (wavelength extension down to the atmospheric cutoff) and accommodated the possibility of a modest multiplex. A spectrograph with such a design would probably have been competitive with CODEX for some of the IGM applications, but HROS has not been selected for the suite of the three first light instruments of the TMT. We are not aware of further developments.

1.6 CODEX in the context of other facilities

CODEX will work both in synergy and in competition with a number of other facilities on several scientific topics.

One of the most prominent areas of synergy between CODEX and other instruments and facilities is exoplanet science. The combination of CODEX with a high-contrast imager on the E-ELT is of particular interest because of its wide range of important applications. An imager equipped with an extreme AO system and a coronographic device (e.g. EPICS) will be capable of directly detecting at least some of the more massive planets discovered by CODEX using the radial velocity method, as well as other planets in the same systems. The combination of these instruments will be able to provide us with a full characterisation of the planets' orbits as well as with basic knowledge on planetary atmospheres, true masses and temperatures.

We note that a more detailed description of the synergies between all E-ELT instruments involved in exoplanet science (CODEX, EPICS, METIS, HARMONI) is planned to be laid out in a future, joint document .

CODEX will also be needed to obtain crucial radial-velocity follow-up observations of transiting exoplanet candidates discovered by various space missions. For example, the planned PLATO satellite will be capable of detecting the transits of Earth-sized planets in the habitable zone of nearby solar-type stars. However, to confirm

[2]Strassmeier, K. et al. 2004, AN 325, 27

[3]Barnes, S.; MacQueen, P. 2008, in Ground-based and Airborne Instrumentation for Astronomy II. Edited by McLean, Ian S.; Casali, Mark M. Proceedings of the SPIE, Volume 7014, pp. 70141H-70141H-10

the planetary origin of the detected photometric signal and to precisely measure the mass of the transiting body in these cases a radial velocity precision of better than 10 cm/s will be necessary, which only CODEX will be able to provide.

Another important synergy is that between CODEX and GAIA. Together these instruments will be able to probe stellar evolution theory by comparing physical stellar parameters derived by GAIA from accurate positions on the Hertzsprung-Russel diagram in combination with theoretical stellar evolutionary tracks with those derived by CODEX from (i) measurements of the radioactive element Th and (ii) from asteroseismology of metal-poor stars.

Several future facilities such as LSST, JDEM and EUCLID will seek to constrain the properties of Dark Energy, mostly using surveys of SNIa, weak lensing, and galaxy clustering. However, a redshift drift measurement by CODEX would probe the expansion rate in a redshift range that will remain largely inaccessible to most other methods even in the ELT era (the only exception being SNIa surveys). CODEX measurements of the redshift drift at z = 2-4 would therefore provide an important complement to the (indirect) constraints on the expansion rate at $z < 2$ obtained by other techniques.

Finally, CODEX will also work in synergy with ALMA and SKA to constrain the possible variability of physical 'constants'. High-redshift molecular rotational absorption lines discovered by ALMA and HI 21cm absorption detected by SKA can be compared to optical metal lines observed with CODEX to constrain various combinations of constants involving the fine structure constant (alpha), the proton-to-electron mass ratio μ and the proton g-factor. In addition, SKA may be able to detect "conjugate" satellite lines of OH which by themselves will constrain a particular combination of α and μ.

1.7 Scientific arguments for CODEX as a first/early light instrument

The discovery of an Earth Twin (a rocky planet in the habitable zone) will with reasonable certainty be the result with the strongest immediate impact. The impact in this case will go far beyond the exo-planet community and will definitely capture the imagination not only of scientists but also of the general public. At the time of first light for the ELT several candidate stars should be known and there will be fierce competition for the crown of the discovery of the first Earth Twin. The long-term impact of a discovery of the variability of fundamental constants is potentially even larger as it may trigger major developments in Theoretical Physics. The leap in wavelength accuracy afforded by CODEX means thereby that such a discovery would not be riddled by the discussions about systematic uncertainties which plague current observations. The case is, however, high-gain high-risk as there is obviously no guarantee that fundamental constants do indeed vary at a level detectable with CODEX. The signal of the redshift drift increases linearly with time. The redshift drift measurement therefore benefits strongly from an early start of measurements. Starting this measurement early in the operational life of the E-ELT may be time well spent at a time when the pressure on the E-ELT is not yet as high as it will become when all anticipated AO systems and a large instrument suite are available. In addition, since the precision of the measurement increase with the square of the signal to noise ratio, an increase of *e.g.* 50% in the duration of the experiment would reduce the required E-ELT observing time by more than a factor of two for the same relative precision. It appears also prudent to remember here the role which accurate spectroscopy has played in the development of quantum mechanics. Finally CODEX has a very large base of potential users with a wide range of interests which should generally translate into a large discovery potential.

2 Show Cases

Show Case 1: A direct measurement of the accelerating expansion of the Universe: Detecting and measuring the cosmological redshift drift of the Lyman-alpha forest[4]

2.1.1 Background

The universal expansion was the first observational evidence that General Relativity might be applicable to the Universe as a whole. For decades astronomers tried to settle the question if the Universe is indeed decelerating as expected for a Universe with a critical density of ordinary matter – a model strongly favoured by many theoretical astrophysicists. The discovery that the expansion of the Universe appears to have begun accelerating thus came rather unexpected. The physical reason for this acceleration is entirely unclear at present and considered as one of the big mysteries of present-day physics. Ironically the infamous cosmological constant originally introduced by Einstein in order to explain a static non-expanding Universe – a model popular at the time – can explain this late acceleration of the Universe very well. Introducing a cosmological constant and setting it to a value which corresponds to an equivalent energy density similar to that of ordinary matter appears, however, rather arbitrary. Modification of General Relativity as a theory of gravity and the presence of a new form of energy dubbed "dark energy" – two other possibilities invoked to explain the acceleration – are thus under vivid study by theoretical and observational astrophysicists.

Probably the best way to probe the nature of the acceleration is to determine the expansion history of the Universe. Observables that depend on the expansion history include distances and the linear growth of density perturbations, and so surveys of type Ia SNe, weak gravitational lensing and the signature of the sound horizon in the galaxy power spectrum are generally considered to be excellent probes of the acceleration.

In practice, however, extracting information on the expansion history from these surveys requires a prior on the spatial curvature, a detailed understanding of the linear growth of density perturbations and hence a specific cosmological model. A model-independent approach to determine the expansion history is thus highly desirable. This is exactly what the experiment described here aims to achieve. The idea was first explored by Sandage (1962) who showed that the evolution of the Hubble expansion causes the redshifts of distant objects partaking in the Hubble flow to change slowly with time. Just as the redshift, z, is in itself evidence of the expansion, so is the change in redshift, $\dot{z}$, evidence of its de- or acceleration between the epoch z and today. This implies that the expansion history can be determined, at least in principle, by means of a straightforward spectroscopic monitoring campaign.

The redshift drift is a direct, entirely model-independent measurement of the expansion history of the Universe which does not require any cosmological assumptions or priors whatsoever. However, the most unique feature of this experiment is that it directly probes the global *dynamics* of the metric describing the Universe. All other existing cosmological observations, including those of the CMB, SNIa, weak lensing and baryonic acoustic oscillations, are essentially *geometric* in nature in the sense that they map out space, its curvature and its evolution. Many of these experiments also probe the dynamics of localised density perturbations but none actually measures the *global* dynamics. In this sense the redshift drift method is qualitatively different from all other cosmological observations, offering a truly independent and unique approach to the exploration of the expansion history of the Universe. Loeb (1998) first discussed the Lyman α (Lyα) forest as a promising target for a $\dot{z}$ measurement and assessed the prospects for a successful detection in the context of currently existing observational technology. As we will discuss here the revolutionary light collecting power of the E-ELT in combination with an ultra-stable, high-precision, high-resolution spectrograph like CODEX should provide for the first time the required accuracy for a successful redshift-drift measurement.

2.1.2 The redshift drift of spectroscopic features in an expanding Universe

In any metric theory of gravity one is led to a very specific form of the metric by simply assuming that the Universe is homogeneous and isotropic. The evolution in time of this so-called Robertson-Walker metric is entirely specified by its global scale factor, $a(t)$. The goal is to measure or reconstruct this function. What a redshift-drift experiment proposes to measure is the change of a with time by its wavelength-stretching effect on photons

[4]This showcase corresponds to case C2 of the E-ELT Design Reference Mission. Most of the material in this show case is based on Liske et al. (2008).

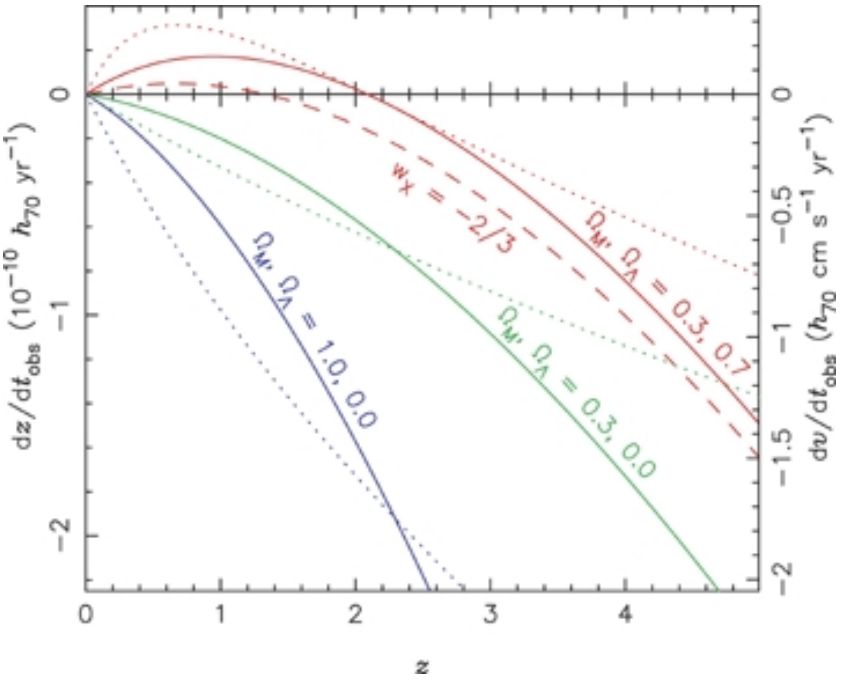

Figure 2: The solid (dotted) lines and left (right) axis show the redshift drift $\dot{z}$ ($\dot{v}$) as a function of redshift for various combinations of $\Omega_{\rm M}$ and Ω_Λ as indicated. The dashed line shows $\dot{z}$ for the case of dark energy having a constant $w_X = -\frac{2}{3}$ (and $\Omega_{\rm M}, \Omega_X = 0.3, 0.7$).

traversing the Universe. For an object at a fixed comoving distance the redshift drift is related to the evolution of the Hubble parameter ($H(t) \equiv \dot{a}/a$) as

$$\dot{z} \equiv \frac{{\rm d}z}{{\rm d}t_{\rm obs}}(t_0) = (1+z)H_0 - H(z). \tag{1}$$

$\dot{z}$ is a small, systematic drift as a function of time in the redshift of a cosmologically distant source as observed by us today. This effect is induced by the de- or acceleration of the expansion, i.e. by the change of the Hubble parameter H. Since H_0 is known, this drift is a direct measure of the expansion velocity at redshift z. Measuring $\dot{z}$ for a number of objects at different z hence gives the function $\dot{a}(z)$. Given $a(z)$ *and* $\dot{a}(z)$, one can reconstruct $a(t)$. A measurement of $\dot{z}(z)$ therefore amounts to a purely dynamical reconstruction of the expansion history of the Universe.

2.1.3 Size of the expected signal – the need for ultra-stable high-precision spectroscopy with cm/s accuracy

Predicting the redshift drift $\dot{z}(z)$ requires a theory of gravity. Inserting the Robertson-Walker metric into the theory's field equation results in the Friedman equation, which specifically links the expansion history with the densities, Ω_i, and equation of state parameters, w_i, of the various mass-energy components of the Universe. In the case of general relativity the Friedman equation is given by:

$$H(z) = H_0 \left[\sum_i \Omega_i (1+z)^{3(1+w_i)} + \Omega_k (1+z)^2 \right]^{\frac{1}{2}}, \tag{2}$$

where $\Omega_k = 1 - \sum \Omega_i$.

Fig. 2 shows the expected present-day redshift drift, $\dot{z}(z)$, for various values of $\Omega_{\rm M}$ and Ω_Λ (solid lines), and for a case where the dark energy's equation of state parameter $w \neq -1$ (dashed line). The redshift drift is also shown in velocity units (dotted lines), where $\dot{v} = c\,\dot{z}\,(1+z)^{-1}$. The existence of a redshift region where $\dot{z} > 0$ is the hallmark of $\Omega_\Lambda \neq 0$. Note the scale of Fig. 2. At $z = 4$ the redshift drift is of order 10^{-9} or 6 cm s^{-1} per

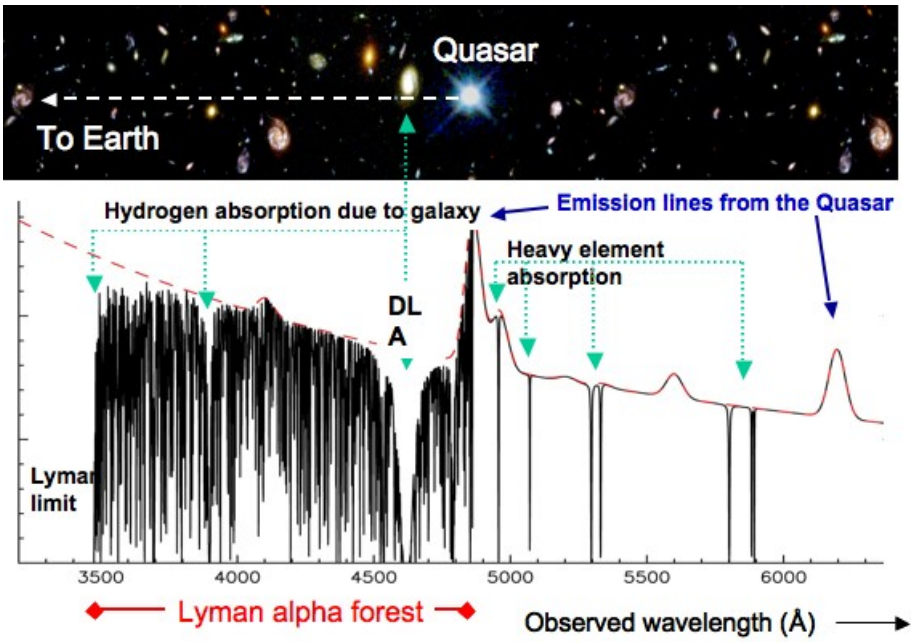

Figure 3: The Lyα forest and associated metal absorption in a QSO spectrum (figure courtesy of John Webb).

decade. For comparison, the long-term accuracy achieved in extra-solar planet searches with the high-resolution echelle spectrograph HARPS on the ESO 3.6-m Telescope is of order 1 m s^{-1}. Measuring the redshift drift due to the cosmic expansion is extremely challenging.

2.1.4 The optimal target - the Lyα forest and the associated metal lines in QSO absorption spectra

A priori, it is not at all obvious which spectral features of which set or class of objects might be best suited for a redshift-drift measurement. Clearly though, potential candidate targets should boast as many of the following desirable attributes as possible.

1. They should faithfully trace the Hubble flow. Although peculiar motions are expected to be random with respect to the Hubble flow, the additional noise introduced by them could potentially conceal the cosmic signal.a
2. The targets should have the sharpest possible spectral features to minimise the error on individual redshift measurements.
3. The number of useful spectral features per target should be as high as possible in order to maximise the amount of relevant information per unit observing time.
4. The targets should be as bright as possible.
5. They should exist over a wide redshift range, and particularly at high z, where the signal is expected to be largest.

As discussed in detail in Liske et al. (2008) the Lyα forest in QSO absorption spectra actually offers the best compromise to these somewhat contradicting requirements. The term 'Lyα forest' refers to the plethora of absorption lines observed in the spectra of all quasi-stellar objects (QSOs) shortwards of the Lyα emission line (see Fig. 3). Since the absorbing gas is physically unconnected with the background source against which it is observed it elegantly avoids the conflict between requirements (1) and (4) above. However, as the gas is in photoionization equilibrium with the intergalactic ultraviolet (UV) background, its temperature is of order 10^4 K. Consequently, the absorption lines are not particularly sharp and the typical line width is $\sim$30 km s^{-1}. On the other hand, QSOs are among the brightest sources in the Universe and exist at all redshifts out to at least $z \sim 6$. Furthermore, each QSO spectrum at $z \gtrsim 2$ shows on the order of 10^2 absorption features.

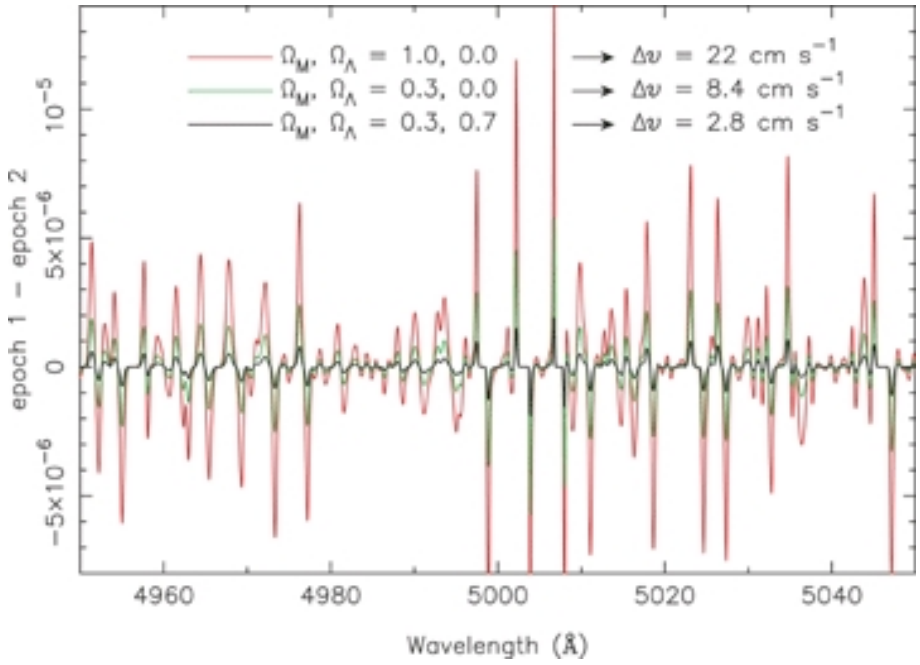

Figure 4: Flux difference between two artificial, noiseless spectra of the same Lyα forest at $z \approx 3$ simulated for two observing epochs separated by $\Delta t_0 = 10$ yr and for various combinations of $\Omega_{\rm M}$ and Ω_Λ as indicated. The redshift drift implied by these parameters is also given.

Fig. 4 demonstrates the effect of the redshift drift on the Lyα forest by showing the difference between two simulated spectra of the same Lyα forest at different epochs.

2.1.5 Photon noise – how well can we do with realistic QSO samples?

The CODEX spectrograph is being designed to achieve a stable wavelength calibration with cm/s accuracy. As discussed extensively in Liske et al. (2008) uncertainties due to peculiar velocities in the intergalactic medium and other astrophysical nuisance effects are expected to be much smaller than the expected cosmological redshift drift signal. The precision of the redshift-drift experiment proposed here should thus be limited by photon noise. The accuracy, σ_v, to which a radial velocity shift between two spectra of the same object can be determined then depends chiefly on the number and sharpness of the relevant spectral features and the spectra's S/N. The number density of the absorption lines that constitute the Lyα forest strongly depends on redshift. Using extensive Monte Carlo simulations Liske et al. (2008) have derived the following relation between the σ_v of a pair of Lyα forest spectra on the one hand, and the spectra's S/N and the background QSO's redshift on the other hand:

$$\sigma_v = 2 \left(\frac{\rm S/N}{2370}\right)^{-1} \left(\frac{N_{\rm QSO}}{30}\right)^{-\frac{1}{2}} \left(\frac{1+z_{\rm QSO}}{5}\right)^{-1.7} \ {\rm cm\ s^{-1}}, \tag{3}$$

where the last exponent changes to -0.9 at $z_{\rm QSO} > 4$. The S/N is per $0.0125\mathring{A}$ pixel and $N_{\rm QSO}$ is the number of QSO spectra used for the experiment. In addition to the Lyα forest QSO spectra also display higher order H I lines and a variety of metal absorption lines. Using the H I Lyβ lines in addition to the Lyα lines, as well as all available metal lines within and to the red of the Lyα forest significantly improves a given spectrum's sensitivity to radial velocity shifts by a further factor of 0.67.

Can the E-ELT achieve the S/N required by equation (3)? In Fig. 5 we plot essentially all known bright, high-redshift QSOs as a function of their redshift and photon flux. The background colour image and solid contours show the value of σ_v that would be achieved if a total integration time of $t_{\rm int} = 2500$ h was invested into observing a single QSO of a given photon flux and redshift. As requested by the midterm review board this calculation uses the full, wavelength-dependent system transmission of the baseline design as presented in the executive summary, including the effects of the atmosphere, telescope (i.e. coatings) and instrument, as well as the instrument's wavelength coverage. The improvement of σ_v afforded by the Lyβ forest and the metal lines as well as the deterioration caused by a realistic scheduling of observations have also been included.

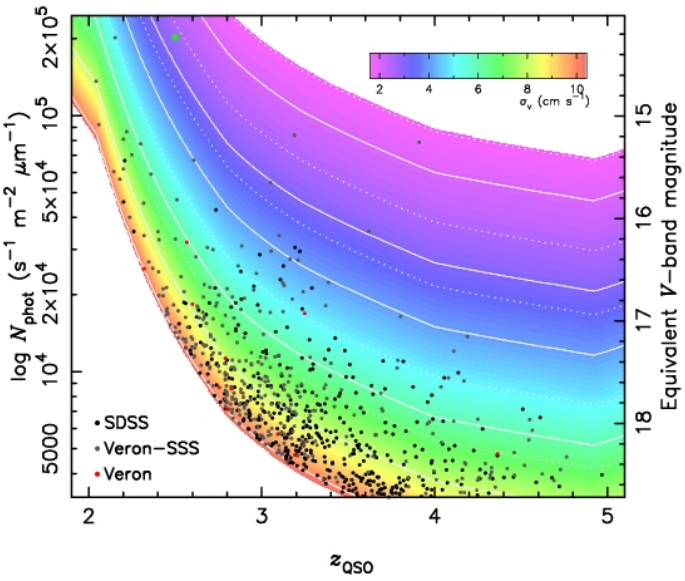

Figure 5: The dots show the known, bright, high-redshift QSO population as a function of redshift and estimated photon flux at the centre of the Lyα forest. Along the right-hand vertical axis we have converted the photon flux to a corresponding Johnson V-band magnitude. The background colour image and solid contours show the value of σ_v that can be achieved for a given photon flux and redshift, assuming $D = 42$ m, $t_{\rm int} = 2500$ h and our estimate of the full system transmission. The contour levels are at $\sigma_v = 2, 3, 4, 6, 8$ and 10 cm s^{-1}. The dotted contours show the same as the solid ones, but for $D = 35$ m or, equivalently, for $t_{\rm int} = 1736$ h.

Fig. 5 demonstrates that, although challenging, a reasonable measurement of $\dot{z}(z)$ is within reach of the E-ELT. There exists a number of QSOs that are bright enough and/or lie at a high enough redshift to provide reasonable values of σ_v. We find 10 objects at $\sigma_v < 4$ cm s^{-1} and 3 objects at $\sigma_v < 3$ cm s^{-1}, with good coverage of the redshift range 2.5–4. One object even gives $\sigma_v = 1.8$ cm s^{-1}. However, for a smaller telescope with $D = 35$ m the number of objects with $\sigma_v < 4$ cm s^{-1} reduces to only 4 (cf. dotted contours).

2.1.6 Mapping the evolution of the accelerating expansion of the Universe at z<2<4

A realistic redshift drift experiment will have to include several QSOs as targets and the total available integration time will have to be divided somehow among them. There are several possibilities, both for how to select the targets and how to divide the time among them. The choice of the selection strategy will depend on the precise goal of the redshift drift experiment. In practice it is likely that operational and scheduling constraints would limit the available choices but we have nevertheless investigated three alternative scenarios which may be perceived to be representative of three different approaches.

1. The simplest possible goal is to aim for the most precise $\dot{z}$ measurement possible, i.e. the smallest overall σ_v. This may be considered a 'pure experimentalist' approach where virtually no prior observational information or theoretical expectation is used to (mis-)guide the design of the experiment.

2. Another approach is to emphasise the most basic and yet most unique (and perhaps most captivating) feature of the redshift drift experiment, which is being able to *watch*, literally and in real time, the Universe changing its rate of expansion. In this case the aim is to prove the existence of a dynamical redshift drift effect and hence to measure a non-zero value of $\dot{z}$ with the highest possible significance.

3. As explained above, the discovery and the unknown physical source of the acceleration of the universal expansion provide a strong motivation for any observation seeking to determine $H(z)$, and this is also true for the direct and dynamical method of measuring $\dot{z}$. From this point of view the goal should be to place the strongest possible constraints on the acceleration.

Fig. 6 shows Monte-Carlo simulations of the results of three such possible redshift-drift experiments, using targets selected from Fig. 5. In the case of scenario 1. above we find that observing 20 QSOs for a total of 4000 h

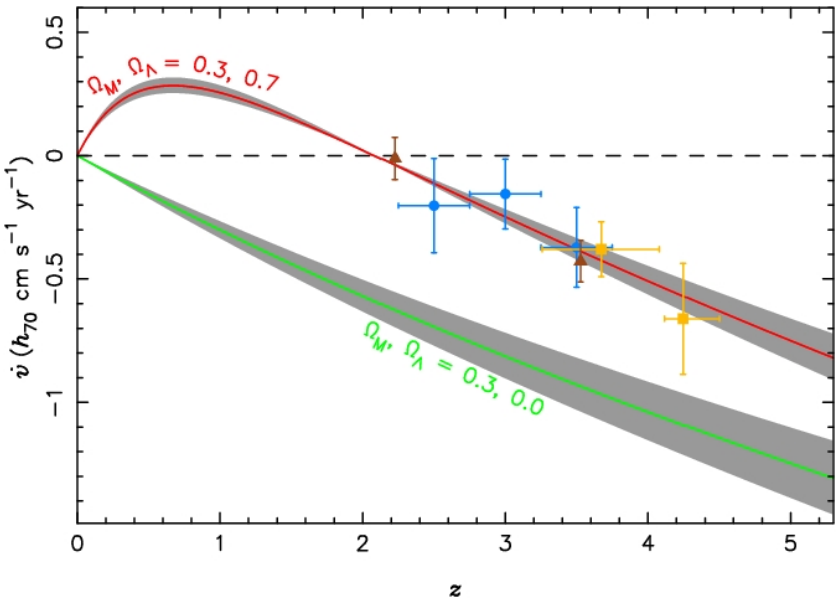

Figure 6: Monte-Carlo simulations of three different implementations of a redshift drift experiment as outlined in the text. Plotted are values and errors of the 'measured' velocity drift $\dot{v}$, expected for a total experiment duration of $\Delta t_0 = 30$ yr, a total integration time of 4000 h and for standard cosmological parameters ($h_{70} = 1$, $\Omega_{\rm M} = 0.3$, $\Omega_\Lambda = 0.7$). Blue dots: selection by σ_v, $N_{\rm QSO} = 20$ (binned into three redshift bins), equal time allocation. Yellow squares: selection by $|\dot{v}|/\sigma_{\dot{v}}$, $N_{\rm QSO} = 10$ (in two redshift bins), equal time allocation. Brown triangles: selection by best combined constraint on Ω_Λ, $N_{\rm QSO} = 2$, optimal time distribution. The solid lines show the expected redshift drift for different parameters as indicated, and $h_{70} = 1$. The grey shaded areas result from varying H_0 by ± 8 km s^{-1} Mpc^{-1}. See Liske et al. (2008) for more details.

over 30 yr delivers an overall precision of $\sigma_v = 2.7$ cm s^{-1}(blue dots in Fig. 6). For scenario 2. we find that the redshift drift can be detected with a significance of 4.3σ (yellow squares). Scenario 3. is discussed in more detail below.

2.1.7 Testing the standard paradigm of gravity/cosmology

Measuring a $\dot{z}$ value > 0 is equivalent to proving the existence of past acceleration of the expansion (cf. Fig. 2). Unfortunately, due to the atmospheric cut-off it is not possible to observe the Lyα forest from the ground at $z \lesssim 2$ where the transition from $\dot{z} < 0$ to > 0 is expected. However, by complementing a $\dot{z}$ measurement at the lowest possible redshift ($z \approx 2$) with another measurement at high redshift it is – at least in principle – possible to show that $\dot{z}$ must turn positive for any reasonable functional form of $\dot{z}(z)$, and that the expansion of the Universe must therefore have accelerated in the past. Note that this conclusion only requires that gravity can be described by a metric theory and that the Universe is homogeneous and isotropic on large scales. Otherwise it is entirely model-independent. Whether this is possible in practice depends, however, rather sensitively on the availability of bright QSOs at the lowest redshift where the blue cut-off of the system transmission does not yet lead to a significant increase of the measurement errors. As is apparent from Fig. 5 with the wavelength dependence of the system transmission of our baseline design it is not possible to achieve reasonable σ_v values for any of the currently known QSOs at $z_{\rm QSO} \lesssim 2.5$. This conclusion depends, however, sensitively on the exact assumptions regarding the system transmission at the bluest wavelength and the exact redshift (distribution) of the brightest QSOs in the narrow redshift range $2 < z < 2.5$. If for example the reflectivity of the telescope and Coudé train mirror coatings at 5000 Å could be maintained all the way into the blue, and if the blue end of the instrument's wavelength range could be reduced from 3700 to 3500 Å, then the measurement error for the very bright QSO at $z_{\rm QSO} = 2.15$ in Fig. 5 would decrease from $\sigma_v = 5$ cm s^{-1} to 3.8 cm s^{-1}, making a meaningful constraint on the acceleration feasible. Alternatively, the discovery of a *single*, similarly bright QSO at slightly higher redshift, say $z_{\rm QSO} \approx 2.5$ (marked by a green star in Fig. 5), would have a similar effect. Either of these improvements would allow us to confidently detect the existence of past acceleration. This is demonstrated by the brown triangles in Fig. 6, where the low-z point corresponds to the green star in Fig. 5. Note that in light of major wide-area QSO surveys being planned or under way and the importance of a QSO reference frame for GAIA the discovery of suitably bright QSOs in the desired redshift range appears more or less guaranteed.

Beyond the 'mere' detection of the acceleration how well can these observations constrain the standard general relativistic model of cosmology? In Fig. 7 we present the expected constraints in the Ω_Λ-$\Omega_{\rm M}$ plane from the two $\dot{z}$ measurements shown as brown triangles in Fig. 6, assuming $t_{\rm int} = 4000$ h and $\Delta t_0 = 30$ yr. The red and blue solid lines show the individual constraint lines for a fixed $h_{70} = 1$ and the grey shaded areas around them are the error bands that correspond to the respective values of σ_v for each object.

The coloured ellipses in Fig. 7 show the joint 68 and 90 per cent confidence regions that result from the combination of the two $\dot{v}$ measurements. Here we have assumed that an external constraint places 1σ limits of ± 8 km s^{-1} Mpc^{-1} on H_0 (Freedman et al. 2001) before marginalising over this parameter. By comparing the error bars on the brown triangles in Fig. 6 with the grey shaded region around the red line we can see that this uncertainty in H_0 is small relative to the errors on $\dot{v}$. Hence the ellipses in Fig. 7 are almost those that would be obtained for a fixed H_0.

Projecting the joint constraints onto the vertical axis we find that the 95 per cent lower limit on the cosmological constant is $\Omega_\Lambda > 0.16$ (indicated by the hashed region in Fig. 7), while $\Omega_\Lambda = 0$ is excluded at the 98.2 per cent confidence level. Note that we can also exclude $q_0 = 0$ at a similar level of 97.6 per cent. These numbers do not depend sensitively on the adopted prior on H_0, for the reason explained above. Doubling the error on H_0 to ± 16 km s^{-1} Mpc^{-1} has almost no effect at all. Even if we use a flat prior and simply marginalise over the range $0 \leq H_0 \leq 140$ km s^{-1} Mpc^{-1} we can still reject $\Omega_\Lambda = 0$ at 98.1 per cent confidence, although the 95 per cent lower limit now reduces to 0.08. For a shorter experiment duration of $\Delta t_0 = 25$ yr we can still exclude $\Omega_\Lambda = 0$ at 95.7 per cent confidence.

Thus we conclude that, assuming general relativity to be valid, the E-ELT will enable us to confirm the existence of a cosmological constant using purely dynamical evidence – by measuring the redshift drift in QSO absorption lines over a period of $\sim$30 yr – *without assuming flatness, using any other external cosmological constraints or making any other astrophysical assumptions whatsoever*.

If we do wish to assume spatial flatness the constraints on Ω_Λ improve of course: marginalising over H_0 we find a 2σ range of $[0.41, 0.74]$. $\Omega_\Lambda = 0$ is excluded at 98.8 per cent confidence, while for a shorter experiment duration of $\Delta t_0 = 25$ yr we can still exclude $\Omega_\Lambda = 0$ at 96.8 per cent confidence. Note that these latter values are not very much higher than in the general case above. The difference is of course that in the flat case the best fit along the $\Omega_\Lambda = 0$ axis is obtained for an unfeasibly low H_0 value of $h_{70} = 0.1$, while in the general case this value is 1. Hence, for flat cosmologies any external H_0 prior has a strong impact on the lower limit one can place on Ω_Λ, in contrast to the general case. For example, applying the relatively weak prior that H_0 is known to within ± 16 km s^{-1} Mpc^{-1} results in the rejection of $\Omega_\Lambda = 0$ at > 99.99 per cent confidence for any $\Delta t_0 > 12$ yr or, alternatively, for $\Delta t_0 = 15$ yr and any $t_{\rm int} > 1900$ h.

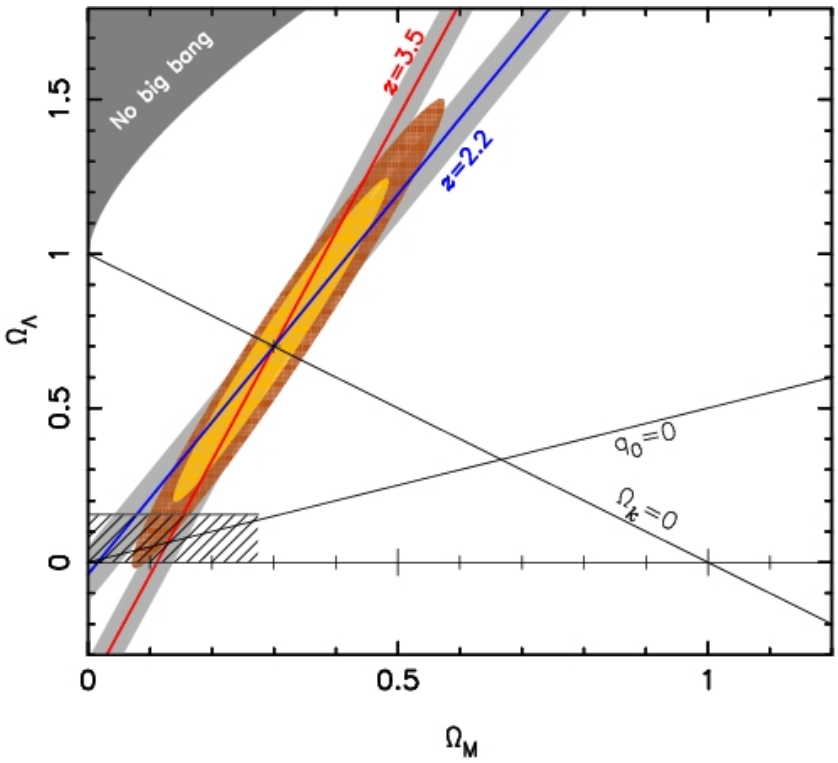

Figure 7: Expected constraints in the Ω_Λ-Ω_M plane from two measurements of the redshift drift at two different redshifts as indicated for a duration of the redshift-drift experiment of $\Delta t_0 = 30$ yr and a total integration time of 4000 h. The two measurements correspond to the brown triangles in Fig. 6. The red and blue solid lines and the grey shaded bands show the individual constraints provided by each of the two objects assuming a fixed $h_{70} = 1$. The coloured ellipses show the joint 68 and 90 per cent confidence regions that result from combining the two measurements, marginalising over H_0 using an external prior of $H_0 = (70 \pm 8)$ km s^{-1} Mpc^{-1}. The hashed region indicates the 95 per cent lower limit on Ω_Λ. Flat cosmologies and the boundary between current deceleration and acceleration are marked by solid black curves. The dark shaded region in the upper left corner designates the regime of 'bouncing universe' cosmologies which have no big bang in the past.

Finally, we make two remarks concerning the combination of $\dot{z}$ measurements with other cosmological observations: (i) the cosmological constraints provided by a redshift drift experiment will be unique and therefore new in the sense that they cannot be provided by any other cosmological observation. $\dot{z}$ probes $H(z)$ in a redshift range that is virtually inaccessible to other methods (such as SNIa, weak lensing) and this will remain true even in the ELT era. In terms of characterising $H(z)$, $\dot{z}$ measurements at $z \gtrsim 2$ will nicely complement the data at $z \lesssim 2$ provided by SNIa surveys. In the Ω_Λ-Ω_M plane these datasets offer similar but nevertheless distinct constraints. (ii) The datasets that are most complementary to the redshift drift in the Ω_Λ-Ω_M plane are those that constrain the geometry of the Universe, such as the fluctuation power spectrum of the CMB, which can break the remaining degeneracy in the $\dot{z}$ constraints. In fact, the WMAP 3-year data constrain the quantity $\Omega_\Lambda + 0.72\,\Omega_\mathrm{M}$ (Spergel et al. 2007), so that the CMB degeneracy line is almost exactly orthogonal to the $\dot{z}$ constraints shown in Fig. 7. Combining these constraints would lead to individual 2σ errors in Ω_Λ and Ω_M of ~ 0.08 and ~ 0.06, respectively.

References

Liske et al., "Cosmics dynamics in the era of extremely large telescopes", 2008, MNRAS, 386, 1192

Loeb A., 1998, ApJ, 499, L111

Pasquini et al., "CODEX: Measuring the Expansion of the Universe (and beyond)", 2005,ESO Messenger, 122, 10

Sandage A., 1962, ApJ, 136, 319

Technical Requirements

FOV	few arcsec
total energy in fibre	$\geq$ 80%
spectral resolution	$\geq$100 000
spectral sampling	$\geq$3
wavelength range (micron)	0.35 -0.67
wavelength accuracy	
RV stability	2 cm/s over 30 yr
throughput	$\gtrsim$0.2
typical magnitude	15-17
source size	point sources
minimum exposure time	photon noise limit (typically 15 min)
maximumm cumulative exposure time	a few hundreds of hours
target density	low
background	dark time
sky subtraction	yes
sky coverage	$\geq$ 90 % of available sky

The redshift drift experiment makes extreme demands regarding the precision, stability and efficiency of the spectrograph. The redshift drift experiment thereby relies heavily on the large E-ELT photon collecting area and a high throughput of $\geq 20\%$ to push the photon noise sufficiently below the signal to be measured. Note that an efficiency of $\geq 20\%$ is comparable or higher than what has been achieved for the best high-resolution spectrographs currently available. These are, however, located at the more luminous Nasmyth or Cassegrain focii, and have either lower resolution, or much lower radial velocity precision. Achieving the required efficiency is therefore a major challenge. It is of particular importance to push the low end of the instrument's wavelength range as blue as possible and to maintain a high throughput of $\geq 20\%$ as far into the blue as possible. Neither the protected aluminium/silver coating nor the bare aluminium coating are therefore ideal. The protected aluminium/silver coating is preferred because of its higher transmission over most of the relevant wavelength range. A higher transmission than offered by the protected aluminium/silver coating in the blue may, however, turn out to be crucial for establishing directly with the redshift drift experiment alone that the expansion of the Universe must indeed have started to accelerate.

For the expansion Show Case there are currently more bright targets known in the Northern Hemisphere. This is, however, entirely due to the larger area surveyed in the North. By the time the redshift drift experiment would be

performed this imbalance is unlikely to persist in light of major wide-area QSO surveys planned for the Southern Hemisphere and the large improvements expected in this respect due to GAIA.

We end here with reiterating that the requirements with regard to the radial velocity accuracy and stability of the spectrograph together with the large E-ELT collecting area and a high throughput of the telescope-Coudé-spectrograph system extending far into the blue are absolutely indispensable for the success of the redshift drift experiment.

Show Case 2: Earth twins in the Habitable Zone of solar-type stars[5]

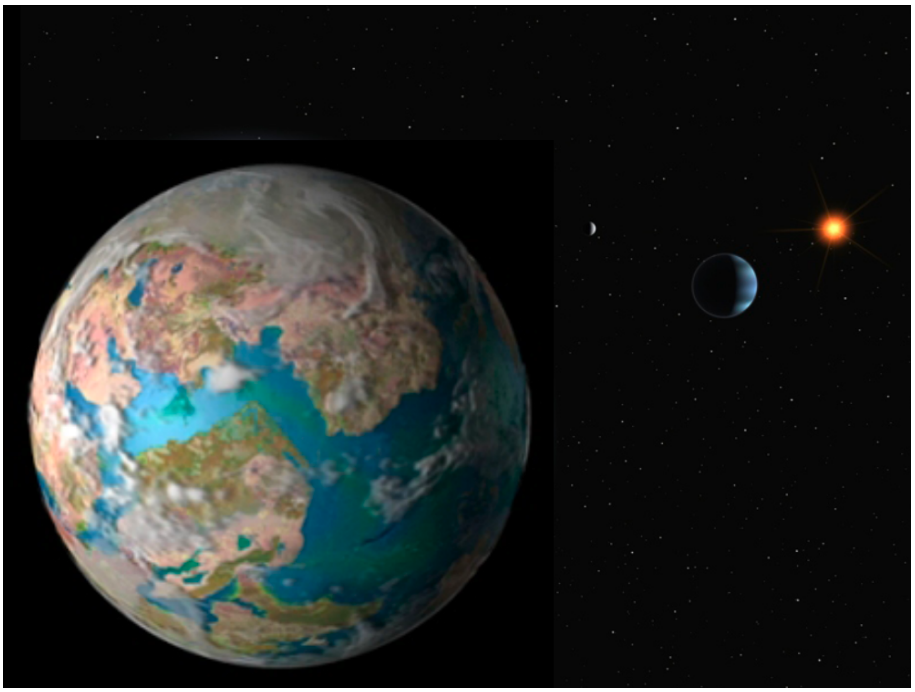

Figure 8: Artistic view of a planetary system including an Earth twin around a solar-type star.

2.2.1 Background

The question of the existence of other worlds has been asked in human history for millennia but it is only recently that scientific evidence has confirmed what many had anticipated: planets do exist and are common outside the Solar System. The discovery 14 years ago of an extra-solar planet orbiting the solar-type star 51 Peg (Mayor & Queloz 1995) has encouraged the launch of numerous new search programs, leading now to a steadily increasing number of exoplanet detections. More than 300 other planetary companions have been found to orbit dwarfs of spectral types from F to M, as well as more massive evolved stars. From this sample, we have learned that giant planets are common and that the planetary formation process may produce an unexpectedly large variety of configurations covering a wide range of planetary masses, orbital shapes, and planet-star separations. Figure 9 illustrates the large variety of the sample of known exoplanets in mass and separation.

The growing number of exoplanets has made possible a meaningful statistical analysis of their properties, as well as those of their host stars (see e.g. Udry & Santos 2007 for a review). These studies are providing important constraints on the physical and chemical processes involved in the formation of planetary systems. It is now known that planets can form far from their host stars, and later migrate inwards as a result of interactions with the proto-planetary disc or with other planets in the system. Giant planets are also known to be more easily found orbiting metal-rich stars, an indication that the giant planets are formed by accretion onto a core (the "core-accretion process"). In general, the diversity of observed planets can generally be explained as the result of a balance between the quantity of available material in the proto-planetary disk, the planet formation timescales, and the lifetime of the disk itself.

The large majority of the known exoplanets have been found due to the induced Doppler shift of spectral features in spectra of the primary star, the so-called radial-velocity (RV) technique. Because of the limitations inherent to the RV technique, most of the candidates detected so far are giant gaseous planets, similar in nature to Jupiter. However since 2004, research teams using the RV technique have been making the headlines several times for their discoveries of low-mass extrasolar planets, some of which having masses as small as a few times the mass of the Earth Fig. 9). ESO's HARPS spectrograph has played a key role in the discovery of low-mass planets with an impressive contribution to the detections of Neptune-mass planets and super-Earths. Sixteen out of twenty planets

[5]This showcase forms part of case S3 of the E-ELT Design Reference Mission.

known today with masses below 20 $M_\oplus$ have been discovered by HARPS. This new era started with the discovery of Ara c, a 10 $M_\oplus$ planet, by Santos et al. (2004) (see Pepe et al. 2007 for an update of the parameters). The recent detections of the planetary system HD 69830 containing three Neptune-mass planets (Lovis et al. 2006) and HD 40307 with its three Super-Earths (Mayor et al. 2009), illustrate the huge potential of HARPS-type instruments (Fig. 10).

The discovery of small-mass planets is especially important for the understanding of the formation and evolution of planetary systems. Five years of sub-m/s radial-velocity measurements of quiet stars in the HARPS-GTO planet-search programme have unveiled the tip of a large population of Neptune-mass and super-Earth planets at separations $\geq$ 0.3 AU around $\sim$30 % of G and K dwarfs in the solar neighborhood. This agrees well with planet population models (Mordasini et al. 2008, Ida & Lin 2008). These models moreover predict the existence of a large population of Earth-mass planets at all separations, many of them in the habitable zone (the region where a terrestrial planet can hold liquid water on its surface, Kasting et al. 1993) around stars. One of the main drivers of extrasolar planet searches is to understand the origin and the frequency of potentially life-bearing planets like the Earth. There is thus strong motivation to search for rocky planets orbiting within the habitable zones of their stars. The main obstacle to their discovery is the small amplitude of the radial-velocity signal (9 cm/s for the Earth-Sun system).

The high resolution and long-term stability of CODEX coupled with the large collecting area of the E-ELT will provide the possibility to measure stellar radial velocities with precision at the cm/s level, offering thus a unique opportunity to detect Earth twins around other stars. We discuss here some of the requirements to reach such an ambitious goal, and give some estimate of the telescope time needed to conduct a successful observational campaign.

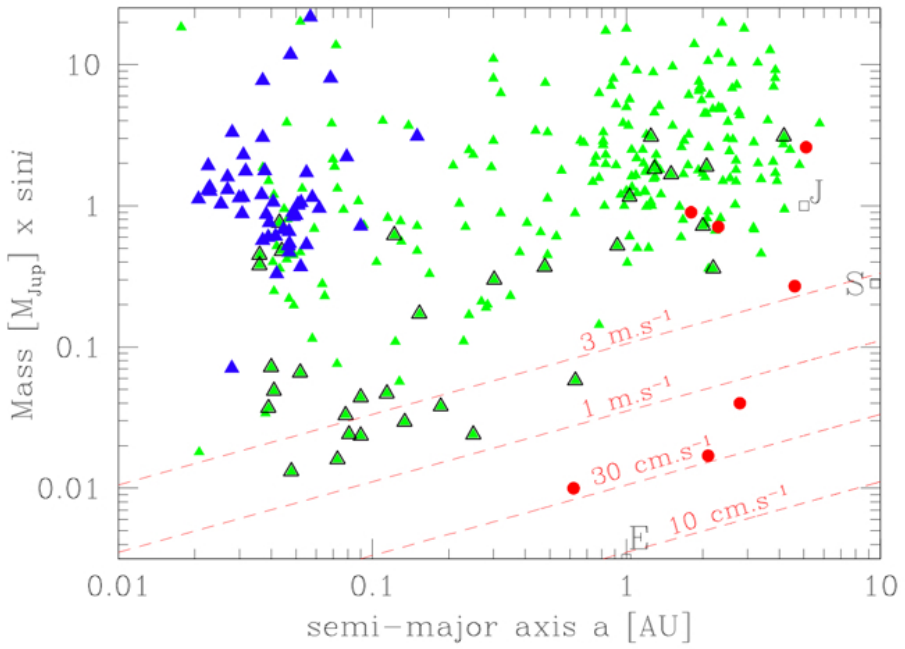

Figure 9: Mass-separation diagram of 300 known exoplanets. The triangles refer to exoplanets found by radial velocities. The dark triangles refer to transiting exoplanets. The circles refer to exoplanets found by microlensing. The bold triangles correspond to exoplanets discovered with HARPS. Lines of radial-velocity semi-amplitude of 3, 1, 0.3 and 0.1 m/s are shown, assuming a 1 $M_\odot$ primary star (from Bouchy et al. 2009).

2.2.2 Discovering Neptunes and super-Earths with radial velocities, the HARPS experience

The HARPS program at high precision.

Among the different surveys conducted as part of the GTO time of the HARPS consortium, the one aiming at finding the smallest possible exoplanets has been assigned the largest fraction of the observing time ($\sim$ 50 %). This "high-precision" HARPS-GTO program has been targeting close to 400 bright, non-active FGK dwarfs. These were mainly selected from the sample obtained from the volume-limited CORALIE search for planets to which

some stars with already known planets have been added. Figure 10 shows two examples of low-mass planetary systems from these surveys: HD 69830 (Lovis et al. 2006) and HD 40307 (Mayor et al. 2009). In both cases at least three low-mass planets have been found with minimum masses similar to or smaller than Neptune, five of these have masses below 10 $M_\oplus$. These "super-Earths" are probably mainly solid (icy and/or rocky). Other examples are HD 181433 with one super-Earth (7.6 $M_\oplus$) in a 3-planet system and HD 47186 with one Neptune-mass planet (22.8 $M_\oplus$) as well as a Saturn-mass companion (Bouchy et al. 2009). Undoubtedly, all these exciting discoveries are important steps towards the first detection of a true Earth twin.

After 5 years of observations, a lot has been learned about the RV behaviour of the stars surveyed by HARPS. The most stable systems exhibit RV dispersions at the level of ∼80 cm/s over several years, very close to the instrumental limits. Many others show variability at the 2-3 m/s level that often turns out to be due to orbiting low-mass planets. Most of these objects are actually found in multi-planet systems, leading to complex, low-amplitude RV curves. This is well illustrated by the HD 69830 and HD 40307 systems (Fig. 10). The total RV dispersion before fitting any Keplerian model amounts to 3.7 m/s for HD 69830 and 2.9 m/s for HD 40307. After fitting for the RV velocity of the clearly detected planets the rms dispersion of the residuals is only ∼0.8 m/s in both cases. This clearly demonstrates the need for sub-m/s precision and for a large number of measurements. Such characteristics of the RV curves were not anticipated and led to a change in observing strategy (Santos et al. 2004). The HARPS GTO team changed focus to a smaller sample of stars, gathering more measurements per star. In this way the cause of the RV variability can be identified more quickly and the planetary systems can be resolved more easily.

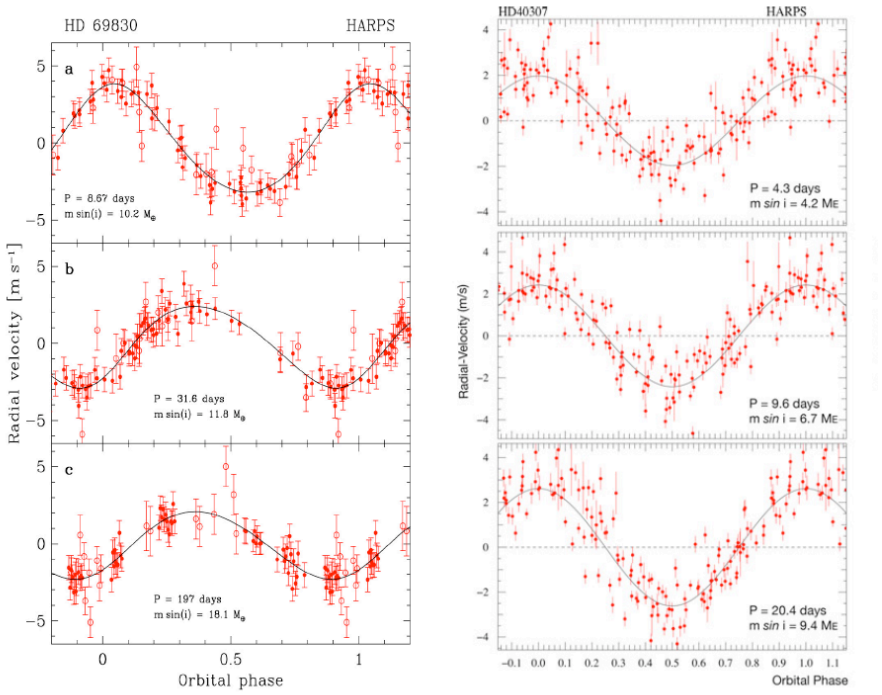

Figure 10: Examples of multi-planet systems detected with HARPS: three Neptunes in HD 69830 (Lovis et al. 2006) and three super-Earths around HD 40307 (Mayor et al. 2009).

An emerging population of Neptune-mass planets and super-Earths as a probe for the existence of Earth twins

Interestingly, the distribution of measured planetary masses appears to be bimodal (see Fig. 11). A new population of more difficult to detect low-mass planets has begun to emerge at Neptune- and super-Earth masses which appears not to be the low-mass tail of the mass distribution of giant gaseous planets. Preliminary results from the HARPS high-precision program suggest that the recently published discoveries only represent the tip of an iceberg. A very recent census of planetary candidates among stars of the "high-precision" GTO program has revealed about 45 pos-

sible low-mass planets ($m_2 \sin i < 30 M_\oplus$) with orbital periods of less than 50-60 days. About 30 % of solar-like stars with a large enough number of measurements to safely conclude on the existence of low-mass planets possess such close-in giants and super-Earths (Mayor et al. 2009). The mass distribution of these planet candidates confirms the trend seen in the published sample. These preliminary numbers strongly suggest the existence of a separate population of low-mass planets in the habitable zone. More than 80% of the planets are thereby in multi-planet systems. The discovery of similar small-mass objects at larger separations (a few AU) with the microlensing technique (e.g. Bennett et al. 2008) further suggests that the population of low-mass planets extends to larger separations. Interestingly this is in good agreement with the predictions of theoretical modeling of planet populations (e.g. Mordasini et al. 2008, Ida & Lin 2008; Fig. 11). The models are predicting the existence of a large population of even smaller-mass planets at all separations, among them a large fraction of Earth-like planets in the habitable zone. The model predictions are further strong motivation for programs aiming to detect potentially habitable planets.

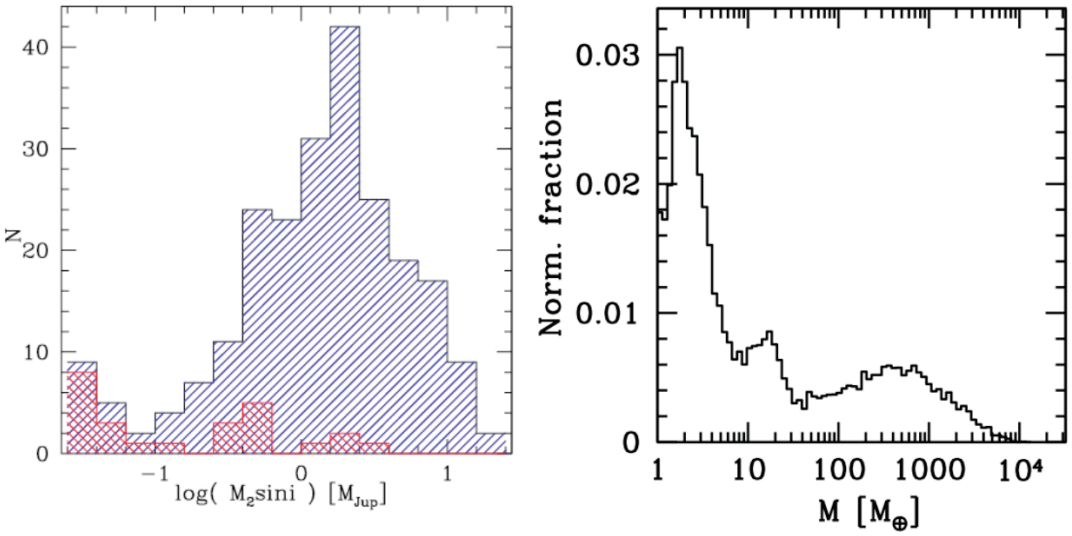

Figure 11: Mass distribution of known extrasolar planets (left). A new population has begun to emerge at low mass. Such a population was predicted by theoretical models of planet populations (right, from Mordasini et al. 2008).

2.2.3 Limitations: instrumental, photon, and stellar noise

The minimum mass detectable from radial-velocity measurements is directly proportional to the amplitude of the reflex motion of the primary star. The detection threshold is thus directly linked to the long-term radial-velocity precision. There are three categories of noise for such measurements: photon noise, instrumental noise, and astrophysical "noise". These are essentially independent from each other and should add in quadrature.

A) **Instrumental limitations.** The exciting results obtained with HARPS have motivated new studies aiming to push down further the precision of Doppler spectroscopy to reach the 1 cm/s level. The experience with HARPS suggests that this should indeed be possible provided that special attention is is given to the following (Pepe & Lovis 2008): i) spectrograph stability; ii) sufficiently high resolution (R > 150 000) to resolve the spectral lines (important to minimize line blends or characterize line shape variations); iii) adequate spectral sampling; iv)precise wavelength calibration; v) efficient image scrambling; vi) precise guiding and centering (rms < 0.02 arcsec). The CODEX design gives emphasis to all these important aspects.

B) **Contamination effects.** Contamination of the target spectrum by external sources also limits the precision of RV measurements, especially if the contaminant contains spectral features. Minimizing these effects leads to instrumental and target selection requirements. The most relevant of these are as follows.

- Light from a close-by object can contaminate the target spectrum. The atmospheric seeing and thus the level of contamination will thereby change from one observation to the next. As a rough estimate there should be a 7 to 10 magnitude difference between the flux of the target and that of the contaminant. High-resolution, high-contrast observations with instruments equipped with AO capabilities will be required to check for visible companions closer than typically 3 arcsec from the target.

- Light from the Moon and the Sun is another potential contaminant. For high-precision RV measurements, one would have to avoid: (i) twilight observations; (ii)observations during full moon, or when the target is too close to the moon; (iii)observations with cloudy sky and/or cirrus.

- Sky lines are yet another potential contaminant. Unfortunately, accurate modeling and removal of the spectral lines produced by the Earth's atmosphere is very difficult. Spectral regions with atmospheric lines brighter than 1/10000 of the spectral line of the observed science target need to be avoided for high-precision radial velocity measurements.

C) **Photon noise:** The uncertainty of the RV measurements due to photon noise scales inversely with the signal-to-noise ratio (S/N) of the spectra. With HARPS, it is possible to reach a precision of 1 m/s for a K dwarf with magnitude V=7mag in a 1 minute exposure. With the assumptions made for the CODEX ETC the photon noise error for a radial velocity measurement of the same star would be $\sim$4 cm/s after 1 minute (or the same 4 cm/s in 16 minutes for a V=10 star). There will thus be plenty of stars, bright enough, for photon-noise not to be a major limitation with CODEX at the E-ELT.

D) **Stellar jitter:** Besides instrumental, environmental and photon-noise other phenomena intrinsic to stellar atmospheres, have to be taken into account. We will call these effects "stellar noise" in the following.

P-mode oscillations. Stars with an outer convective envelope can stochastically excite p-mode oscillations at their surface through turbulent convection. These solar-like oscillations have typical periods of a few minutes in solar-type stars and typical amplitudes per mode of a few tens of cm/s in radial velocity (e.g. Bouchy & Carrier 2001, Kjeldsen et al. 2005). The observed signal is the superposition of a large number of these modes, which may cause RV variations up to several m/s. Amplitudes of the RV variations become larger for early-type and evolved stars. Low-mass, non-evolved solar-type stars are therefore easier targets for planet searches. However, even in the most favourable cases, it remains necessary to average out this signal to achieve high precision for radial velocity measurements. This can be done by integrating over a few oscillation periods. Usually, an exposure time of 15 min is sufficient to decrease this source of noise well below 1 m/s for dwarf stars. Estimates based on stellar asteroseismology models show that for the most quiet stars, it is possible to reduce the remaining radial velocity perturbations below 10 cm/s in about 20-30 minutes (Eggenberger P., private comm).

Granulation and super-granulation. Granulation is the photospheric signature of the large-scale convective motions in the outer layers of stars with convective envelopes. The granulation pattern is made of a large number of cells with upward and downward motions tracing the hot matter coming from deeper layers and the matter cooling at the surface (Fig. 12). On the Sun, typical velocities of these convective motions are 1-2 km/s in the vertical direction. However, the large number of granules on the visible stellar surface ($\sim 10^6$) efficiently averages out these velocity fields, leaving some remaining "jitter" at the m/s level for the Sun, probably less for K dwarfs (e.g. Pallé et al. 1995, Dravins 1990). The typical timescale for the evolution of granules is about 10 minutes for the Sun. On timescales of a few hours to about one day, other similar phenomena occur, called meso- and super-granulation. These are thought to be due to larger convective structures in the stellar photosphere that may induce additional stellar noise, similar in amplitude to the granulation itself. Granulation-related phenomena represent a significant noise source when aiming at sub-m/s RV precision, and observing strategies must aim to minimize their impact.

Magnetic activity. Magnetic phenomena at the surface of solar-type stars induce radial-velocity variations through the temporal and spatial evolution of spots, plages, and convective inhomogeneities (Saar & Donahue 1997; Saar et al. 1998). When the star spot pattern is long-lived, variations of asymmetries in line profiles are modulated by the rotational period of the star and can mimic a planetary signal (e.g. Queloz et al. 2001; Bonfils et al. 2007). When the star is observed longer than the typical lifetime of star spots, the signal becomes incoherent and is detected as radial-velocity noise, potentially limiting the detection of the radial velocity signature of planets. Typical values of stellar jitter are below 1 m/s for slowly rotating, chromospherically quiet G-K dwarfs (Mayor et al. 2009). How small or large the stellar-induced velocity jitter for the most quiet stars suitable for planet searches actually is is not known yet. The distribution of the velocity rms in the HARPS high-precision programme peaks at 1.4 m/s but note that this includes all sources of noise discussed above, instrument and photon noise, stellar jitter, as well as undetected planets.

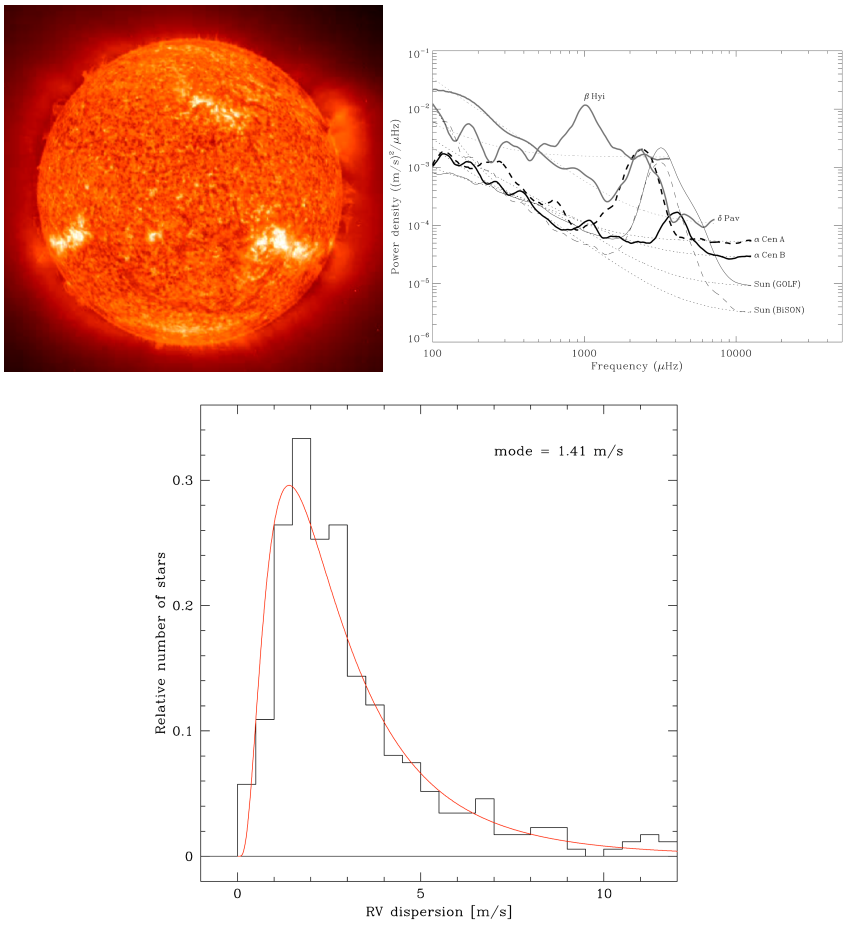

Figure 12: *Top left.* Granules at the surface of the Sun. The small scale granular pattern is evolving on a time scale of about 10 minutes. Larger scale patterns (meso- and super-granulation) evolve on longer time scales (several hours). *Top right.* Frequency structure of the radial-velocity jitter observed on several solar-type stars (from Kjeldsen et al. 2005). Envelopes of p-modes are prominent at the milli-Hertz level whereas power due to granulation and activity-related effects is growing towards lower frequencies. *Bottom.* Distribution of the raw radial-velocity dispersion for the stars in the HARPS high-precision sample. The rms includes all possible sources of ”noise”: instrumental, photon noise, stellar jitter, as well as still undetected low-mass planets. The low value of the mode around 1.4 m/s suggests that prospects for major improvements with CODEX are excellent.

2.2.4 Timescales of intrinsic variations and optimal observing strategy

Doppler spectroscopy has reached neither its instrumental nor its astrophysical limits. Stellar noise is potentially a major limitation. However, so far clever observing strategies have made it possible to avoid its detrimental effect. We will discuss now several of these in turn.

P-mode oscillations. Solar-like p-mode oscillations are clearly detected with HARPS. As already mentioned with HARPS it is possible to reduce the associated noise by integrating the signal over 10-15min. For HARPS observations of late-G and K dwarfs this reduces the residual noise below $\sim$20 cm/s. For CODEX we anticipate that the noise level will be reduced further to a few cm/s for integration of 20-30min.

Stellar granulation and stellar activity. On intermediate and long time scales, RV measurements are affected by stellar granulation and stellar activity, respectively. A strategy aiming at statistically averaging the perturbing effects is possible with enough observations covering a span larger than the typical time scale of the effects (hours or stellar rotation period). Simulations are needed to quantify the amount of observations required to reach a given level of precision. As a rough estimate one can assume that the residual noise will decrease inversely with the square root of the number of measurements.

For the impact of stellar oscillations and granulation, this has been recently investigated by Dumusque et al.

(in prep). Based on publicly available HARPS radial-velocity measurements for 6 stars (β Hyi, δ Eri, α Cen B, τ Ceti, μ Ara and α Cen A), they generated synthetic high-frequency observations using models of the stellar noise in Fourier space (Fig. 13, top left panel). The rms of the synthetic velocities were then calculated and binned according to different observing strategies (top right panel). In this way the authors derived detection limits in the planet mass-separation plane for each strategy. For a given planet mass, the detection limit depends only weakly on the period. For longer periods, the lower amplitude of the RV signal is compensated by larger temporal bins used for the averaging. The lower panels of Figure 13 illustrate this. For a quiet K V star like α Cen B and with the suggested observing strategy, it would be possible to detect planets with 5-6 times the mass of Earth with an orbital period of 200-330 days, residing in the habitable zone. The estimates include instrumental errors (centering and guiding effects) for HARPS and a contribution from photon noise. These would obviously improve for a more stable instrument like CODEX.

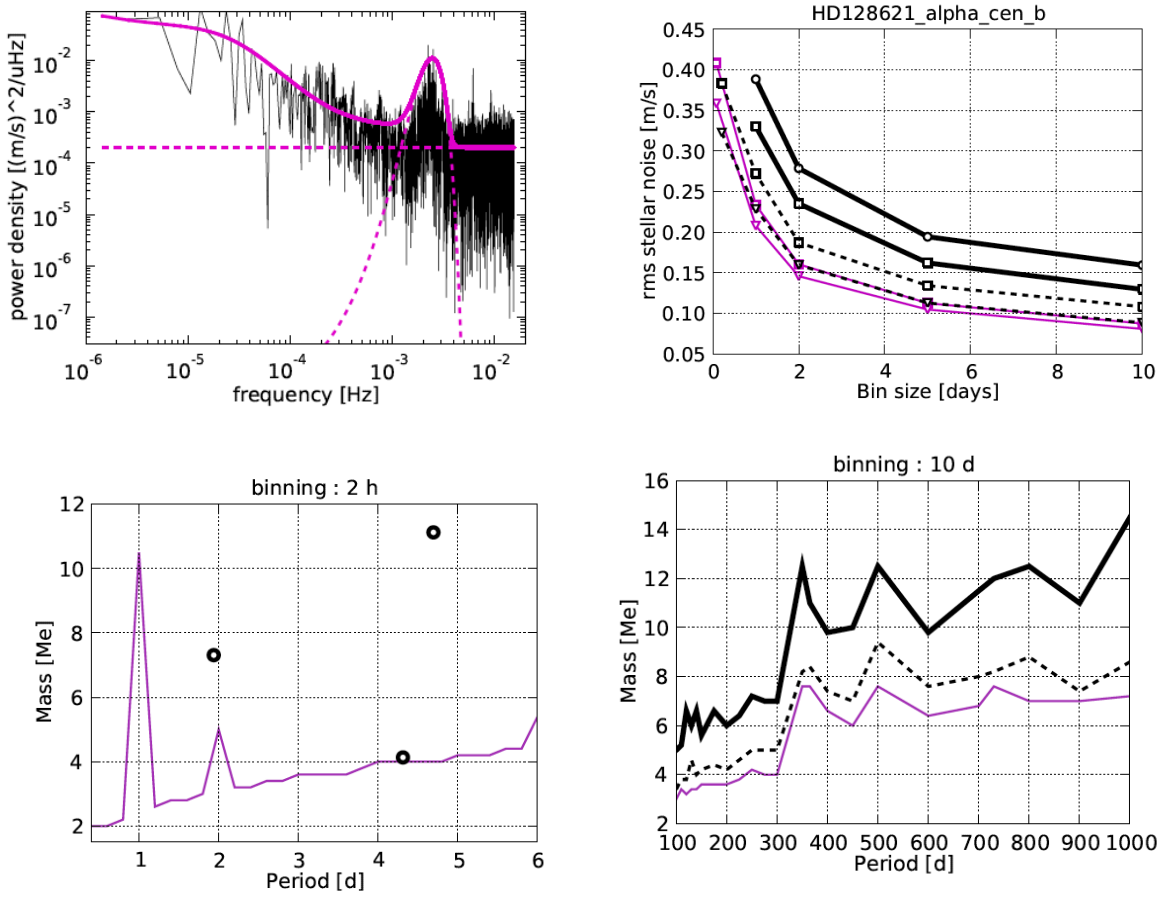

Figure 13: Estimates of planet detection limits in the mass-period diagram for stars of different levels of activity. The estimates have been obtained from numerical simulations based on actual HARPS asteroseismology measurements used to model the observed stellar noise of the stars (see text). *Top left.* Example of the observed frequency structure of the stellar noise superimposed with the corresponding model (α Cen B case). *Top right.* rms of the velocities of the model data for different binning laws. *Lower panels.* Model estimates of planet detection limits in the mass-period diagram for 6 observed stars. Note that the detection limit does depend little on the period as for longer periods the velocities can be averaged into "larger" temporal bins. Open circles represent actual HARPS detections of low-mass planets.

Quiet G-K dwarfs exhibit a jitter level well below 1 m/s (Pepe & Lovis 2008). The lowest level for the quietest stars is not known. The minimum value observed with HARPS is at the level of the instrumental limitations. Binning the observations over time scales comparable to the rotational periods of the stars permits to significantly average out stellar noise. A precision of 35 cm/s has already obtained for a few test cases as e.g. HD 69830 (Lovis et al. 2006). Further work will be needed to quantify the ultimate limitation imposed by stellar activity.

2.2.5 From HARPS via ESPRESSO to CODEX

We have discussed the main limitations for the precision of RV measurements in the last two sections. We will now turn to the improvements we can expect regarding the detection of low-mass planets as we progress from HARPS at the La Silla 3.6m via ESPRESSO at the VLT to CODEX at the E-ELT. Let us first assume that the observational strategy reduces the stellar noise below the instrumental and photon noise and that the stellar noise can be neglected. Fig. 14 compares the planet population which is then expected to be detected by HARPS, ESPRESSO, and CODEX as the instrumental limit for the radial-velocity precision is improved from 1 m/s to 10 cm/s, and to 1 cm/s. A RV semi-amplitude of the planet being equal to twice the precision is thereby set as a conservative detection criterion. The figure is based on the predictions of the planet formation models of synthetic planetary populations by the Bern group for solar-mass stars (Mordasini et al. 2009). The models follow the evolution and growth of small-mass seeds in a gaseous disk until the gas has disappeared leaving behind planets of various masses and separations to the central star. The Figure very clearly demonstrates that CODEX at the E-ELT (precision well below 10 cm/s is required to detect Earth-mass planets at separation of $\sim$1 AU from solar-type dwarfs. It further suggests that the expected number of such planets will be large. The model estimates are likely to be a lower limit as terrestrial planets should also form from collisions of large planetesimals on longer time scales, a path which is not included in the models.

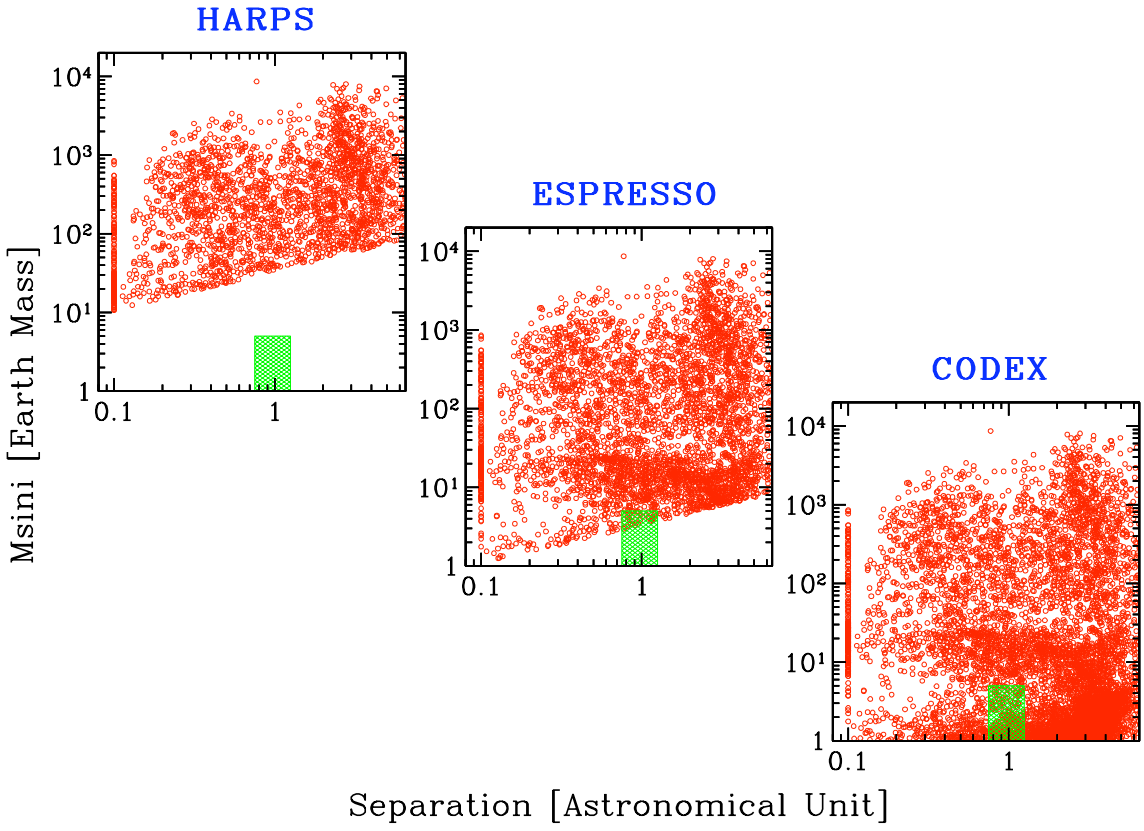

Figure 14: Expected planet population at separations of $\sim$ 1AU to be detected by Doppler spectroscopy with the HARPS/3.6m (precision of 1 m/s; left), ESPRESSO/VLT (precision of 10 cm/s; middle) and CODEX/E-ELT (precision of 1 cm/s; right) spectrographs, after applying observational limits for radial-velocity measurements on the predictions of planet population synthesis models. The detection criterion is set as the RV semi-amplitude being equal to twice the precision. The figures are based on the predictions of the planet formation models for solar-mass stars by the Bern group (Mordasini et al. 2009). Note that we have assumed that the stellar noise has been reduced to below the instrumental noise by suitable averaging (see text). From the figure, it clearly appears that a spectrograph like CODEX is required to detect Earth-like planets in the habitable zone of solar-type stars (colored square area) and that we can expect to detect sizable samples of such planets.

2.2.6 Searching for Earth twins in the Habitable Zone of solar-type stars with CODEX

Target sample and observing time requirement

We will now discuss a possible target sample and the observing time requirements for a realistic observing campaign with CODEX. The choice of individual exposure times is determined by the necessity to reduce the stellar noise. The requirement to stay 20 or 30 minutes on the target translate into a magnitude limit. To be definite we assume that we want to achieve a residual noise level of 4 cm/s (safely above the expected instrumental errors) For a sample of stars with V$\leq$10.5 the photon noise of a 20-30 minutes exposure will be sufficiently low not to dominate the RV measurement error. In the HARPS GTO study of a volume-limited sample of stars 10 % of all stars where found to show little activity. There are hundreds of non-active late G to K dwarfs with V$\leq$ 10.5 which are suitable for the search of an Earth twin. Even if part of this sample has to be rejected because of contamination or the presence of a secondary star, or due to longer-term magnetic-cycle effects, the remaining number of suitable targets will exceed by far the number of stars that can be monitored with the E-ELT in a reasonable amount of observing time. Availability of suitable targets should thus not be a limiting factor.

An optimized survey will require 3 to 4 observations of a given star per night, repeated every day (or every other day) during an observing run (of e.g. 10 days), and with regularly scheduled runs (once a month) over the visibility period of the star (8 months per year). Such an observational strategy requires thus typically a minimum of $\sim$100 individual observations per star, per year, which corresponds for an exposure time of 20 minutes and overheads of 5 minutes to 42 hours per year per star. Good candidates will need to be followed over at least 2 variation periods (i.e. about 2 years) to confirm a potential detection. Each star will thus require 84 hours of observation in total. The total required observing time will scale accordingly with the size of the sample which will be determined by the scientific questions/objectives the observing campaign aims to answer.

Scientific objectives

The scientific objectives of a search for Earth-mass planets in the habitable zones of their parent stars are truly exciting. The detection of a sizeable sample of such planets will

- hopefully prove the existence of planets similar to the Earth and determine the frequency of Earth twins around nearby stars,
- determine statistical properties of low-mass planets and give priceless constraints for planet-formation models,
- characterize the multiplicity of planet systems with Earth twins,
- and build-up a list of suitable targets for future space missions aiming at characterizing the atmosphere of potentially habitable planets in search for tracers of life.

With CODEX on the E-ELT we should be able to answer the long-standing question of the existence of other planets similar to our own on which – at least in principle – life could develop.

References

Bennett et al., " Low-Mass Planet with a Possible Sub-Stellar-Mass Host in Microlensing Event MOA-2007-BLG-192", 2008, ApJ 684, 663

Bonfils et al., "The HARPS search for southern extra-solar planets. X. A $m \sin i = 11\,M_\oplus$ planet around the nearby spotted M dwarf GJ 674", 2007, A&A 474, 293

Bouchy F., Carrier F., "P-mode observations on ? Cen A", 2001, A&A 374, L5

Bouchy et al., "The HARPS search for southern extra-solar planets. XVII. Super-Earth and Neptune-mass planets in multiple planet systems HD47186 and HD181433", 2009, in press (arXiv:0812.1608)

Dravins D., "Stellar granulation. VI - Four-component models and non-solar-type stars", 1990, A&A 228, 218

Ida S., Lin D., "Toward a Deterministic Model of Planetary Formation. IV. Effects of Type I Migration", 2008a, ApJ 673, 487

Ida S., Lin D., "Toward a Deterministic Model of Planetary Formation. V. Accumulation Near the Ice Line and Super-Earths", 2008b, ApJ 685, 584

Kasting et al., "Habitable Zones around Main Sequence Stars", 1993, Icarus 101, 108

Kjeldsen et al., "Solar-like Oscillations in ? Centauri B", 2005, ApJ 635, 1281

Lovis et al., "An extrasolar planetary system with three Neptune-mass planets", 2006, Nature 441, 305

Lovis et al., "An emerging new population of Neptune-mass and super-Earths planets", 2008, in IAU Symp 253 on Tranisiting planets, 2009, in press

Mayor M., Queloz D, "A Jupiter-Mass Companion to a Solar-Type

Star", 1995, Nature 378, 355
Mayor et al, "The HARPS search for southern extra-solar planets. XIII. A planetary system with 3 super-Earths (4.2, 6.9, and 9.2 $M_{\oplus}$)", 2009, A&A 493, 639
Mordasini et al. "Giant Planet Formation by Core Accretion", 2008, in Extreme Solar Systems, ASP Conference Series, Vol. 398, 235
Mordasini et al. "Extrasolar planet population synthesis I: Method, formation tracks and mass-distance distribution", 2009, A&A submitted
Noyes et al., "Rotation, convection, and magnetic activity in lower main-sequence stars", 1984, ApJ 279, 763
Pallé et al., "A measurement of the background solar velocity spectrum", 1995, ApJ 441, 952
Pepe F., Lovis C., "From HARPS to CODEX: exploring the limits of Doppler measurements", 2008, Physica Scripta, Vol 130, 14007
Pepe et al., "he HARPS search for southern extra-solar planets. VIII. μ Arae, a system with four planets", 2007, A&A 462, 769
Queloz et al., "No planet for HD 166435", 2001, A&A 379, 279
Saar S., Donahue R., "ctivity-related Radial Velocity Variation in Cool Stars", ApJ 485, 319
Saar et al., "Magnetic Activity-related Radial Velocity Variations in Cool Stars: First Results from the Lick Extrasolar Planet Survey", 1998, ApJ 498, L153
Santos et al., "The HARPS survey for southern extra-solar planets. II. A 14 Earth-masses exoplanet around μ Arae", 2004, A&A 426, L19
Udry S., Santos N.C., "Statistical properties of exoplanets", 2007, ARA&A 45, 397
Wright et al., "Chromospheric Ca II Emission in Nearby F, G, K, and M Stars", 2004, ApJS 152, 261

Technical Requirements

FOV	few arcsec
minimum energy in fibre	$\geq$ 80 %
spectral resolution	$\geq$ 150 000
wavelength range (micron)	0.38 -0.68
spectral sampling	$\geq$4
wavelength accuracy	
RV stability	2-5 cm/s over 10 yr
typical magnitude	$<$ 11
source size	point sources
minimum exposure time	typically 15 min
maximum cumulative exposure time	few tens of hours
target density	low
background	grey
sky subtraction	yes
sky coverage	$\geq$ 90%

The planet search makes extreme demands with regard to precision, stability and resolution of the spectrograph. The throughput gain of the protected silver/aluminium coating compared to the Al coating is of course beneficial, but we stress that it is not critical for the Earth twins programme and its bright targets and the aluminium coating would not have any significant negative impact on this programme. Sufficiently large samples of targets are in principle available in both hemispheres. Target selection is nevertheless a critical aspect for discovering Earth twins. Pre-existent high-precision radial-velocity data will be necessary to select low activity, slowly rotating solar-type stars and to discard targets hosting more massive planets. Most of this data will most likely have been taken with HARPS and hopefully ESPRESSO. A site located in the Southern Hemisphere (or a site from which a significant fraction of the Southern Hemisphere can be observed at low airmass) is thus favourable. Note, however, that this imbalance may become less relevant with HARPS-NEF – a "copy" of HARPS to be built for the WHT.

Show Case 3: Galactic Archaeology: Unraveling the assembly history of the Milky Way with nucleochronometry

2.3.1 Introduction

To understand how galaxies were assembled is one of the key questions of modern astrophysics. Cosmological numerical simulations have taught us a lot how this should happen through hierarchical merging in the context of a ΛCDM cosmology. Observationally we still have few constrains on this phenomenon, even for the Milky Way. One of the key physical parameters to be determined are the time-scales on which the different pieces of a galaxy are assembled. The Milky Way consists of four components: Halo, Bulge, Thin Disc and Thick Disc. The absolute and relative ages of these components and the time interval for the formation of each of them are subject to very active research and are in fact one of the main objectives of the GAIA satellite (Turon et al. 2008). The accurate parallaxes measured by GAIA will allow to construct Hertzsprung-Russel diagrams for the different populations in the components of our Galaxy. Comparison of these diagrams with theoretical isochrones will allow to determine ages.

Radioactive dating, which has been termed nucleocosmochronometry, offers an exciting independent avenue to age determinations. The basic technique is the same as used for dating meteorites (Tilton, 1988) or stars (Butcher, 1987) and relies on comparing the present abundance ratios of radioactive and stable nuclear species to the ratios predicted for their production. The only radioactive nuclei with a sufficiently long lifetime for astronomical applications, and relative ease of observation are ^{232}Th (mean lifetime 20.3 Gyr) and ^{238}U (mean lifetime 6.5 Gyr).

We will explain here, why a spectrograph like CODEX at the E-ELT is needed to bring this technique to full fruition. Existing or planned facilities on existing 8-10m class telescopes do provide some useful information, but only an instrument like CODEX can lead to an accurate radioactive dating of stars throughout the Galaxy. The use of an E-ELT for this purpose is in fact one of the recommendations of the ESA-ESO Working Group on Stellar populations (Turon et al. 2008).

2.3.2 Radioactive dating

The technique.

A sample of radioactive nuclei decays exponentially with time. If the the *mean lifetime* (τ) and the initial and present number of nuclei are known, one can obtain the time interval that has elapsed since the nuclei were produced. In practice one measures the present number of nuclei of the unstable species (n_X) relative to the number of nuclei of a stable element (n_R) which is related to the number of unstable nuclei initially produced (n_{X0}).

To determine ages, the two nuclei are assumed to have a common nucleosynthetic origin and that n_{X0} is simply proportional to the number of nuclei of the stable species, n_R. The proportionality constant is called the "production ratio" and is usually given the symbol β.

It can be shown (Ludwig et al. 2009) that the uncertainty on the radioactive age $\sigma(t)$ is related to the uncertainty in the abundances of the radioactive and reference elements by,

$$\sigma(t) = \tau \ln 10 \left\{ \sigma^2[\log \beta] + \sigma^2[A(X)] + \sigma^2[A(R)] \; - \; 2\,\sigma[A(X)]\;\sigma[A(R)]\;\mathrm{Cor}\,[A(X), A(R)] \right\}^{1/2},$$

where $\mathrm{Cor}\,[.,.]$ denotes the linear correlation coefficient. In deriving the above equation it was assumed that β is uncorrelated with A(X)[6] and A(R). We shall ignore here the error for β assuming that future advances in the theory of the $r-$process will make this term negligible with respect to the errors for the abundances. The covariance term tells us that correlation between errors for the element abundance may help us in reducing the total error. This is indeed the case, since in practice the radioactive elements (Th and U) and the reference elements (Eu, Hf,...) are observed as ionised species and have similar line formation properties. This means that abundance errors due to inaccurate atmospheric parameters ($T_{\rm eff}$, $\log g$,...) cancel out to a large extent when abundance ratios X/R are considered. We can thus estimate the abundance errors as being due to only the "observational error" and ignore the uncertainties in atmospheric parameters and the covariance term. If we further assume that the abundance errors for the radioactive and stable element are roughly equal, the above equation simplifies to

$$\sigma(t) \sim \tau \ln 10 \left\{ 2\sigma^2[A(X)] \right\}^{1/2}.$$

[6] We use the usual spectroscopic notation A(X) = log(X/H)+12.

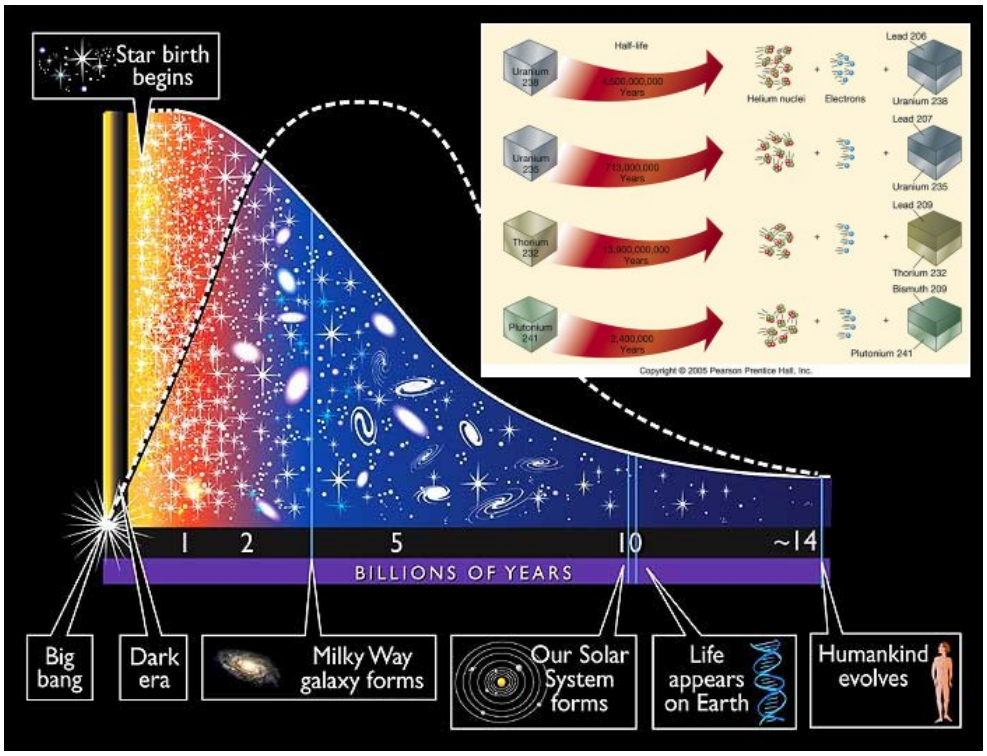

Figure 15: Probing the Milky Way with Galactic Archaeology

For Th the mean lifetime is $\tau = 20.3\,\mathrm{Gyr}$. Assuming an error for the abundance of 0.03 dex translates into an error of $\sim 2\,\mathrm{Gyr}$ for the age of an individual star. This is only slightly larger than the errors for age estimates obtained by using stellar evolution theory for open clusters (Grundahl et al. 2008).

Current status of radioactive dating of stars.

Age determination for stars in the Galactic disc based on observations of Th have been performed by Butcher (1987) and more recently with the use of sophisticated chemical evolution models by Del Peloso et al. (2005). There are, however, severe limitations to the current studies: *i)* the studies rely on a *local* sample of stars and it is mandatory to determine the age of more distant portions of the disc; *ii)* the error for the abundance ratios of individual stars is about 0.15 dex, clearly sub-optimal in view of what we discussed in Sect. 3.2.1 .

For the Galactic halo the measurement of the Th abundance in giant stars with metallicities down to ~ -2.5 was first performed by François et al. (1993). Later on it was realized that the Th II 401.9 nm line in cool giants can be blended with a ^{13}CH line (Norris et al. 1997, Bonifacio et al. 1998). The use of Th for radioactive dating thus requires a careful determination of the abundance of carbon and oxygen (the carbon abundance is linked to the oxygen abundance via the formation of the CO molecule) and of the isotopic ratio of carbon. More recent measurements (Johnson & Bolte 2001, Honda et al. 2004) have taken this into account. Measurements have, however, been only been made for a handful of stars. Accurate measurements were possible only in cases where the Th abundance was enhanced by at least a factor of two relative to other metals. The Th line then stands out with respect to the blending lines of the iron-peak elements Co and V. The increased sensitivity to weak absorption features of CODEX will lead to a major improvement in the determination of Th abundances. It will become possible to measure Th in extremely metal-poor stars and in stars in which Th is not enhanced relative to Fe.

Considerable attention has been given in recent years to r-enhanced stars. In 1994 Sneden et al. discovered that the abundances of the very metal-poor giant CS 22892-052 show big enhancements in the r-process elements. In 2001, Cayrel et al. discovered another such star, CS 31082-001, for which uranium was measured for the first time in a metal-poor star. The HERES project (Christlieb et al. 2004, Barklem et al. 2005) , was specifically designed to discover more of these r-process-element enhanced metal-poor stars (r-enhanced stars, for short), and succeeded in discovering a further 41 such stars. Up to now uranium has been measured, only in three r-enhanced stars, CS 31082-001, BD +17°3248 and HE1523-0901. The resonant UII line in spectra of two of these stars is shown in Fig. 16. The majority of the other r-enhanced stars is fainter than these three stars. This makes an accurate abundance measurements difficult. In some cases, like CS 22892-052, the measurement has been impossible due to

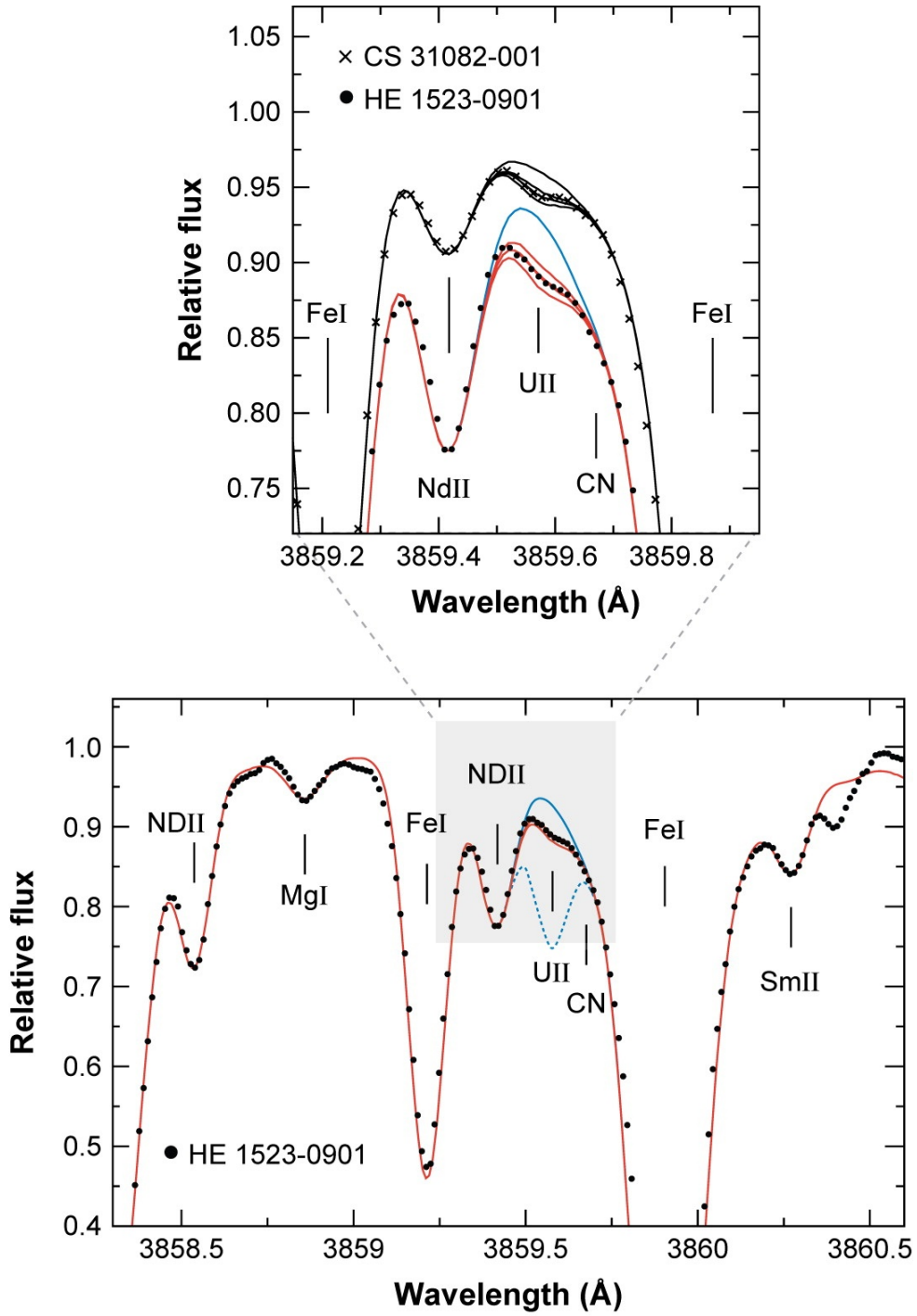

Figure 16: The U II 385.9 nm resonance line in the two metal-poor r-enhanced giants CS 31082-001 (Cayrel et al. 2001) and HE 1523-0901 (Frebel et al. 2007). To date the only two objects in which it has been possible to use the U/Th chronometer.

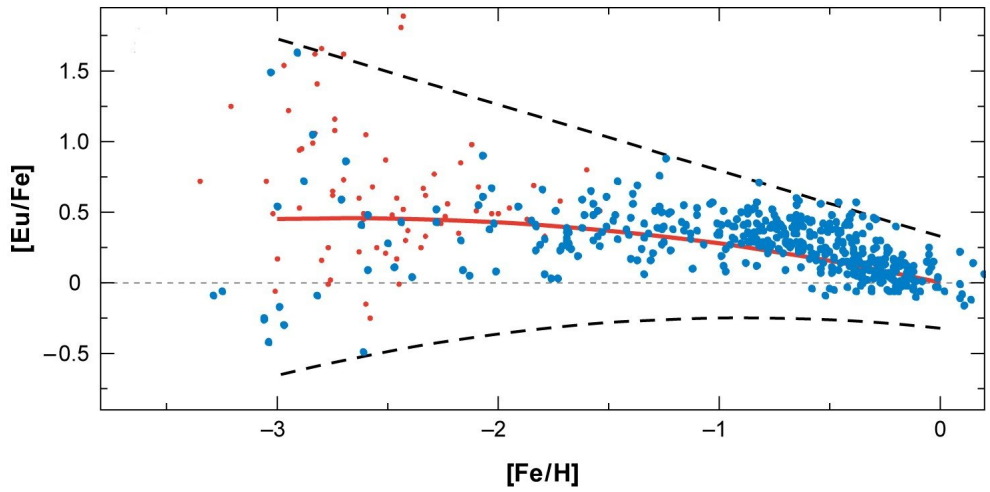

Figure 17: The evolution of Eu with metallicity (from the review of Sneden et al. 2008). The large scatter is due to the inhomogeneity of the Galaxy, not to observational error. The average [Eu/Fe] is clearly larger than zero. The evolution of Th at low metallicities is not known, but since both Eu and Th are pure r-process elements it is reasonable to expect a similar evolution.

a high carbon-enhancement. Some stars like CS 31082-001 have been suggested to have an "actinide boost", which may be the result of fission recycling (Schatz et al. 2002). Such an "actinide boost" can reconcile discrepancies between the ages derived from Th/U and Th/stable and U/stable ratios.

r-enhanced stars are clearly very interesting targets for a determination of radioactive ages. They are, however, very rare and do not represent more than 5% of the stellar population of the Galactic halo (François et al. 2007). Only for a subset of these it is possible to measure Th and U. We also need to better understand the nucleosynthesis in these stars, since their production ratios might be different from those appropriate for non r-enhanced stars. Note that the number of known r-enhanced stars can, however, be expected to grow substantially due to the great effort which is currently going into the discovery and study of metal-poor stars.

2.3.3 Difficulties of the radioactive dating.

Galactic evolution of Th and U

Unfortunately the Galactic evolution of Th and U is poorly known, especially at low metallicities. If the Th/Fe and U/Fe ratios were decreasing with decreasing metallicity, as is the case for Sr/Fe, measurements at low metallicity would become extremely difficult. It appears. however, reasonable to assume that this is – as for the pure r-process element Eu – not the case. The average Eu/Fe ratio is larger than solar in metal-poor stars (Fig. 17).

Atomic and molecular data.

The oscillator strengths of the relevant transitions of Th and U are known with reasonable accuracy. Unfortunately the same cannot be said for blending atomic and molecular features. In particular for the Th II 401.9 nm line there is a ^{13}CH line for which neither the wavelength nor the oscillator strength are well known. In the case of the U II 385.9 nm line there is a blending CN line as well as a strong Fe I line to the red (see Fig. 16) for which accurate oscillator strengths and damping constants are missing. However, by the time CODEX would be operating these should be known with sufficient accuracy due to better experimental determinations or theoretical calculations.

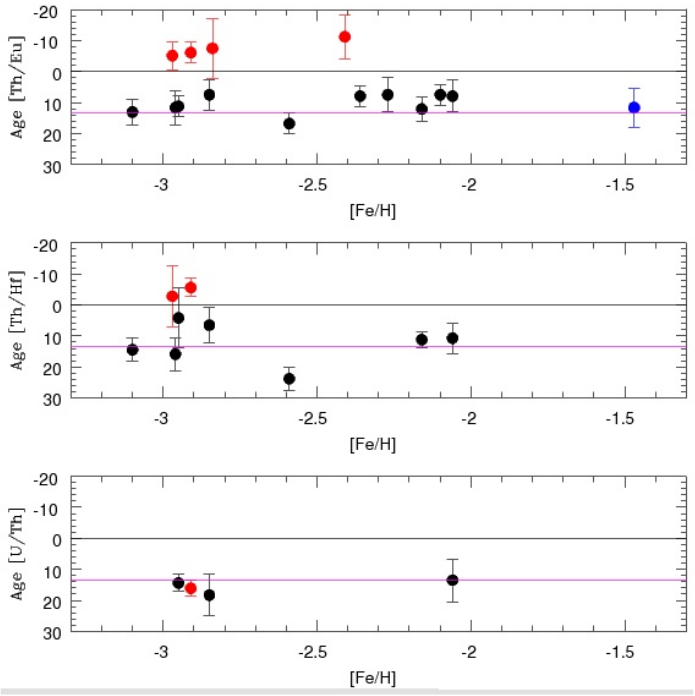

Figure 18: Radioactive ages from different pairs of lines used for the chronometry. Note the different behaviour of actinide-boosted stars with respect to the non actinide-boosted. (Courtesy of V. Hill)

Production ratios.

At present another weak point of radioactive dating are poorly known production ratios. Figure 18 shows how different line pairs used for the nucleochronometry can suggest different ages and how in actinide boosted stars ratios such as Th/Eu or Th/Hf can provide substantially wrong ages. The age estimates for well studied stars may span a range of 10–15 Gyr depending on the line pair and on the assumed production ratios (figures 2 and 3 of Ludwig et al. 2009). Our present knowledge of the r-process is still rudimentary, but the field is very actively working on remedying this. This includes theoretical modeling as well as laboratory measurements of relevant nuclear cross sections. Observations of stars and meteorites provide increasingly useful constraints on the production ratios. Observations of Th and other neutron capture ratios in Globular Clusters with well known ages from main sequence fitting or white dwarf cooling will provide strongly improved constraints on the production ratios. The globular clusters M15 (Sneden et al. 2000) and M4 and M5 (Yong et al. 2008) already provide a good starting point. All three clusters are r-enhanced, which makes the measurement of Th easier. In the coming years more GCs will be investigated in this way. It appears reasonable to assume that the combined efforts will lead to accurate production ratios by the time CODEX will be operating.

2.3.4 The role of CODEX

The Galactic Halo.

The age of the Galactic halo is currently best constrained by the ages of the Globular Clusters, which can be determined in several ways. Main sequence fitting and the white dwarf cooling sequence are probably the most accurate methods. The oldest globular clusters are determined to have an age of ~ 13.8 Gyr while some clusters appear to be 2 to 3 Gyr younger (Gratton et al. 2003). The best age determinations have an accuracy of ~ 1 Gyr. Note, however, that for the same Globular Cluster, age determination which differ by several Gyr can be found in the literature, even if the the same technique (e.g. MS fitting) but different photometry, reddening, metallicity and theoretical isochrones are used.

The most metal-poor Globular Clusters are measured to have a metallicity of ~ -2.5. In contrast metallicities of stars which are part of the of the field population in the halo extend down to ~ -4.0, or less. The ages of stars in this metal-weak tail of the halo population is poorly constrained. The determination of the ages of field stars is difficult. A measurement of the age of 100 giants with metallicity $\lesssim -3.0$ with CODEX using cosmochronometry

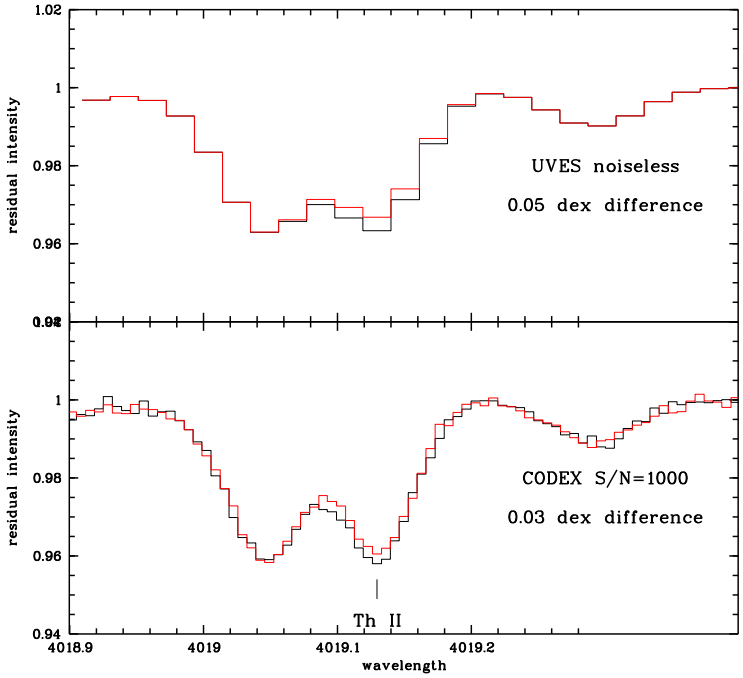

Figure 19: Comparison of the performance of UVES (top panel) and CODEX (bottom panel). With UVES an accuracy of 0.05 dex is not attainable even in the absence of noise. With S/N=1000 CODEX will reach an accuracy of 0.03 dex.

should provide an estimate of the age and formation history of the metal-weak halo with an accuracy of 0.2 Gyr. A spread in the measured ages significantly above this value would be an indication that the metal-weak halo formed over a period longer than 0.2 Gyr.

We will now demonstrate that the required accuracy and number of targets is indeed within the capabilities of CODEX. Fig. 19 shows two synthetic spectra for the halo giant CS 22873-055 (metallicity ~ -3, Cayrel et al. 2004) assuming A(Th)[7] $= -2.89$ (red line) and A(Th) $= -2.86$. The top panel shows what is currently obtainable with UVES at the highest resolution in the blue arm (R$\sim$ 80 000), with image slicer # 2, without any addition of noise. The bottom panel shows what will be achievable with CODEX, with a S/N ratio of 1000. The required accuracy (0.03 dex) is clearly beyond the capabilities of UVES. It is however within reach of an instrument with the resolution and pixel-size of CODEX, provided a S/N~ 1000 can be reached. Consider the star CS 22873-055 with a visual magnitude V=12.65. The E-ELT ETC [8] in spectroscopic mode with a resolution R=120 000 gives a S/N~ 1000 for a 1h integration in seeing limited mode (0.″8 seeing)

About 50 halo giants with metallicity $\lesssim -3$ are already known and studied with high resolution spectra, so that their atmospheric parameters are well known. Stars down to V=15 are interesting targets for our purpose. We would then typically need 6 hours of integration for each star to reach the required S/N ratio. The observation of 100 targets takes then 600h, i.e. 75 nights, a conceivable amount of time in a 4 to 5 year observing campaign.

The Galactic Bulge.

The bulge is one of the main components of the Milky Way. The population of the bulge is predominantly old. The metallicity shows a peak at higher than solar metallicity with a metal-poor tail that extends at least down to [Fe/H]=–1.5 (Minniti & Zoccali 2008). High-resolution spectroscopy carried out at the VLT has enabled a detailed view of the chemical composition of bulge stars. Chemical evolution arguments suggest that the formation of the bulge occurred on a rather short time-scale (1 Gyr or less) while colour-magnitude diagrams suggest an age of about 10 Gyr, somewhat younger than the halo and the thick disc.

Verifying this with a more direct age measurement is clearly very important. The new wide-field camera on the Hubble Space Telescope will be employed for a ”Treasury Program”, which will map bulge populations in four low-extinction fields in five photometric bands (Brown et al. 2008). This extensive data set will allow to select giant

[7]The solar Th abundance is 0.08 (Caffau et al. 2008).

[8]http://www.eso.org/observing/etc/bin/elt/elt/script/eltsimusp , the ETC provides a maximum resolution of 100 000, however an estimate for the S/N for higher resolution can be obtained by scaling the S/N provided by the ETC for R=100 000 by a factor $\sqrt{(R/10^5)}$.

stars of different metallicity for which accurate Th dating will be possible with CODEX at the E-ELT. The distance of the bulge implies that we will have to work with objects of V magnitude around 16. It is thus unlikely that large samples of giants can be observed with the required S/N ratio. However, even observing only 10 giants for each metallicity bin, will allow to reach an accuracy for the age determination of 0.6 Gyr. This will be sufficient to study details of the assembly of the bulge for populations of different metallicity.

The Galactic Thick Disc.

The existence of a thick disc with scale-height of the order of one parsec, or larger, was first highlighted by Gilmore & Reid (1983), but only after the extensive investigations of Fuhrmann (1998,2000,2004,2008) it became clear that this Galactic component is distinct of the thin disc and is considerably older. In fact Fuhrmann claims the existence of an age gap of the order of 2 Gyr between the youngest stars in the thick disc and the oldest stars in the thin disc. The conclusions of Fuhrmann, although rather convincing, are still based on ages derived from comparison of the data to theoretical evolutionary tracks. The possibility of directly dating the thick disc using Th chronometry will allow to confirm or refute the existence of the age gap. The RAVE survey should provide radial velocity measurements for about 1 million stars. This large kinematic data set will allow to select *bona fide* thick disc giants suitable for a Th measurement.

The Galactic Thin Disc

The radioactive age of the Galactic thin disc has been the object of an investigation of Del Peloso et al. (2005). Their measurements were, however, for a very local sample of stars. Applying the method to more distant stars with the desired accuracy of 0.2 Gyr, will allow to investigate the ages of thin disc stars at different galactic locations and to establish the existence or absence of radial age gradients along the thin disc.

References

Barklem, P. S., Christlieb, N., Beers, T. C., et al., "The Hamburg/ESO R-process enhanced star survey (HERES). II. Spectroscopic analysis of the survey sample", 2005, A&A, 439, 129

Bonifacio, P., Molaro, P., Beers, T. C., & Vladilo, G., "CS 22957-027: a carbon-rich extremely-metal-poor star", 1998, A&A, 332, 672

Brown, T. M., Sahu, K., Zoccali, M., et al., "The WFC3 Galactic Bulge Treasury Program: A First Look at Resolved Stellar Population Tools", 2008, ApJ in press, arXiv:0812.0023

Butcher, H. R., "Thorium in G-dwarfs as a chronometer for the Galaxy", 1987, Nature 328, 127.

Caffau, E., Sbordone, L., Ludwig, H.-G., et al., "The solar photospheric abundance of hafnium and thorium. Results from CO^{5}BOLD 3D hydrodynamic model atmospheres", 2008, A&A, 483, 591

Cayrel, R., Hill, V., Beers, T. C., et al., "Measurement of stellar age from uranium decay", 2001, Natur, 409, 691

Cayrel, R., Depagne, E., Spite, M., et al., "First stars V - Abundance patterns from C to Zn and supernova yields in the early Galaxy", 2004, A&A, 416, 1117

Christlieb, N., Beers, T. C., Barklem, P. S., et al., "The Hamburg/ESO R-process Enhanced Star survey (HERES). I. Project description, and discovery of two stars with strong enhancements of neutron-capture elements", 2004, A&A, 428, 1027

Cowan, J. J., Sneden, C., Burles, S., et al., "The Chemical Composition and Age of the Metal-poor Halo Star BD +17deg3248", 2002, ApJ, 572, 861

Del Peloso, E. F., da Silva, L., Porto de Mello, G. F., & Arany-Prado, L. I., "The age of the Galactic thin disk from Th/Eu nucleocosmochronology. III. Extended sample", 2005, A&A, 440, 1153

François, P., Spite, M., & Spite, F., "On the Galactic Age Problem - Determination of the Th/eu Ratio in Halo Stars", 1993, A&A, 274, 821

François, P., Depagne, E., Hill, V., et al., "First stars. VIII. Enrichment of the neutron-capture elements in the early Galaxy", 2007, A&A, 476, 935

Frebel, A., Christlieb, N., Norris, J. E., et al., "Discovery of HE 1523-0901, a Strongly r-Process-enhanced Metal-poor Star with Detected Uranium", 2007, ApJ, 660, L117

Fuhrmann, K., "Nearby stars of the Galactic disk and halo", 1998, A&A, 338, 161

Fuhrmann, K., "Nearby stars of the Galactic disk and halo. II", 2000, http://www.ing.iac.es/ klaus/

Fuhrmann, K., "Nearby stars of the Galactic disk and halo. III.", 2004, AN, 325, 3

Fuhrmann, K., "Nearby stars of the Galactic disc and halo - IV", 2008, MNRAS, 384, 173

Gilmore, G., & Reid, N., "New light on faint stars. III - Galactic structure towards the South Pole and the Galactic thick disc", 1983, MNRAS, 202, 1025

Gratton, R. G., Bragaglia, A., Carretta, E., et al., "Distances and ages of NGC 6397, NGC 6752 and 47 Tuc", 2003, A&A, 408, 529

Grundahl, F., Clausen, J. V., Hardis, S., & Frandsen, S., "A new standard: age and distance for the open cluster NGC 6791 from the eclipsing binary member V20", 2008, A&A, 492, 171

Hill, V., Plez, B., Cayrel, R., et al., "First stars. I. The extreme r-element rich, iron-poor halo giant CS 31082-001. Implications for the r-process site(s) and radioactive cosmochronology", 2002, A&A, 387, 560

Honda, S., Aoki, W., Kajino, T., et al., "Spectroscopic Studies of Extremely Metal-Poor Stars with the Subaru High Dispersion Spectrograph. II. The r-Process Elements, Including Thorium", 2004, ApJ, 607, 474

Johnson, J. A., & Bolte, M., "Th Ages for Metal-poor Stars", 2001, ApJ, 554, 888

Ludwig, H.-G., Caffau, E., Steffen M., et al., "Accuracy of spectroscopy-based radioactive dating of stars", 2009, A&A submitted

Minniti, D., & Zoccali, M., "The Galactic bulge: a review", 2008, IAUS, 245, 323

Norris, J. E., Ryan, S. G., & Beers, T. C., "Extremely Metal-poor Stars. The Carbon-rich, Neutron Capture Element–poor Object CS 22957-027", 1997, ApJ, 489, L169

Schatz, H., Toenjes, R., Pfeiffer, B., et al., "Thorium and Uranium Chronometers Applied to CS 31082-001", 2002, ApJ, 579, 626

Sneden, C., Cowan, J. J., & Gallino, R., "Neutron-Capture Elements in the Early Galaxy", 2008, ARA&A, 46, 241

Sneden, C., Johnson, J., Kraft, R. P., et al., "Neutron-Capture Element Abundances in the Globular Cluster M15", 2000, ApJ, 536, L85

Sneden, C., Preston, G. W., McWilliam, A., & Searle, L., "Ultrametal-poor halo stars: The remarkable spectrum of CS 22892-052",

1994, ApJ, 431, L27
Tilton, G. R., "Principles of radiometric dating", 1988, in Meteorites and the Early Solar System (eds. Kerridge, J. F. & Matthews, M. S. Univ. Arizona Press, Tucson, p.249
Turon, C., Primas, F., Binney, J., et al., "Galactic Populations, Chemistry and Dynamics", 2008, ESA-ESO Working Groups, Report No. 4
Yong, D., Karakas, A. I., Lambert, D. L., Chieffi, A., & Limongi, M., "Heavy element abundances in giant stars of the globular clusters M4 and M5", 2008, ApJ , in press, arXiv:0808.2505
Zwitter, T., Siebert, A., Munari, U., et al., "The Radial Velocity Experiment (RAVE): Second Data Release", 2008, AJ, 136, 421

Technical Requirements

FOV	few arcsec
total energy in fibre	$\geq$80%
spectral resolution	120 000
spectral sampling	3
wavelength range (micron)	0.38 -0.68
wavelength accuracy	N/A
RV stability	N/A
typical magnitude	15
source size	point sources
minimum exposure time	photon noise limit (typically 15min)
cumulative exposure time	up to several tens of hours
target density	low
background	
sky coverage	$\geq$ 90% of available sky
sky subtraction	

The metal lines usable for radioactive dating are rather narrow and a high resolving power of $R \sim 120000$ is desirable. The primary demand is for a sufficient photon flux to reach the extreme signal-to-noise necessary to measure accurate abundances from very weak lines. Large telescope aperture and throughput are thus also highly desirable. The U_{II} resonance line is at 385.9 nm and that wavelength the throughput is higher for the protected silver/aluminium coating. For other wavelengths of interest this coating also has a higher throughput. For the study of halo, thin and thick disc the hemisphere of the location is not relevant. For the study of the bulge a southern location is, however, strongly preferred. A tropical northern location would be acceptable, a location further north would essentially mean losing the bulge.

Show Case 4: Probing the interplay of galaxies and the Intergalactic Medium from which they form. [9]

2.4.1 Background

Our understanding of the formation and assembly of galaxies is still far from satisfactory despite the enormous progress seen in the last decade with multi-wavelength imaging data for large samples of galaxies at redshift up to 4 and beyond. Key for further progress is a better understanding of the complex interplay of galaxies and the surrounding Intergalactic Medium (IGM). The IGM provides the reservoir for the ongoing infall of fresh gas into galaxies. It acts at the same time as a repository for the gas driven out of galaxies due to the energy and momentum input from stellar and AGN driven winds responsible for self-regulating the gas supply, star formation and black hole growth as well as the chemical and structural evolution of galaxies. Metals play a very important role for most if not all aspects of the complex life cycle of gas in galaxies and the IGM.

Absorption line spectroscopy is a powerful tool for studying this life cycle. The most ambitious searches for weak associated metal absorption features (based on Voigt profile fitting of CIV lines) have detected CIV associated with HI absorption with column densities of $\log N_{\rm HI} \gtrsim 14.5$. At lower HI column densities the detection of associated CIV absorption peters out (Cowie & Songaila 1998). Searches based on what is called the pixel-optical depth method reach to moderately smaller column densities/densities (Songaila 1998, Schaye et al. 2003, Pieri & Haehnelt 2004, Schaye 2005, Aguirre et al. 2008). The IGM outside of galaxies is clearly enriched with metals.

Transporting metals from the galaxies or protogalaxies where they are produced into the (low density) IGM is, however, not a trivial matter. A variety of mechanisms have been proposed. Some have argued for supernova-driven (Couchman & Rees 1986, Dekel & Silk 1986) or 'miniquasar'-driven (Haiman, Madau & Loeb 1999) winds. Others have argued for ejection via galactic mergers (Gnedin & Ostriker 1997 and Gnedin 1998) or photoevaporation during reionisation (Barkana & Loeb 1999).

It is major unsolved questions when this enrichment occurred and what kind of galaxies are responsible for it. Two competing models have emerged which aim to explain the metal enrichment of the IGM. The first model proposes that early and widespread Population III star formation in pre-galactic structures at $z \gtrsim 10$ is responsible (e.g. Nath & Trentham 1997, Madau, Ferrara & Rees 2001). In this model the metals are produced early in rather shallow potential wells. In the second model the IGM is enriched due to winds from more massive starbursting galaxies at lower redshift, $z \leq 5$ (e.g. Aguirre et al. 2001, Adelberger et al. 2003). In the latter model the metals are produced later in much deeper shallow potential wells.

The two models are most different in their predictions for the expected metallicity (and temperature and ionization state) in low-density regions of the IGM far-away from galaxies which take up most of its volume. The associated metal absorption of the low-column density Lyα forest which probes these low-density regions is thus of particular interest. With the sensitivity currently achievable only the densest few percent of the cosmic volume have been probed for metals. As we will demonstrate with the large collecting power and throughput of CODEX at the E-ELT it will be possible to push the detection threshold for metals to much lower densities.

Figure 20 shows a high-resolution large box-size hydrodynamical simulation of the IGM at $z = 3$ performed with the numerical code GADGET-II (Springel 2005). The top left panel shows the density distribution of the IGM which has settled into a characteristic cosmic web of filaments and sheets of gas which traces a corresponding web of dark matter. Galaxies are located in the dark matter haloes at the intersection of the prominent filaments. The top right panel shows the temperature of the gas. Bubbles of hot gas develop around the haloes at the intersection of the filaments due to supernova driven galactic winds. The metallicity distribution is presented in the bottom left panel. The filaments are typically enriched to a metallicity level of about 0.001 $Z_{\odot}$. In the bottom right panel the (projected) CIV column density is shown.

2.4.2 What should be measured?

With an accurate determination of the fraction of the Universe (or 'volume filling factor') enriched by metals it should – at least in principle – be possible to differentiate between the early/late models for the enrichment of the IGM. A large volume filling factor would favour early enrichment by stars forming in shallow potential wells, out of which metals are more easily transported into low density regions. The left panel of Fig. 21 demonstrates the sensitivity of the metallicity in underdense regions to the properties of galactic winds. A simulation with a galactic wind implementation meant to mimic "strong" galactic winds with wind velocities of 600 km/s is compared to a simulation with "weak" galactic wind implementation with wind velocities of 100 km/s. The right panel

[9] This showcase corresponds to case C7 of the E-ELT Design Reference Mission.

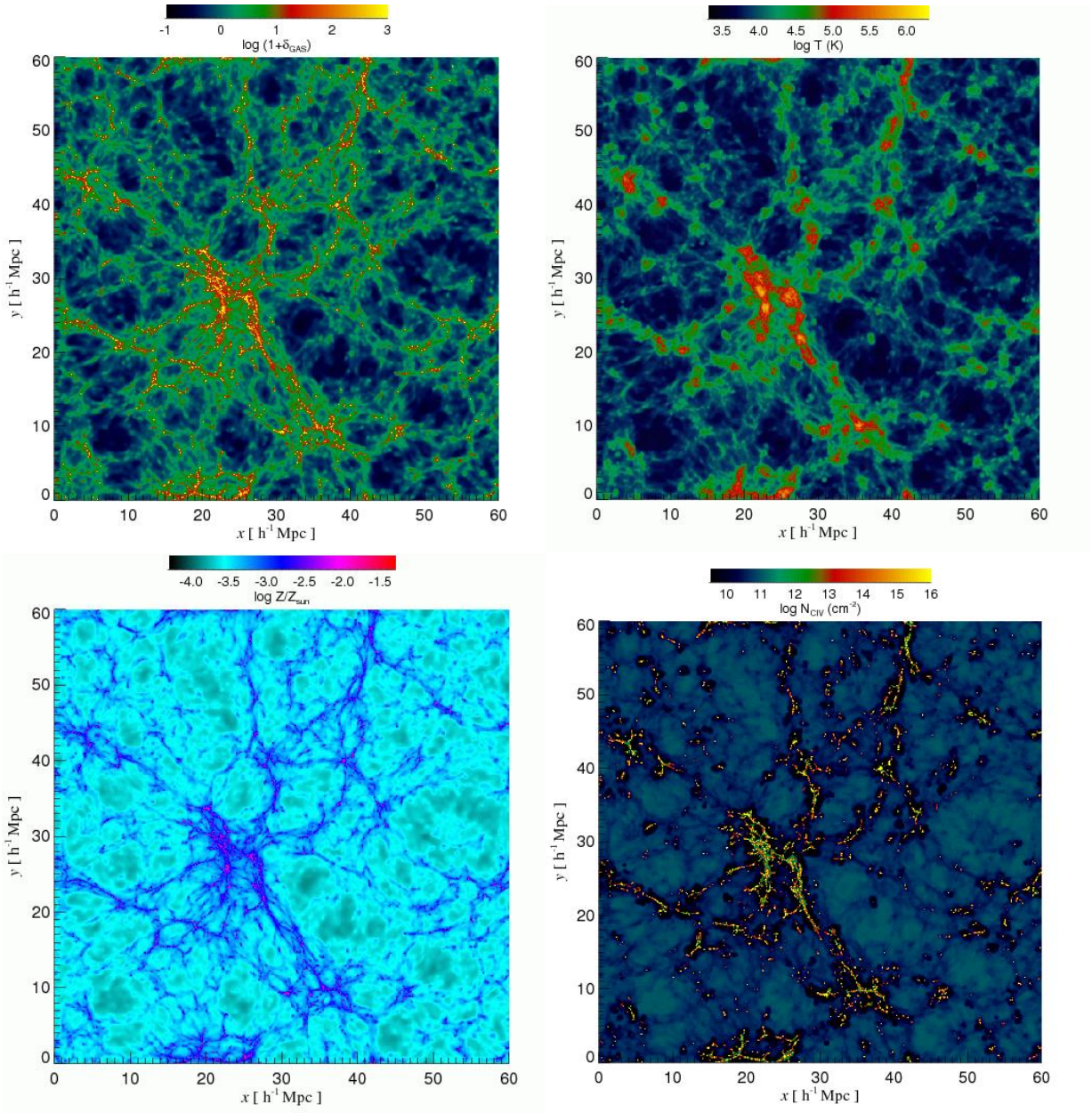

Figure 20: The cosmic web of filaments and sheets at $z = 3$ as simulated using the hydrodynamical code GADGET-II. The simulated box has a linear size of 60 comoving Mpc/h and is for a ΛCDM model. The simulation follows the evolution of 2×400^3 gas and dark matter particles. Cooling and star formation are included using simple prescriptions (e.g. Viel, Haehnelt and Springel 2004), while feedback in the form of strong galactic winds (speed around 600 km/s) powered by the thermal energy of Supernova explosions is simulated using the energy driven prescription of Springel & Hernquist (2003). Projected IGM density (top left), IGM temperature (top right), IGM metallicity (bottom left) and CIV column density (bottom right) are shown for a slice of thickness 2.5 comoving Mpc/h. Outflows are produced by supernova explosions that power galactic winds with an initial velocity of 600 km/s. CIV traces the density structures of the cosmic web down to very small mass haloes. Note that the IGM environment surrounding the haloes is depleted of CIV due to the large temperatures produced by the winds.

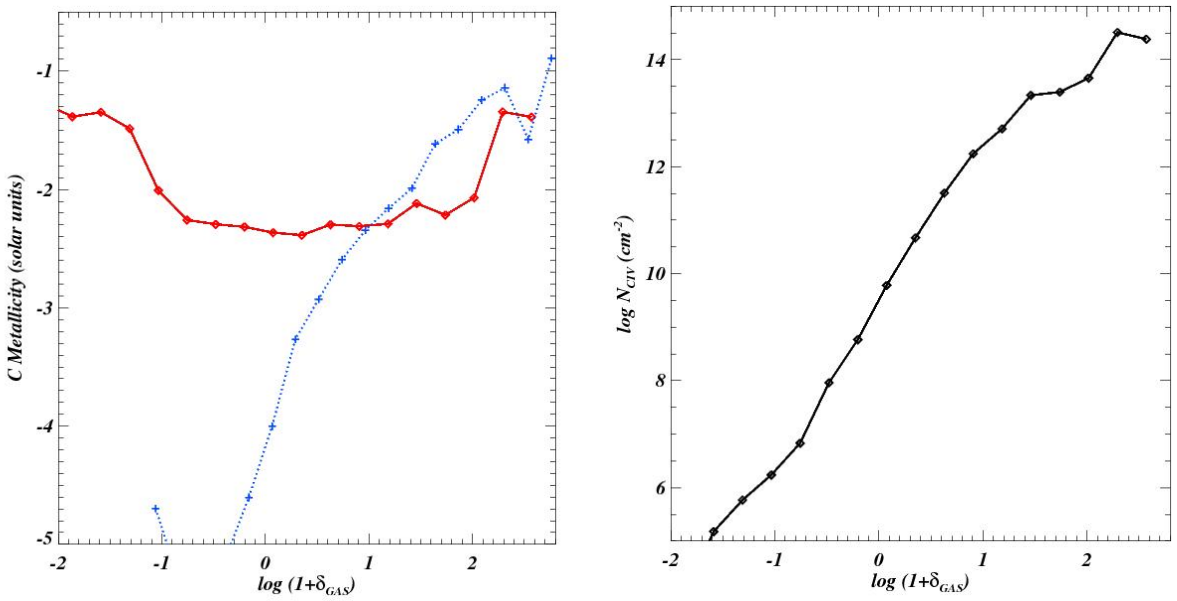

Figure 21: (Left) Comparison of the mean metallicity as traced by carbon for simulations with different implementations of galactic winds. The red solid curve is for "strong" galactic winds (velocity 600 km/s) while the blue dotted curve is for "weak" galactic winds (wind velocity 100 km/s). (Right). The CIV column density vs. matter overdensity. The two figures are a simplistic illustration of the sensitivity of the metallicity in underdense regions to galactic winds.

demonstrates how pushing to weaker CIV absorption features will enable progressively lower-density regions to be probed. Note that these simulations are meant for illustrative purposes only. We consider neither of the wind implementations particularly realistic. Note also that the CIV column in the right panel will depend strongly on the temperature of the gas and the spectrum of the meta-galactic UV background. Especially at low column density there will also be large differences between the projected column density plotted here and the column density of actual absorption features.

Depending on the enrichment mechanism, the abundances of intergalactic metals will vary as a function of various environmental factors, such as the gas density, temperature, and the distance to particular types of galaxies. The gas density and temperature can be constrained using the absorption lines observed in the spectra of relatively bright background sources (quasars, gamma-ray bursts, galaxies). These measurements will improve if more transitions are observed and if the intrinsic line widths can be measured which typically requires a resolving power larger than 100000). Observing in absorption rather than emission allows to trace gas to lower densities. The optical depth is proportional to the ion density, whereas the emissivity is proportional to the density squared. To study the environments of galaxies, it is desirable to find and localize many galaxies near sight lines to bright background sources. Measured abundances are expected to have large stochastic fluctuations. It will thus be important to measure the probability distribution function (pdf), not just the mean.

A number of studies have investigated the correspondence between metal absorption (mainly CIV and OVI) observed along single lines-of-sight and the location of Lyman-Break galaxies (LBGs) identified in the same field. A tight correlation between the location of LBGs and CIV absorption with $N_{\rm CIV} \geq 10^{12.5}$ cm^{-2} was found (Adelberger et al. 2005). Unfortunately, this is, however, not sufficient to settle the question whether LBGs are responsible for the metal enrichment in their neighborhood (Porciani & Madau 2005). A promising approach to solve this question is the use of spectra for multiple lines-of-sight to pairs and groups of QSOs, separated by less than an arcmin, in order to benefit from the combined information in the transverse and longitudinal directions. For galaxies at small impact parameters to the lines of sight it will then be possible to study the metal enrichment by a given galaxy at different separations, and in favourable cases also the dynamics of the absorbing gas. Fig. 22 gives a pictoral representation of the use of two close lines of sight intercepting a galactic outflow at different impact parameters. The two spectra illustrate how the metal absorption (in this case due to the CIV doublet) may change with increasing distance from a galaxy with stronger and more complex features absorption features in the sightline closer to the galaxy.

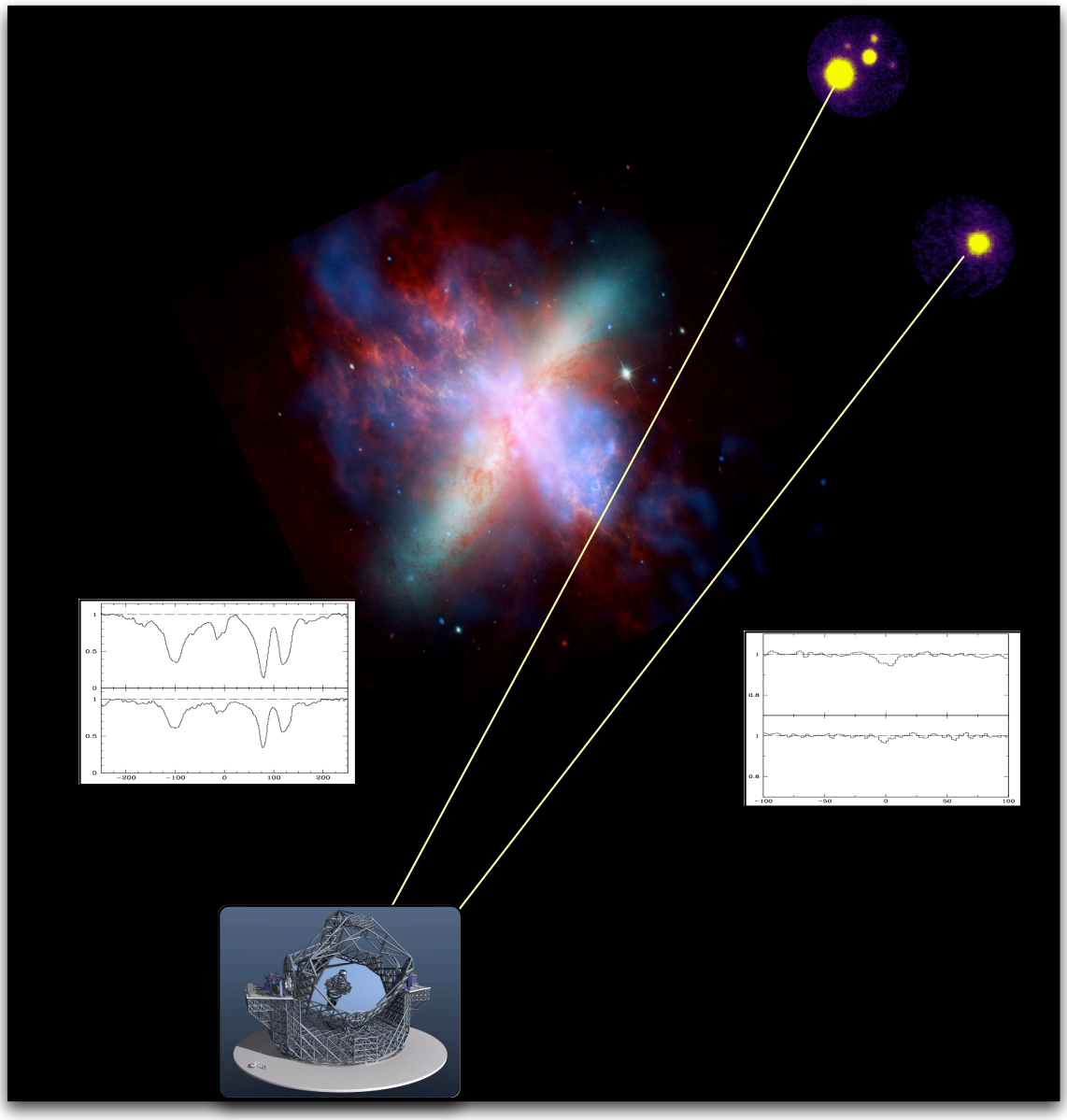

Figure 22: Pictorial view of the use of multiple lines to probe the nature and effects of galactic winds on the IGM. The two white boxes illustrate how the CIV absorptions due to galactic winds may change with impact parameter.

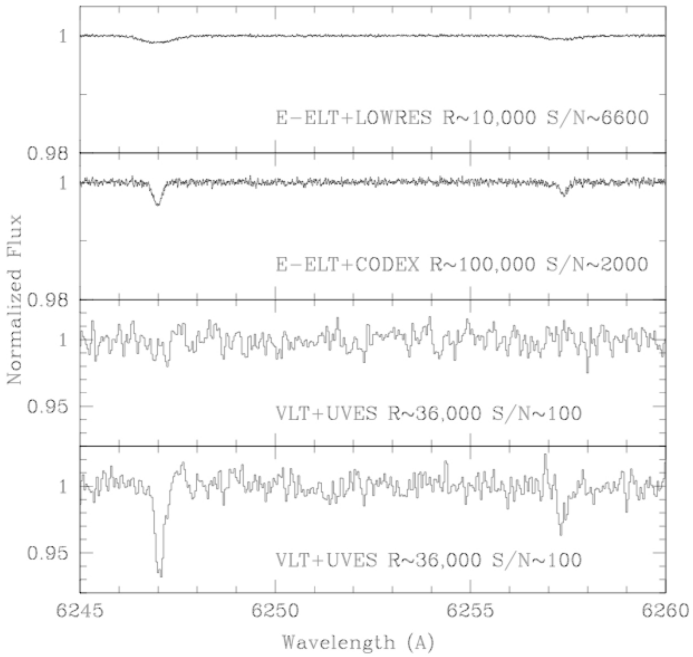

Figure 23: From bottom to top: a) CIV absorption with $\log N_{\rm CIV} = 12.05$ associated with a HI line of column density $\log N_{\rm HI} = 14.72$ (due to gas with an overdensity of $\delta = 6.8$ at $z = 3.03$). A resolving power of $R = 36\,000$ and a signal-to-noise of $S/N \simeq 100$ were assumed. b) CIV absorption associated with a HI line due to gas at the mean cosmic density at the same redshift ($\log N_{\rm HI} = 13.53$). Resolution and S/N are the same as in a). The CIV column density was estimated based on the observed ratio of column densities $N_{\rm CIV}/N_{\rm HI}$. c) same as panel b but with $R = 100\,000$ and $S/N = 2000$. d) Same as c) but with $R = 10,000$ and $S/N = 6600$. The exposure time would be the same in all cases (20 h for an $R \sim 16$ quasar) if the spectra in the two lower panels would be taken with UVES/VLT and in the two upper panels with CODEX/E-ELT.

2.4.3 The need for an E-ELT

Searching for metals in the low-density IGM is difficult. At low densities, $n_{\rm H} \sim 10^{-6} - 10^{-3}$ cm^{-3} the metal abundances are low, $Z \leq 10^{-2} Z_{\odot}$ and the expected total metal column densities drop fast with decreasing density. The low-density IGM is thereby highly ionized by the meta-galactic UV background from galaxies and quasars. Assumptions regarding the ionization balance are thus required in order to convert ion abundances into heavy element abundances.

The most prominent transitions are in the rest-frame ultraviolet and the transitions that can be detected most easily are CIV (1548, 1551), SiIV (1394, 1403), OVI (1032, 1038), CIII (977), and SiIII (1207). As already mentioned briefly statistical methods like the pixel-optical depth method can push the detection threshold to lower densities. Synthetic absorption spectra drawn from large-scale hydrodynamical simulations have proved to be an indispensable tool for testing these methods and to help guide the interpretation of the observational data. Further improvements will, however, require a significant increase in flux and thus telescope size and system throughput.

Note that the ionization corrections depend on the intensity and spectral shape of the radiation field, on the gas density and temperature, and, unless the gas is in ionization equilibrium, also on its history. Ionization equilibrium is generally assumed to hold and should be an excellent approximation for the hydrogen and helium in the IGM, but not always for the heavy elements. The gas density, temperature and the intensity of the meta-galactic UV background can all be measured from the absorption spectra. The major uncertainties are therefore the spectral shape of the UV radiation field and, for systems rarer than Lyman limit systems, the ionizing radiation from local sources (Schaye 2006).

At $z \sim 3$ metal systems corresponding to a few times the mean density are expected to show very low metal absorption column densities ($10^{11} - 10^{12}$ cm^{-2} for CIV, $10^{12} - 10^{13}$ cm^{-2} for OVI).

Figure 23 demonstrates that in order to detect and measure the properties of a CIV system with $N({\rm CIV}) \sim 10^{11}$ cm^{-2} a S/N of the order 10^3 is needed. Even for a bright quasar ($V \simeq 17$) more than 1500 hours of observing

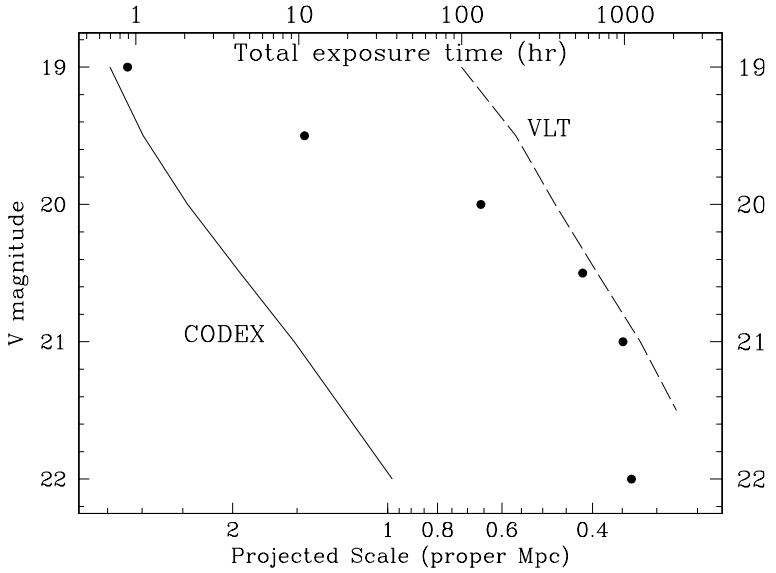

Figure 24: The dots show the limiting V magnitude required to obtain spectra for a sample of 50 known QSO pairs with $z > 1.5$ and $\Delta z < 0.25$ at $\delta < 10^{\circ}$ with separations less than a given scale (scale at the bottom). Notice the small difference going from $V = 21$ to $V = 22$ due to the relatively small number of quasars presently known in this range. The dashed and solid curve show the total exposure time (scale at the top) required to reach a S/N~ 10 at 5500 Å for a sample of 50 QSO spectra taken with UVE/VLT and CODEX/E-ELT, respectively.

time with UVES at the VLT would be required to reach this limit. An ELT is clearly needed to push the search for associated metal absorption into this low-overdensity regime.

The tomographic studies of galactic winds with multiple lines of sight mentioned above are limited by the dearth of close QSO pairs bright enough to be observed with 8-10m class telescopes with spectrographs of sufficiently high-resolution (R $\geq$ 100 000) to reliably identify the metal absorption lines, in particular in the Lyman forest region.

For QSOs with typical limiting magnitude $V \sim 19$ for which a S/N~ 10 at 5500 Å is reached in about 2 hours of exposure time with UVES at the VLT, typical separations would be as large as $6.5'$, corresponding to more than 3 proper Mpc at these redshifts (see Fig. 24). In order to get to the scales of interest, ≤ 350 kpc ($\sim 40''$), approximately the maximum sphere of influence of individual galaxies on the IGM and comparable to the expected coherence length of the undisturbed IGM, will require to take spectra of QSOs of about 21^{st} mag. This is expected to require less than half an hour of integration per object with CODEX at the E-ELT.

References

Adelberger, K. L., Steidel, C. C., Shapley, A. E., & Pettini, M. 2003, ApJ 584, 45

Adelberger, K. L., Shapley, A. E., Steidel, C. C., Pettini, M., Erb, D. K., & Reddy, N. A. 2005, ApJ 629, 636

Aguirre, A., Dow-Hygelund, C., Schaye, J., & Theuns, T. 2008, ApJ 689, 851

Aguirre, A., Hernquist, L., Schaye, J., Katz, N., Weinberg, D. H., & Gardner, J. 2001, ApJ 561, 521

Barkana, R., & Loeb, A. 1999, ApJ 523, 54

Couchman, H. M. P., & Rees, M. J. 1986, MNRAS 221, 53

Cowie, L. L., & Songaila, A. 1998, Nature 394, 44

Dekel, A., & Silk, J. 1986, ApJ 303, 39

Gnedin, N. Y. 1998, MNARS 294, 407

Gnedin N. Y., Ostriker J. P., 1997, ApJ 486, 581

Haiman, Z., Madau, P., & Loeb, A. 1999, ApJ 514, 535

Madau, P., Ferrara, A., & Rees, M. J. 2001, ApJ 555, 92

Nath B. B., Trentham N., 1997, MNRAS, 291, 505

Schaye, J., 2006, IAUS "The Scientific Requirements for Extremely Large Telescopes", 232, 313

Pasquini et al., "CODEX: Measuring the Expansion of the Universe (and beyond)", 2005, ESO Messenger 122, 10

Pieri, M. M., & Haehnelt, M. G. 2004, MNRAS 347, 985

Porciani, C., & Madau, P. 2005, ApJ 625, L43

Songaila A. 1998, AJ, 115, 2148

Springel, V. 2005, MNRAS 364, 1105

Springel, V., & Hernquist, L. 2003, MNRAS 339, 289

Schaye et al. 2003, ApJ, 596, 768

Viel, M., Haehnelt, M. G., & Springel, V. 2004, MNRAS 354, 684

Technical Requirements

FOV	few arcsec
total energy in fibre	$\geq$ 80%
spectral resolution	≥ 100.000
spectral sampling	$\geq$3
wavelength range (micron)	0.37 - 0.75
wavelength accuracy	
RV stability	
typical magnitude	17-21
source size	point sources
minimum exposure time	photon noise limit (typically 15min)
cumulative exposure time	up to few hundred hours
target density	$\leq$ 0.01-1 arcmin^{-2}
background	dark time
sky subtraction	yes
sky coverage	$\geq$ 90% of available sky

The metal lines in the low-density IGM are expected to be rather narrow and a high resolving power $R \geq 100000$ is desirable. The primary demand is for a sufficient photon flux to reach the extreme signal-to-noise necessary to detect the very weak lines. Large telescope aperture and throughput are thus also highly desirable. For the work on QSO pairs and groups a FOV of several arcmin and a modest multiplex would also be benificial. Sensitivity is of prime importance for this showcase which argues for the most efficient coating. There is flexibility in the choice of redshift/wavelength and the blue cut-off is less important for this Show Case. Targets can be chosen all over the sky and there is thus no particular preference in terms of hemisphere.

Show Case 5: Testing Fundamental Physics: Taking the test of the stability of fundamental constants to new limits

2.5.1 Background

The values of fundamental constants in physics have no theoretical explanation and have to be determined experimentally. If General Relativity in a 4-dimensional space time, together with the the standard model of particle physics and the weak equivalence principle were sufficient to describe the Physics of the Universe, fundamental constants should be indeed constant in space and time. Even a small variability of these constants would thus have far reaching implications (for a review see Uzan 2003).

Why should fundamental constants vary? In string theory and other theories with extra hidden spatial dimensions physical constants are defined in a higher dimensional space-time. The scale of these hidden dimensions is generally expected to vary with time which then results in variations of what should be considered "effective" constants in the "observable" dimensions. Another possible explanation for a variability of fundamental constants is related to the contribution of dark energy to the energy density of the Universe. The quintessence scalar field is proposed as as an alternative to the cosmological constant term as an explanation for dark energy. The coupling between such a scalar field with the electromagnetic field would be another possible reason for variability of fundamental constants.

The most stringent stability tests have been made with respect to dimensionless constants to which the characteristic wavelengths of spectral lines are sensitive like the fine structure constant ($\alpha = \mathrm{e}^2/(\hbar c)$) and the ratio of the electron to proton mass ($\mu = m_p/m_e$). As we will discuss in more detail in the next section there is some (rather controversial) evidence for a variability of α and μ from QSO absorption spectroscopy.

If the fine structure constant and the ratio of the electron to proton mass is varying, then all the gauge and Yukawa couplings are also expected to vary. The expected relation between the variation of α and μ is model dependent and depends on the context of a particular Grand Unified Theory (GUT) for the forces in the Universe. Simultaneous measurements of the variability of α and μ at similar redshift could thus be a discriminant of different GUTs.

The ratio of the rate of variation of μ and α is expected to be ≤ 50, but larger values are also possible. The variability of μ would be related to a " running" of the coupling constant of the strong force which is expected to be faster than that of the fine structure constant (Fritzsch 2008).

2.5.2 Astronomical and laboratory bounds on the variability of α and μ

Predictions for the element ratios produced during primordial nucleosynthesis and for the power spectrum of the CMB are sensitive to the value of the fine structure constant. The resulting limits are, however, rather weak and only constrain the fine structure constant in the Early Universe to differ not more than a few percent from its present-day laboratory value. The wavelength of spectral features of astronomical objects probe variations of the fine structure constant and the proton-to-electron mass ratio over cosmological time scales and/or distances and can be measured very accurately. Wavelength measurements of metal lines of intervening absorption systems observed in the spectra of distant QSOs are thus providing the most sensitive astronomical tests of the stability of α and μ. The energy levels of nuclei nuclei are subject to relativistic corrections which are sensitive to the mass number of the nucleus. For this reason the wavelength shift of spectral lines due to changes of the value of α can be be positive as well as negative and depends on the particular transition responsible for the spectral line. Relativistic corrections have been calculated for the most frequently observed resonance lines. Measuring the relative wavelength shifts of a variety of multiplets of spectral lines significantly increases the sensitivity to a variation of α and is the basis of what is called the many-multiplet method. Fig. 25 shows an example of FeII absorption lines at $z = 1.84$ in a QSO absorption spectrum.

Unfortunately the results of current measurements are ambiguous. Murphy and collaborators have measured the wavelength of several spectral lines in a sample of 143 absorption systems in the redshift interval 0.2$< z_{\rm abs} <$4.2 and found evidence for a variation of the fine structure constant, $\Delta\alpha/\alpha$ = (-5.7 ± 1.1) ppm (left panel of Fig. 26). However, two other groups could not confirm the evidence for variability at the level claimed by Murphy et al. Chand et al. 2004 and Srianand et al 2007 found an average value of (-0.1 ± 1.5) ppm in a sample of 23 absorption systems, while others found (-0.12 ± 1.79) ppm and (5.66 ± 2.67) ppm in two systems at $z = 1.15$ and 1.84, respectively (Levshakov et al 2007). These latter measurement are all consistent with no variability of α and at face value appear to rule out the result of Murphy et al. In response to this Murphy et al. have reanalyzed some of the data of Chand et al. and got significantly different results and larger errors for the same data set (right panel of Fig. 26). It is currently not clear how to explain these discrepancies other than with systematic uncertainties of the wavelength calibration.

Laboratory measurements with cooled atomic clocks have also failed to detect a possible variation of the fine structure constant. The most stringent laboratory constraint on the change of the fine structure constant with time is

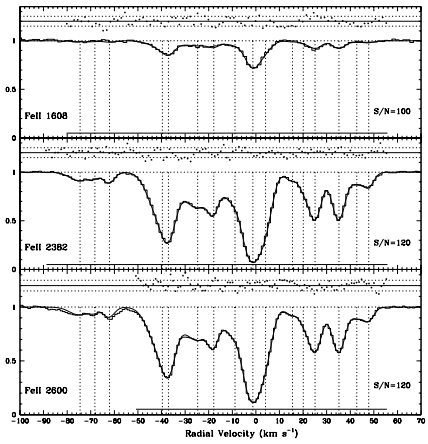

Figure 25: Example of a comparison of Fe II lines for which wavelength shifts occur in opposite directions if α is varied. The spectral features are associated with the $z_{\rm abs}$ = 1.84 damped Lyα system towards Q 1101–264 (Levshakov et al 2007). The synthetic line profiles obtained by Voigt profile fitting are plotted together with the normalized (continuum-fitted) observed flux. The different components of the Voigt profile decomposition are marked by vertical tick marks. The normalized residuals of the fit are shown on the top by the dotted curve together with the 1σ errors. In this example the error of the $\Delta\alpha/\alpha$ measurement is $\sigma_{\Delta\alpha/\alpha}$ = 2.6 ppm.

$\dot{\alpha}/\alpha = (-1.6 \pm 2.3) \times 10^{-17}$ yr^{-1} (Rosenband et al 2008). It is not obvious how to compare the measurements based on QSO absorption systems with the laboratory measurements. The claimed detection of variability at a level of 6 ppm (part-per-million) is based on spectroscopic measurements which reach up to redshift 4 corresponding to a lookback time of about 12Gyr. If the variability of the fine structure constant is in time rather than space and depends linear on time this should correspond to a variation of 5×10^{-16} yr^{-1} in apparent conflict with the above laboratory measurements.

Tests of the stability of μ with astrophysical spectroscopic measurements are also ambiguous. The most stringent limits come here from observations of the Werner and Lyman series of molecular hydrogen in damped Lyα absorption systems (DLAS). The wavelength of different electron-vibro-rotational transitions have a different dependence on the reduced mass and can be used to constrain a possible variability of μ. The fact that only a handful of systems have been investigated for this purpose reflects the difficulty of these measurements. Only few DLAS show H_2 and the restframe wavelengths of the H_2 lines are at $\approx$ 1000 Å, in the middle of the Lyman forest. With an optical spectrograph they are thus only observable at $z_{\rm abs} \geq 2$. Intense searches for H_2 systems are under way and a larger number of suitable absorption systems should be available in the near future. UVES observations of DLA systems at $z_{\rm abs}$ =3.0 and 2.4 towards QSO 0347-383 and QSO 0405-443 , respectively, have given $\Delta\mu/\mu = (24 \pm 6)$ ppm (Reinhold et al 06). However, the same UVES data have been used to claim a null detection with $\Delta\mu/\mu = 2.6 \pm 3$ ppm by King et al. (2008).

2.5.3 Towards new limits

The current measurements of α and μ are obviously performed at the limit of what can be done with current spectrographs. CODEX with its novel calibration technique will dramatically improve this situation. With the anticipated wavelength accuracy of CODEX the measurements error should become dominated by photon noise rather than errors of the wavelength calibration. The large collecting power of E-ELT will thus be very important as it will reduce the photon noise of these measurements which are performed for rather faint targets.

We discuss now in somewhat more detail how well we expect CODEX at the E-ELT to do. Measuring the variability of μ or α implies the measurement of a tiny variation of the position of one or a few lines with respect to other reference lines. In that respect the measurements are not much different from radial velocity searches for exoplanets, but with the added difficulty that only few lines can be used and that QSOs are much fainter than the stellar sources used for exoplanet searches. The relation between $\Delta\alpha/\alpha$ and the small wavelength shift characterized by a corresponding Doppler velocity can be written as,

$$\frac{\Delta\alpha}{\alpha} \approx \frac{\Delta v}{2c}\Delta Q \tag{4}$$

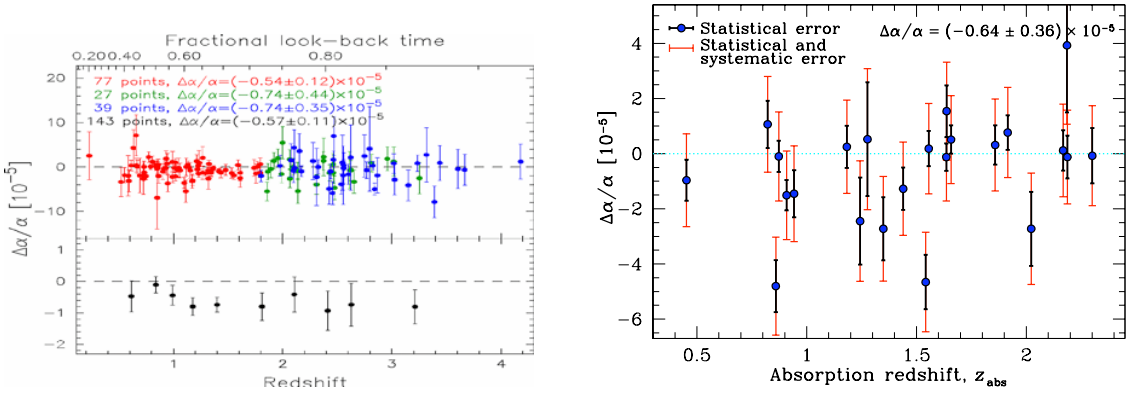

Figure 26: *Left:* Results of Murphy et al. (2004) from 143 absorption systems obtained with the HIRES spectrograph at Keck. The authors claim the detection of a variability of the fine structure constant with 5σ significance, $\Delta\alpha/\alpha$ = $-5.7 \pm 1.1 \cdot 10^{-6}$. *Right:* Results of the reanalysis of the $\Delta\alpha/\alpha$ measurements of Chand et al. based on 23 absorption systems obtained with UVES at the VLT by Murphy et al. (2008). The weighted mean is $\Delta\alpha/\alpha$= $-6.4\pm$ 3.6 ppm. The statistical error is $\geq$ 6 ppm for an individual absorption system, but the scatter suggests a remaining large systematic error. The total error is estimated to be as large as $\sigma_{\Delta\alpha/\alpha}$ $\approx$15 ppm for individual absorption systems.

where ΔQ is the difference in the theoretically computed coefficients which describe the sensitivity of the wavelength to α. Typical values of ΔQ are of order 0.02-0.05.

The precision with which the wavelength of a spectral transition can be determined from an absorption line depends on the S/N of the spectrum and the Full Width Half Maximum (FWHM) of the absorption line. The wavelength error therefore decreases with decreasing intrinsic linewidth and with increasing resolving power of the spectrograph (the latter until the intrinsic line width is resolved). For the idealized assumption of a perfect Gaussian line shape the wavelength error is given by (Landman et al. 1982),

$$\sigma_0 = \frac{1}{(2\pi \ln 2)^{1/4}} \frac{1}{S/N} \sqrt{\Delta_{\rm pixel} \rm FWHM}.$$

Fig. 27 shows the expected wavelength accuracy of CODEX at the E-ELT in the photon noise limit. [10].

A wavelength accuracy of a few ms^{-1} is reachable for single lines with relatively short exposures even for faint sources provided the errors due to the wavelength calibration and the correction for the motion of the Earth are sufficiently small. An error of 3 m s^{-1} for the measurement of the wavelength shift of a pair of lines corresponds to an error of $\sigma_{\Delta\alpha/\alpha}$ of 0.05-0.1 ppm for α depending on the sensitivity coefficients ΔQ of the spectral lines used.

CODEX at the E-ELT will decrease the error for measurements of the variability of α and μ by two orders of magnitude. This should easily resolve the current controversy around the claimed detection of a variability of α and μ. As discussed in the Introduction a convincing detection of variability would have far reaching implications revealing new physics beyond the Standard Model of Physics, and possibly providing insights into the nature of dark energy. Unfortunately there is little theoretical guidance on the expected rate of change of any of these constants. The significant improvements of the measurement errors expected for CODEX at the E-ELT should thus be very worthwhile. The improved wavelength calibration should thereby enable photon noise limited measurements so that there is a good reason to believe that unlike for presently available spectrographs systematic uncertainties of the wavelength calibration will not be the dominant source of error.

Several space-based missions such as ACES, μSCOPE, STEP expect to significantly improve existing laboratory bounds on the expected variability of fundamental constants. There is therefore the exciting prospect that if variability were detected, it could be investigated from very different angles.

[10]Note that we made here the standard assumption regarding telescope aperture and telescope throughput as described in section 1.4

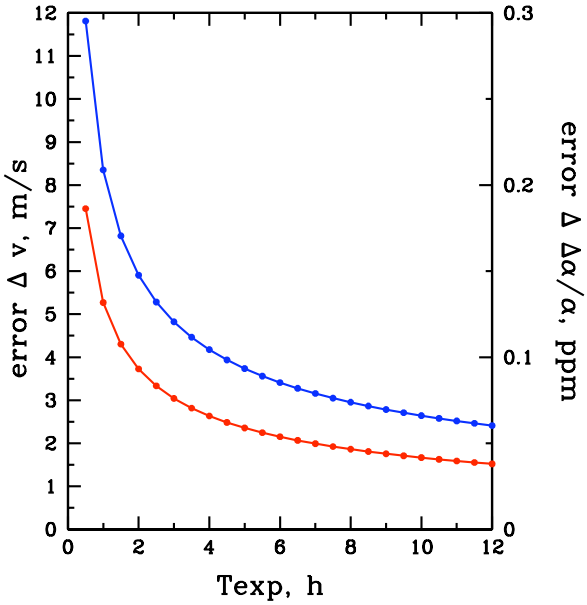

Figure 27: Expected wavelength accuracy with CODEX at the E-ELT for a single Gaussian absorption line with a Doppler parameter b= 2 km s^{-1} as a function of the exposure time for QSOs with magnitudes of V=16 (lower red curve and V=17 (upper blue curve).

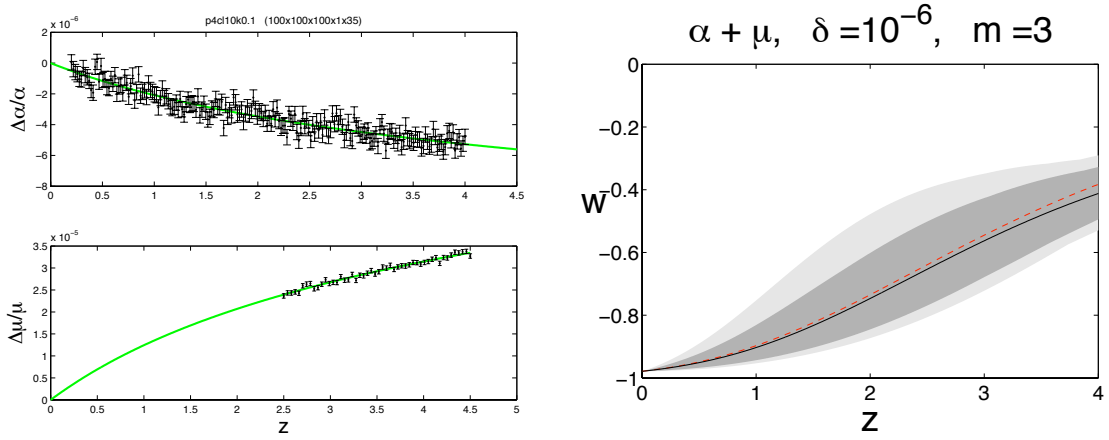

Figure 28: *Left:* Monte Carlo realization of a mock data set based on a model where the evolution of α and μ is due to the evolution of a scalar field representing an evolving dark energy component of the energy density of the Universe (Avelino et al. 2006, Nunes private communication). The assumed errors of 0.5 ppm for $\Delta\alpha/\alpha$ and $\Delta\mu/\mu$ are expected to be reached easily with CODEX at the E-ELT. The ratio of the rate of change of α and μ was assumed to be -6. *Right:* The solid curve shows the equation of state parameter $w(z)$ inferred from the mock data set. The shaded regions represent the 1- and 2-σ confidence limits. The dashed curve shows the assumed evolution.

2.5.4 Varying fundamental constants and dark energy

As already mentioned in certain models where a scalar field is responsible for the observed dark energy component of the energy density and the scalar field couples to electromagnetic fields the evolution of the dark energy density and the variation of μ and α are related. Avelino et al (2006) have demonstrated the possibility that in such models the evolution of the scalar field and of the equation of state of the dark energy can be inferred from the evolution of α and μ with redshift, similar to the reconstruction of the effective potential from the motion of a particle. Nelson Nunes kindly performed such an analysis for a set of mock observations as may be realistically performed with CODEX at the E-ELT. He thereby assumed that α and μ have been measured with an accuracy of 0.5ppm [11] for a sample of 200 and 50 systems, respectively.

The left panel of Fig. 28 shows a Monte-Carlo realization for the evolution of α and μ for such a data set. The assumed evolution of the equation of state parameter *w(z)* is shown in the right panel of Fig. 28 by the red dotted curve. The black continuous curve shows the evolution inferred from fitting the simulated measurements with a polynomial of order m=3 (see Avelino et al 2006 for more details). The two shaded regions represent the 1- and 2-σ confidence limits of the reconstructed evolution. Relatively few measurements are sufficient to recognize whether *w(z)* evolves with redshift or not.

References

Avelino P.P., Martins C.J.A.P., Nunes N.J., Olive K.A., 2006, Phys. Rev. D, 74, 083508

Bohlin R.C., Jenkins, E.B., Spitzer L Jr., et al, 1983, ApJS, 51, 277

Chand H., Srianand R.,Petitjean P., Aracil B., 2004, A&A, 417, 853

Churchill C., Vogt S.S., Charlton J.C., 2003, AJ, 125, 98

Fritzsch H., 2008, arXiv:0802.0099

King, J.A., Webb J.K., Murphy M.T.,Carswell R.F., 2008, arXiv:astro-ph/0807.4366

Landman D.A., Roussel-Dupre R., Tanigawa G., 1982, ApJ, 261,732

Levshakov P., Molaro S., Lopez, et al., 2007, A&A, 466, 1077

Murphy M.T., Flambaum V.V., Webb, J. K. et al., 2004, Lecture Notes Phys., 648, 131

Murphy M.T., Webb J. K.,Flambaum, V. V., 2008, MNRAS, 384, 1053

Reinhold E., Buning R., Hollenstein U., Ivanchik A., Petitjean P., Ubachs W., 2006, Phys. Rev. Lett. 96, 151101

Rosenband T., Hume D.B., Schmidt P.O. et al., 2008, Sciencexpress Report, 6 March, p. 1

Srinanand R., Chand H., Petitjean P., Aracil B., 2007, arXiv:0711.1742

Uzan J.-P., 2003, Rev. Mod. Phys., 75, 403

Technical Requirements

FOV	few arcsec
total energy in fibre	$\geq$ 80%
spectral resolution	$\geq$150 000
wavelength range (micron)	0.37-0.68
spectral sampling	$\geq$ 4 pixel
wavelength accuracy	$\leq$ 2 m s^{-1} locally
RV stability	
typical magnitude	16-18
source size	point sources
minimum exposure time	photon noise limit (typically 15min)
maximum cumulative exposure time	few tens of hours
target density	low
background	dark time
sky substraction	yes
sky coverage	$\geq$ 90% of available sky

Measuring the variability of fundamental constants puts strong demands on the wavelength accuracy of the spectrograph. Line widths of metal absorbers are often as small as 1-2 km/s^{-1} and the measurement errors improve for increased resolving power all the way up to $R \sim 300000$. A good sampling of the resolution element is highly desirable. The measurements are anticipated to be photon noise limited. Large telescope aperture and throughput are thus also highly desirable. For the measurement of a variation of α a coating with high sensitivity over a large

[11] CODEX should actually do much better in many cases. This error assumption can thus be considered conservative.

wavelength range stretching into the the mid-IR like the protected silver/aluminium coating would be beneficial as there are plenty of suitable absorbers at all redshifts. The access to the UV down to the atmospheric cut-off provided by the aluminium coating would be important for the study of the variability of the electron-to-proton mass ratio. The Lyman-Werner transitions around 950-1050 A are used for this. Up to now only 3 systems have been studied and all are at redshifts greater than 2.4, while there are quite a few more at redshifts between 2 and 2.5. Hemisphere of site location is not particularly important for this Show Case. About 150 absorbers have been studied with Keck so far and about 25 systems have been studied with the VLT. Studies of the variability of the proton-to-electron mass ratio have been performed for three systems in southern QSOs. However, there is obviously no reason why molecular hydrogen should be found preferably in the Southern Hemisphere.

3 Other Science proposed for CODEX

Note that the cases denoted by * have been communicated to us by the community and have become part of the ELT Science Plan (DRSP).

3.1. Stars and Planets with CODEX

- **Planets around low-mass stars and brown dwarfs: mass ratio dependence on the mass and chemical composition of the primary.** With a precision of tens of cm s^{-1} (expected for $R \sim 19.5$ mag), CODEX can find "super-Earths" at close-in orbits around more than 200 L- and several T-type objects known in the solar neighbourhood. Such CODEX observations would also contribute to our knowledge about the multiplicity of properties of the population of very low-mass stars in the solar vicinity, which is very poorly constrained at present. Comparison to synthetic spectra would advance our understanding of the structure and behaviour of the atmospheres of stars and brown dwarfs.

- **Transmission and reflection spectroscopy of known planets around stars.** The transmission spectrum of a planet atmosphere is obtained when a transiting planet is passing in front of the disk of its parent star, while the reflected spectrum is obtained out of eclipse for both transiting and non-transiting planets. CODEX covers a wavelength range suitable for the detection of features due to ozone, molecular oxygen, water vapour, sodium, as well as ions from the ionospheres of Earth-like planets. Spectral features of sodium, potassium, oxides, and hydrides can be revealed from the transmitted and/or reflected spectrum of warmer giant planets around stars.

- **Radial velocity searches for planets around binary stars, stellar clusters and associations of different age and metallicity.** With CODEX we will be able to study the distribution of planet masses and orbital parameters in stellar clusters with different masses, metallicities and ages. This will provide key information for understanding the origin of the great variety of planetary systems observed.

- **Precise orbital parameters for planets discovered in non-radial velocity searches.** CODEX will provide the high-precision radial velocity measurements required to fully characterize the orbital parameters of planets discovered by photometric transits, astrometry and direct imaging.

- **Follow-up of known planetary systems** The long-term stability and high precision of CODEX will be essential to detect additional planets with longer orbital periods and/or lower mass in previously known planetary systems.

- **Searching for giant planets in the LMC*.** A survey for giant planets in metal-poor intermediate mass giants in the LMC will not only provide the first extra-galactic planets, but will also give an extremely important input for our understanding of giant planet formation. In particular, it will give us crucial hints about the dependence of extrasolar planet formation on two important stellar parameters, mass and metalicity (communicated by Nuno Santos).

- **Searching for exo-planets in open clusters*.** A search for exo-planets in open clusters will provide important information complementary to that gained from planets around field stars. The study of exo-planets in open clusters will allow us to investigate planets around stars with similar chemical composition and age, and common birth environments (communicated by Katia Biazzo).

- **The inner workings of late-type stars, as revealed by systematic abundance studies of globular-cluster stars*.** To fully exploit the archaeological potential that late-type stars in globular cluster stars hold, their surface abundances need to be corrected for modifications brought on by internal mixing processes of various sorts. Detailed observations of elemental and isotopic abundances of, e.g., Li-7 and Li-6, among main-sequence stars in globular clusters can give vital clues as to which are the dominant processes that shape the surface abundances (communicated by Andreas Korn).

3.2 Galactic Astronomy with CODEX

- **Spectral line variations in solar-type stars and 3D hydro-models.** CODEX will enable the study of the short- and long-term variability of stellar line shifts and shapes. The intrinsic variations in line shifts, which appear as "noise" in planet search Doppler data, may hide interesting physics, e.g., short time scale convective motions, internal pulsations/oscillations. Current asteroseismic data do not have high enough signal-to-noise to investigate the line profile shapes. A detailed analysis of line shifts and asymmetries of the data acquired for planet searches may lead to an improvement of the precision of radial velocity measurements. Detailed studies of line profile variations and asteroseismological studies can be carried out for a large number of solar-type and metal poor stars with Fe/H ≤ -3. CODEX observations will therefore provide a unique test bench for a new generation of 3D hydro models.

- **Corrugated stellar surfaces*****.** Absorption lines in stellar spectra do not have the wavelengths 'naively' expected from their laboratory values, merely Doppler-shifted due to stellar radial motion. Subtle deviations are caused by gravitational redshift and convective blueshift, the latter is an important tool for testing models of 3-dimensional stellar hydrodynamics (communicated by Dainis Dravins).

- **The dynamics of the solar neighbourhood brown dwarf population.** Radial velocities measured with CODEX can be combined with trigonometric parallaxes (from ground and space facilities) to derive the dynamical properties of the substellar population in the solar vicinity. Much work has been done so far for F-G-K and early-M stars, but little is known for substellar objects.

- **Spectral line variations in massive stars.** OB stars show a large unexplained broadening of stellar lines that corresponds to highly supersonic velocities and can therefore not be interpreted as classical turbulence. This broadening may be related to internal pulsations and oscillations or to other motions of still unknown origin. The properties and scales of this broadening are unknown and have to be analyzed using tiny differences in the line profiles, thus demanding high resolution, high signal-to-noise ratio spectra obtained on short time scales. At the typical distances of OB stars in the Galaxy (1–2 kpc) this can only be achieved with an ultra-stable instrument with large throughput like CODEX.

- **Abundance anomalies in companions of X-ray bursters.** Studies of atmospheric abundance anomalies due to the explosion of a companion supernovae give us insight into the explosion conditions of SNe. Such studies are based on small differences in the spectra of stars of similar spectral type and require therefore high spectral resolution and signal-to-noise for faint targets.

- **Structure of ionized regions.** High-resolution spectra of HII regions and planetary nebulae will allow us to study their kinematic structure and abundance variations in detail. CODEX at the ELT will allow us to extend such studies to very faint objects while keeping the high resolution needed to separate the different kinematic components. In this way, ejection (for planetary nebulae) and interaction mechanisms (both for planetary nebulae and HII regions) can be studied in detail.

- **Distance and structure of globular clusters.** Measurements of the velocity dispersion of globular clusters can be combined with measurements of stellar proper motions (e.g. from GAIA) to estimate their distances. By determining radial velocities of individual stars it will be possible to constrain the mass concentration at the centre of globular clusters. It should be possible to answer the question whether globular clusters harbour intermediate-mass black holes, and if yes, what is their mass.

- **Kinematics of the Galactic bar.** CODEX at the E-ELT will offer the opportunity to perform detailed studies of the kinematics of the Galactic bar, particularly in the regions where the bar encounters the bulge.

- **Structure of the Galaxy.** Detailed kinematic studies of the different Galactic populations (thin and thick disk, halo stars, young massive clusters, globular clusters) are required to obtain a complete picture of the structure of the Milky Way. Such studies should be linked with abundance studies to shed new light on the origin and age of the different Galactic components. High resolution, high signal-to-noise spectra of thousands of faint stars are needed.

- **The formation of the Galaxy.** The Milky Way is surrounded by the remnants of infalling dwarf galaxies, presently forming streaming groups of stars. Such groups can be identified with precise radial velocity measurements and their origin can be studied with detailed abundance measurements. This requires high-resolution spectra and most of these objects will be faint targets appropriate for CODEX. Older stars are

fossil records of the early chemical evolution of the Milky Way. They are expected to be metal-poor and abundance determinations will require very high quality spectra to investigate the corresponding very weak spectral features.

3.3 Extra-galactic Astronomy and Cosmology with CODEX

- **Detailed chemical abundance study of damped Lyman-alpha systems and their isotopic ratios.** High resolution and high signal-to-noise spectra of QSOs obtained with CODEX at the E-ELT will open the door for the detection of numerous new chemical elements which are not accessible with spectrographs on 8-10m class telescopes. Measurements of these new elemental abundances (light elements and s- and r-process elements) will provide important insights into nucleosynthesis in the early Universe and will increase our knowledge of physical properties of high-redshift galaxies. The same spectra will enable for the first time a determination of the isotopic ratios of C and Mg in low-metallicity interstellar environments, which are very relevant for certain nucleosynthetic processes.

- **H_2-to-CO conversion factor in the ISM of low-metallicity galaxies at high redshift.** For the few damped Lyman-alpha systems in which molecular gas has been detected, spectra with higher signal-to-noise with CODEX will enable the detection of UV transitions of CO molecules. The resulting H_2 and CO abundance measurements can be used to constrain the H_2-to-CO conversion factor in low-metallicity environments. The sampling of different environments is ideal to study possible variations of the conversion factor over a range of an order of magnitude in metallicity.

- **Measuring the sizes of H_2 absorption clouds in damped Lyman-alpha systems.** H_2 clouds are known to be very clumpy. With pencil beam surveys of H_2 in quasar absorption line systems, it will be possible to constrain the size and filling factor of molecular clouds at high redshifts.

- **Probing the kinematics of damped Lyman-alpha systems.** The cm/s radial velocity accuracy and long-term stability of CODEX at the E-ELT will enable the monitoring of temporal variations of the metal and molecular line profiles of DLAs over periods of a few years. This opens a new window for studying the kinematics of these high-redshift galaxies.

- **Chemical abundances of representative samples of Lyman break galaxies.** Lyman break galaxies are star-forming galaxies detected in large numbers at high redshifts. Due to their relatively faint flux, it is generally only possible to obtain low-resolution spectra with 8-10m class telescopes. With CODEX at the E-ELT, we will be able to measure their abundances from UV absorption line studies, similarly to what is done in quasar absorption line systems.

- **Chemical abundances of gamma-ray burst (GRB) host galaxies.** The progenitors of GRBs are very likely massive stars, and hence GRBs are expected to be found in any place where star formation happens, up to very high redshifts. GRB's are therefore a very efficient tool to detect very high-redshift galaxies. CODEX at the E-ELT will allow to study the ISM of these galaxies in great detail, since CODEX will require a less rapid trigger of the observations. Temporal follow-up of GRBs will provide very important further constraints on the physical processes of GRBs and on their progenitors.

- **Primordial nucleosynthesis: abundance measurements of deuterium in quasar absorption line systems.** With the higher resolution spectra of quasars obtained with CODEX at the E-ELT it will be possible to better disentangle the deuterium absorption from Lyman forest interlopers. This should increase the number of deuterium abundance measurements in quasar absorption line systems. The deuterium abundance is an important probe of the cosmological baryon density.

- **Isotopic ratios in the Local Group galaxies.** The high-resolution and high signal-to-noise spectra obtainable with CODEX at the E-ELT will allow a determination of the isotopic ratios of Mg in spectra of cool giants or dwarfs using MgH lines. Other isotopic ratios, such as Ba, Sm, and Eu, are also of great interest and will be measurable with CODEX in giants. This will be possible in Local Group galaxies, such as Sagittarius and the Magellanic Clouds.

- **Detailed abundance studies of extremely metal-poor and metal-rich stars in Local Group galaxies.** The study of extremely metal-poor stars promises to provide important constraints on the early formation of galaxies. Numerous ambitious surveys searching for metal-poor stars with smaller telescopes are under way and should lead to the discovery of an appreciable number of extremely metal-poor stars both in the Milky Way and the dwarf galaxies of the Local Group. Detailed abundance studies will require the high resolution and high signal-to-noise spectra obtainable with CODEX at the E-ELT. The same holds for the metal-rich stellar population of the Large Magellanic Cloud, the Sagittarius galaxy and the bulge of the Milky Way.

- **Multi-epoch observations of Type Ia Supernovae.** Multi-epoch high-resolution spectroscopy of Type Ia Supernovae (SNe) is currently typically performed for two SNe per year and is limited to the initial months with 8-10m-class telescopes. CODEX at the E-ELT will significantly increase the number of SN with high-quality spectra and will allow the follow-up of SNe for a longer time. These observations will provide important information about the circumstellar environment of SNe and about the stellar progenitor system. As a byproduct, the data will allow to study in detail both the interstellar medium of the host galaxy and the intergalactic medium along the line of sight to SNe. Moreover, since Type Ia SNe are relatively homogeneous in luminosity and color, these observations will allow the analysis of the extinction curve of galaxies of various morphological types.

- **Searching for the Progenitors of Type Ia SNe*****.** We propose to obtain E-ELT multi-epoch, high-resolution, optical spectroscopy of relatively nearby Type Ia SN/e (v(r)$<$10,000 km/s). Through the study of time evolution of narrow absorption features originating in the circumstellar environment of the exploding star, we will be able to put stringent constraints on the progenitor's nature and to probe the existence of multiple channels to Type Ia explosion (communicated by Ferdinando Patat).

- **Probing galaxies in cluster with QSO absorption line spectroscopy*****.** QSO/GRB absorption-line spectra provide a sensitive probe of the gas in galaxies that is independent of redshift and brightness of both the background source and the absorber host-galaxy. How does environment affect gas accretion? So far this problem has been studied by selecting absorbers and then following up the line-of-sight environments. Little has been done in terms of systematic studies that instead select the environment and then look for the absorbers. The "Quasars behind Clusters" survey is a notable exception that has delivered its first results on the effect of group and cluster-size environment on the gaseous content of high-redshift galaxies. Future surveys like the LSST will provide large numbers of galaxy clusters and GRB/QSOs suitable for extending such an experiment with exquisite accuracy (communicated by Sebastian Lopez).

3.4 High-precision spectroscopy Tests of Physical Theories with CODEX

- **Tests of General Relativity using high-precision dynamical studies of black hole/star binaries.** Currently, there are about half a dozen bright ($V \sim$ 17-18 mag) secondary stars orbiting black holes in our Galaxy for which CODEX can yield radial velocity measurements with a precision better than 10 cm s^{-1} and with a good orbital coverage. Observations should be carried out during periods of quiescence with minimal disk emission. Given the typical masses of the compact objects (in the range 5–10 $M_{\odot}$) and the typical orbital separations of the companions (2-5 $R_{\odot}$), the radial velocity curves of the systems are expected to show signatures of relativistic gravitoelectric and gravitomagnetic effects in the form of post-Newtonian orbital velocity deviations (similarly to Mercury and its orbital motion around the Sun). The predicted amplitude of these relativistic effects is in the range 0.1–1 m s^{-1} depending on binary system parameters. For comparison, the amplitude of the projected radial velocity curves are in the range 400–700 km s^{-1}. High spectral resolution observations ($R \sim$ 50000) with CODEX and with a good orbital coverage (step of 0.05 in orbital phase) for each of these systems will further test General Relativity. These observations would need to be repeated during various orbital periods in order to increase the signal-to-noise ratio of the relativistic effects. The series of spectra will also allow detailed chemical composition studies of the secondaries, which may provide evidence of the nucleosynthesis processes in the progenitors of the black holes and additional information on their origin and on the physics of the explosion. Furthermore, the spectra will offer the possibility to investigate the interaction of the black holes with the disks and their companion stars.

4 Summary of Technical Requirements

	expansion	planets	stars	metals	constants
FOV	few arcsec	few arcsec	few arcsec	few arcsec	few arcsec
tot. energy in fibre	$\geq$ 80%	$\geq$ 80%	$\geq$ 80%	$\geq$ 80%	$\geq$ 80%
spectral resolution	$\geq$100 000	150 000	120 000	$\geq$ 100 000	$\geq$ 150 000
spectral sampling	$\geq$ 3	$\geq$ 4	$\geq$ 4	$\geq$ 3	$\geq$ 4
wavelength range (μ)	0.35-0.67	0.38-0.68	0.38-0.68	0.37-0.75	0.37-0.68
wavelength accuracy					$\leq$ 1m/s
RV stability	2 cm/s (20yr)	2-5 cm/s (10 yr)			
throughput	$\geq$0.2				
typical magnitude	15-17	$<$11	15	17-21	16-18
source size	point sources	point sources	point sources	point sources	point sources
minimum exposure time	photon noise limit (typically 15min)	typically 15min	phot. noise lim. (typically 15min)	phot. noise lim. (typically 15min)	phot. noise lim. (typically 15min)
maximum cumulative exposure time	few hundreds of hours	few tens of hours	few tens of hours	few hundreds of hours	few tens of hours
target density	low	low	low	$\leq$ 0.01-1 arcmin^{-2}	low
background	dark time	grey-dark time		dark time	dark time
sky subtraction	?	?		yes	yes
sky coverage	$\geq$ 90%	$\geq$ 90%	$\geq$ 90%	$\geq$ 90%	$\geq$ 90%

The table above summarizes the technical requirements of the five Show Cases as given in the tables at the end of each case. As mentioned in the Introduction the Show Cases were chosen to cover a wide range of subject areas and technical demands on the spectrograph in order to aid in the necessary trade-offs in the spectrograph design. The table should therefore form a good base for defining the top level scientific requirements for CODEX.

The most extreme demands with regard to precision and stability of the spectrograph are made by the cosmic redshift drift experiment and the radial velocity searches for planets. The redshift drift experiment thereby relies also heavily on the large E-ELT photon collecting area and a high throughput of $\geq 20\%$ – comparable or higher than what has been achieved for the best high-resolution spectrographs currently available [12] – to push the photon noise sufficiently below the signal to be measured.

All Show Cases ask for a resolution of $R \geq 100000$. Demand for higher resolution comes mainly from the desire to resolve narrow metal lines which would benefit the Fundamental Constant and the Planet case most. There is also a genuine scientific interest in probing the temperatures of metal enriched gas in the IGM and in galaxies at high redshift. Larger resolving power would also enable the measurement of interesting isotopic ratios in QSO spectra. Demand for lower resolution is mainly driven by the desire to look at fainter objects (at high high redshift, galaxies instead of QSOs, or in the case performing tomography of the IGM just fainter QSOs.)

While large spectral wavelength coverage is obviously always welcome the majority of the showcases appears to content with a wavelength range from $0.35 - 0.75$ micron. There are, however, interesting science cases which would benefit from the ability to cover in particular stellar spectral lines all the way to the atmospheric cut-off. The search for metals in the IGM would benefit from redder wavelength as this would allow to search at higher redshift. The work with pairs and groups of QSOs in the IGM Show Case would benefit from a larger FOV and a modest multiplex capability.

In Chapter 12 of the document describing the Technical Specifications of CODEX we have performed a comparison of the technical requirements as derived from the Science Show Cases with the compliance matrix of the present design of CODEX. The technical specifications of the current design still satisfy most of the scientific requirements.

Finally we would like to stress again that the requirements with regard to the radial velocity accuracy and stability of the spectrograph together with the large E-ELT collecting area and a high throughput of the telescope-Coudé-spectrograph system extending as far as possible into the blue are absolutely indispensable for the success of the redshift drift experiment.

[12] Note that these instruments are located at the more luminous Nasmyth or Cassegrain focii, and that they have either lower resolution, or much lower radial velocity precision. The significant challenge of such a high throughput should thus be clear.

5 The impact of the blue-wavelength cut-off due to the coating of the mirrors

At the midterm review we have been asked to consider the impact of the blue wavelength cut-off due to the coating of the mirrors on our Show Cases. There are currently two coatings discussed for the mirrors, a protected silver/aluminium coating and a bare aluminium coating. The protected silver/aluminium coating is superior to the bare aluminium coating at wavelengths > 370 nm (see Fig. 29 below). Aluminium shows the well-known dip near 800 nm, and the protected silver/aluminium coating retains an advantage all the way into the mid-IR. Aluminium, on the other hand, offers higher efficiency at wavelengths < 370 nm (`from http://www.eso.org/sci/facilities/eelt/science/drm/techdata/telescope/`). We have discussed the effect of the two different coatings at the end of the subsection *Technical Requirements* of each of the Show Cases. We give a brief summary of these discussions here.

For the redshift drift experiment a high throughput of $\geq 20\%$ is essential and it is important to maintain this high throughput as far into the blue as possible. Neither the protected aluminium/silver coating nor the bare aluminium coating are therefore ideal. The protected aluminium/silver coating is preferred because of its higher transmission over most of the relevant wavelength range. A higher transmission than offered by the protected aluminium/silver coating in the blue may, however, turn out to be crucial for establishing directly with the redshift drift experiment alone that the expansion of the Universe must indeed have started to accelerate. For the radial velocity search for planets the throughput gain of the protected silver/aluminium coating compared to the Al coating is of course welcome but not critical for the Earth twins program and its bright targets. For the radiative dating of stars in the Milky way the primary demand is again for a sufficient photon flux to reach the extreme signal-to-noise necessary to measure accurate abundances from very weak lines and the protected silver/aluminium coating is therefore preferred. The same is true for the IGM Show Case where there is flexibility in the choice of redshift/wavelength and a possible blue cut-off is less important for this Show Case. Access to the UV down to the atmospheric cut-off provided by the aluminium coating would significantly increase the sample of targets available for the study of the variability of the electron-to-proton mass ratio.

On balance the five Show Cases appear to argue for the protected silver/aluminium coating which is more efficient over most of the optical wavelength range. **The redshift drift experiment argues, however, very strongly for a major effort towards further improvements in coatings in particular at the bluest wavelengths.** Note also that there are other science cases which would be irretrievably lost without access to the atmospheric cut-off. An example is the importance of Beryllium, Oxygen OH and Nytrogen NH transitions with wavelengths close to the atmospheric cut-off for the DRM case “First Star relics in Milky Way Satellites”.

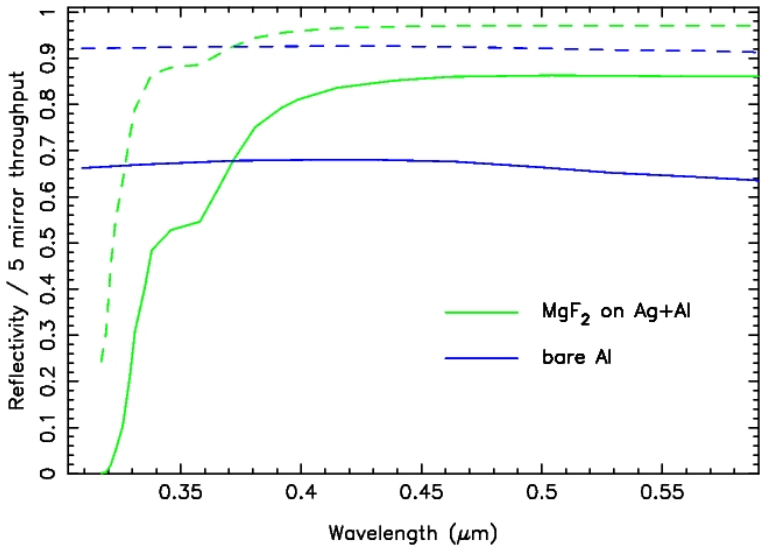

Figure 29: The dashed green line shows the reflectivity for a protected silver/aluminium coating, while the dashed blue line shows the same for a bare aluminium coating. The solid lines show the respective throughputs after 5 mirrors. Only the UV-blue-optical region is shown here to emphasize the dramatic difference between the two coatings in the UV.

6 The impact of the hemisphere of site location

We have discussed the effect of the hemisphere of site location at the end of the subsection *Technical Requirements* of each of the Show Cases. We give a brief summary of these discussions here.

For the expansion Show Case there are currently more bright targets known in the Northern Hemisphere. This is, however entirely due to the larger area surveyed in the North. By the time the redshift drift experiment would be performed this imbalance is unlikely to persist in light of major wide-area QSO surveys planned for the Southern Hemisphere and the large improvements expected in this respect due to GAIA. In case of the radial velocity search for planets sufficiently large samples of targets are in principle available in both hemispheres. Target selection is nevertheless a critical aspect for discovering Earth twins. Much preparatory work will have been performed with HARPS and hopefully ESPRESSO. A site from which a significant fraction of the Southern Hemisphere can be observed at low airmass is thus favourable. Note, however, that this imbalance may become less relevant due to HARPS-NEF at the WHT. For the galactic archaeology study of halo, thin and thick disc the hemisphere of the location is not relevant. For the study of the bulge a southern location is, however, strongly preferred, although a tropical northern location would be acceptable. A location further north would essentially mean losing the bulge. Targets can be chosen all over the sky for the IGM Show Case and there is thus no particular preference in terms of hemisphere. Hemisphere of site location is also not particularly important for the Study of the variability of Fundamental Constants. On balance there appears to be – albeit a rather weak – preference for a southern site location.

7 Preparatory Observations for CODEX

7.1 ESPRESSO at the VLT as a pathfinder for CODEX

ESPRESSO (Echelle Spectrograph for PREcision Super Stable Observations) is a proposed 3rd generation instrument for the VLT which is at present undergoing a Phase A study. ESPRESSO can in many ways be seen as a precursor of CODEX and is meant to ease the path of ultra-stable high-precision spectroscopy from HARPS at a 4m class telescope to the 42m aperture of the E-ELT. Observations with ESPRESSO at very high SNR will be crucial for developing procedures for data acquisition, reduction and analysis which assure the cm/s radial velocity accuracy required for the cosmic redshift drift experiment and the radial velocity searches for earth-like planets in the habitable zones of their parent stars.

7.2 Target selection for the redshift drift experiment

The accuracy with which the redshift drift of the absorption features in the Lyα forest can be measured with CODEX will be limited by photon noise. There are therefore substantial gains to be made from using a sample of as bright as possible QSOs which spans the redshift range $2 < z < 4.5$. From the presently known samples of bright, high-redshift QSOs it is obvious that the sky has not been surveyed to the same depth everywhere. Known bright, high-z QSOs lie predominantly in the North. That means that a fair number of such QSOs remain to be discovered in the South. It is likely that this will be done (or can be done) with upcoming large or even all-hemisphere surveys from VST, VISTA, LSST, SkyMapper and particularly GAIA. These surveys will not only discover new potential targets but they will also provide us with more reliable photometry of the already known QSOs than what is currently available. Low/intermediate resolution spectra of the candidate targets will need to be obtained in order to verify if they are suitable for the experiment (e.g. absence of DLA and LLS) and to allow a flux calibration of the high resolution spectra. Photometrically selected targets would need to be monitored in order to obtain their light-curves and verify that they do not vary in an unfavourable way.

7.3 Target selection for radial velocity searches for planets

Observing campaigns with HARPS and ESPRESSO will provide radial velocities of a large number of stars with sub-m/s accuracy. This will allow the pre-selection of stars with favourable parameters and little stellar activity for the search of earth-mass planets. GAIA should be operational at the time of CODEX and will provide an additional sample.

Once stars with favourable stellar parameters and little activity have been identified, it is important to ensure that the stars do not have physical or optical companions. Contamination by objects as faint as 7 to 10 times magnitudes fainter needs to be avoided. This is best checked with follow-up measurements with NACO where NACO's AO capability is essential to study the stellar environment.

7.4 Target selection for Galactic Archaeology

The radiodating of stellar ages discussed in the Galactic Archaeology Show Case requires substantial preparatory work to find suitable targets.

- **Targets for the galactic halo**.

  - *Thorium measurements in 'normal' giants.* Several hundred stars with [Fe/H] < -3 are already known from HK, HES and SDSS Surveys. Further targets can be extracted from SDSS especially at very cool temperatures $4000\mathrm{K} < T_{\mathrm{eff}} < 4500\mathrm{K}$. Stars in that temperature range should be explored and they are probably most suitable for a Th measurement. VLT with UVES/X-shooter would be adequate to fully characterize a suitable sample. Measurements of T_{eff}, $\log g$, and the detailed chemical composition of at least ~ 100 stars would be required. Many of the HK, HES metal-poor stars lack good and complete photometry. The missing photometric data could be obtained with small telescopes (e.g. REM, Danish) but would need to be taken in good time. For each star one would like at least UBVRIJHK. U band is important. SDSS stars already come with $ugriz$ photometry, which may be sufficient. Acquisition of JHK (e.g with REM) would be nevertheless be desirable.

- *Uranium measurements.* These are likely to be only possible for r-enhanced stars. Up to now, there is a sample of ~ 40 r-enhanced stars from the HERES Survey (Christlieb et al. 2004, Barklem et al. 2005). measurement of U is not going to be possible in all r-enhanced stars but only in those which are not C-enhanced and more likely in those which have an actinide-boost. Larger numbers of r-enhanced stars (an increase by at least a factor of 4 compared to the HERES sample of 253 stars) would be required. A dedicated survey using X-shooter on VLT using candidate targets from SDSS and Skymapper could build up such a sample rapidly.

- **Targets for the thin and thick disc**.

  Large number of both thin and thick disc stars will be available from the RAVE Survey. A high resolution follow-up to fully characterize the possible targets would be needed. 4m class telescopes would be sufficient as a substantial number of candidate targets will be brighter than V=13.

- **Targets for the bulge.** High resolution follow-up of the MP populations with VLT (X-shooter?) could establish a suitable sample for CODEX (see paper by Brown et al. arXiv:0812.0023).

7.5 An ultra-deep UVES and/or ESPRESSO spectrum to search for metals in the low-density IGM

The SNR and the resolution achievable by CODEX at the E-ELT will be needed to reach the most underdense regions of the IGM where the tightest constraints on residuals from enrichment by the first galaxies can be obtained. An ultra-deep spectrum with UVES and/or ESPRESSO would, however, already push current studies to significantly lower densities and would be extremely useful for a study of the systematic uncertainties of the presently adopted techniques (e.g. the pixel optical depth statistics) at very high signal-to noise. It would be feasible to acquire UVES spectra of ~ 2 QSOs with a SNR of ~ 500 (never obtained before at high resolution). With ESPRESSO in the 4UT configuration (at the UVES resolution) even higher SNR could be reached while in the 1UT mode, at a resolution $R \sim 180\,000$, the intrinsic width of metal lines and the presence of very weak and narrow absorptions could be investigated. The ESPRESSO spectra obtained for this purpose could be used as the higher redshift subsample of a sample used to test the stability of fundamental constants.

7.6. Stability of fundamental constants

- **Pre-ESPRESSO**

  - Fine structure constant, α.

    New UVES observations with dedicated exposures would be helpful to investigate wether the accuracy presently achieved is limited by wavelength calibration errors or by photon noise and to characterize the limitations of the wavelength calibration with UVES at the VLT.

    Reobserving the subsample of HIRES/KECK spectra which is accessible from the Southern hemisphere with UVES/VLT would also improve of our understanding of the limits of the wavelenght calibration of both spectrographs.

  - Electron-proton mass ratio, $m_{\rm e}/m_{\rm p}$.

    Most pressing here is to study a larger number of systems showing H_2 at redshift $z \gtrsim 2.5$. There are only three targets bright enough for accurate UVES/VLT observations. This will requires new extensive H_2 survey of DLAs, for which the SDDS DLA sample would provide a suitable base.

- **ESPRESSO**
  There is considerable overlap in the science goals of ESPRESSO and CODEX regarding the test of the stability of fundamental constants. ESPRESSO should provide an order of magnitude improvent of the current limits and CODEX should take this further by another order of magnitude.